

CHARACTERIZATION OF THE HSP70 PROTEIN HOMOLOG (HSP70h) OF CITRUS  
TRISTEZA CLOSTEROVIRUS

By

INES-MARLENE ROSALES VILLAVICENCIO

A DISSERTATION PRESENTED TO THE GRADUATE SCHOOL  
OF THE UNIVERSITY OF FLORIDA IN PARTIAL FULFILLMENT  
OF THE REQUIREMENTS FOR THE DEGREE OF  
DOCTOR OF PHILOSOPHY

UNIVERSITY OF FLORIDA

2001

To my parents, Inés and Moisés

## ACKNOWLEDGMENTS

I would like to express my gratitude to all the people that supported my graduate studies at the University of Florida. I am especially grateful to my former major professor Dr. C.L.Niblett, for his encouragement and friendship along all these years. I would also like to thank my present advisor, Dr. Richard Lee, who gave me guidelines and advice for my research during my entire program, and for being one of the few people who showed a permanent interest for my condition as graduate student. I would like to thank Drs. K. Derrick, Dr. R. Brlansky, and G. Moore for serving in my committee and for their helpful suggestions and comments and for reviewing this manuscript. I would like to extend my gratitude to Debbie Howd and Dianne Anchor for the technical assistance during the EM work, to Dr. J. Grosser for letting me use the facilities at his laboratory and to Dr. Rachel Shireman for her special support and dedication to graduate students in our lab.

I want to give special thanks to the former and current members of the Niblett's and Lee's labs, V. J. Febres, R. Chandrika, K. L. Manjunath, J. Vázquez, R. Harakava, H.Genc, Y. Petersen and M. Dekkers for the limitless help, understanding and friendship that they gave me in the past years. I want to extend my gratitude to all the sincere and unconditional friends that I have made in Gainesville and Lake Alfred, who gave me affection and unconditional support.

My deepest thanks and appreciation go to my parents and family, for the constant support and unconditional love they have provided throughout my life.

My deepest thanks and appreciation go to my parents and family, for the constant support and unconditional love they have provided throughout my life.

Finally, I thank INIA (Instituto de Investigaciones Agropecuarias) for its generous financial support during my graduate studies at the University of Florida. A special recognition goes to Dr. Sergio Bonilla, who took great care of all the administrative issues with UF during this time. Thanks go to Carlos Muñoz and Emilio Ruz for their support and help. My gratitude goes to the people working at “INIA-La Platina” for being my friends from the distance.

## TABLE OF CONTENTS

	<u>page</u>
ACKNOWLEDGMENTS.....	iii
LIST OF TABLES .....	vii
LIST OF FIGURES.....	viii
ABSTRACT.....	x
CHAPTERS	
1. CITRUS TRISTEZA VIRUS: THE DISEASE, THE CAUSAL AGENT AND ITS CHARACTERISTICS .....	1
The Tristeza Disease and Its Causal Agent .....	1
The Disease .....	2
Cytopathology of CTV-infected Tissue .....	3
Natural Resistance to CTV.....	5
Molecular Characteristics of CTV .....	7
Genomic Organization and Replication Strategies.....	7
RNA Populations in Infected Tissue .....	9
LMT RNAs .....	10
Defective RNAs .....	10
Subgenomic RNAs.....	13
Population Structure and Genetic Diversity.....	14
2. PRODUCTION OF A POLYCLONAL ANTISERUM AGAINST THE CARBOXY-TERMINAL END OF THE CTV HEAT SHOCK PROTEIN HOMOLOG (HSP70h) .....	20
Introduction.....	20
Material and Methods.....	22
Results .....	29
Sequence Analysis.....	29
Expression and Purification of the Carboxy-Terminal End of the CTV-HSP70h....	31
Production of the Polyclonal Antiserum.....	43
Discussion.....	45

3. <i>IN VIVO</i> LOCALIZATION OF THE HSP70 PROTEIN HOMOLOG (HSP70h) IN CITRUS TRISTEZA CLOSTEROVIRUS INFECTED PLANTS .....	49
Introduction.....	49
Material and Methods.....	52
Results .....	54
<i>In Vivo</i> Detection of the HSP70h by Tissue Printing.....	54
Immunoprecipitation of an HSP70h-CP Complex from CTV-infected Plants.....	56
SSEM-Immunogold Labeling.....	57
Discussion.....	60
4. THE CTV-HSP70h AS A COMPONENT OF CTV INCLUSION BODIES .....	64
Introduction.....	64
Material and Methods.....	65
Results .....	69
Light Microscopy and Inclusion Body Purification.....	69
Fluorescent Antibody Microscopy.....	71
Analysis by SDS-Polyacrylamide Gel Electrophoresis (SDS-PAGE).....	73
Western Blot Analysis.....	76
Discussion.....	77
5. <i>AGROBACTERIUM</i> -MEDIATED TRANSFORMATION OF DUNCAN GRAPEFRUIT ( <i>Citrus paradisi</i> ; Macf).....	80
Introduction.....	80
Material and Methods.....	85
Results .....	91
Constructs Used in the Transformation Experiments .....	91
Transformation and Regeneration of Transgenic Plants.....	95
PCR Assay of the Putative Transgenic Plants.....	98
Conclusions .....	100
LIST OF REFERENCES .....	102
BIOGRAPHICAL SKETCH.....	116

## LIST OF TABLES

<u>Table</u>	<u>Page</u>
2-1. Sequence of the primers used for the RT-PCR and cloning of the HSP70h from CTV.....	24
2-2. Nucleotide identity among the CTV-HSP70h genes of different isolates of citrus tristeza virus.....	32
2-3. Amino acid identity among the CTV-HSP70h proteins expressed by different isolates of citrus tristeza virus CTV-HSP70h proteins .....	32
2-4. Biological properties and origin of the citrus tristeza virus (CTV) isolates included in the alignment of the amino acid sequences of their HSP70h proteins .....	34
5-1. Set of primers used for PCR assay of the putative transgenic plants.....	91
5-2. Summary of the results of Duncan grapefruit transformation experiments performed with the constructs containing the CTV-HSP70h, the frameshift mutant (HSP70h-HindIII), or the binary vector by itself.....	98

## LIST OF FIGURES

<u>Figure</u>	<u>Page</u>
1-1. Symptoms caused by citrus tristeza virus.....	4
1-2. Representation of the gene expression and genome organization of citrus tristeza virus .....	8
2-1. Nucleotide sequence for the HSP70h gene from the grapefruit stem pitting CTV isolate T3800 .....	33
2-2. Alignment of the amino acid sequences of the HSP70h proteins from several CTV isolates.....	35
2-3. Cluster dendrogram based on the amino acid sequences of the translated p65 gene for the various CTV isolates.....	41
2-4. Domain conservation between HSP70s and HSP70h proteins.....	41
2-5. Silver stained SDS-polyacrylamide gel electrophoresis (PAGE) showing the over-expression of the 149 amino acid fragment fusion protein in <i>E.coli</i> BL21 cells.....	42
2-6. Western blots showing the reactivity of the test bleeds.....	46
2-7. Expression and analysis of the CTV-HSP70h induction in BL21 cells.....	46
2-8. Western blot showing the reaction of the bacterial-expressed CTV-HSP70h protein with the HSV-Tag monoclonal or chicken polyclonal antibody.....	47
3-1. Representation of the citrus tristeza closterovirus genome.....	51
3-2. Tissue prints of infected and healthy citrus stems after incubation with HSP70h and coat protein specific antibodies.....	55
3-3. Interaction of CTV-HSP70h and CTV-CP in CTV infected tissue.....	58
3-4. Serologically specific electron microscopy (SSEM) of trapped citrus tristeza virus (CTV) particles .....	59

3-5. Immunogold labeling of citrus tristeza virus trapped particles using the coat protein specific antibody.....	59
3-6. Immunogold labeling of citrus tristeza virus particles using the CTV-HSP70h-specific antibody. ....	60
4-1. Azure A staining and light microscopy of leaf petiole sections of healthy and CTV infected tissue. ....	70
4-2. Inclusion body purification.....	71
4-3. Immunofluorescence of proteins contained in the CTV inclusions using a TRITC-labeled conjugate. ....	72
4-4. Silver staining of SDS-PAGE gels containing proteins from partially purified CTV inclusion bodies (IB) from citrus tristeza virus (CTV) infected and healthy bark tissue. ....	74
4-5. Western blot detection of the CTV-CP in the purified inclusion bodies. ....	75
4-6. Western blot detection of the CTV-HSP70h in the purified inclusion bodies (IB).....	75
5-1. <i>Agrobacterium</i> -mediated transformation of grapefruit epicotyl segments.....	92
5-2. Nucleotide and amino acid sequences of the CTV-HSP70h and the frameshift mutant cloned in the binary vectors used for transformation. ....	93
5-3. Analysis of the putative transgenic Duncan grapefruit plants by PCR.....	97
5-4. Histochemical GUS-staining of the regenerated shoots.....	99

Abstract of Dissertation Presented to the Graduate School  
of the University of Florida in Partial Fulfillment of the  
Requirements for the Degree of Doctor of Philosophy

CHARACTERIZATION OF THE HSP70 PROTEIN HOMOLOG (HSP70h) OF  
CITRUS TRISTEZA CLOSTEROVIRUS

By

Inés-Marlene Rosales Villavicencio

December 2001

Chairman: Dr. Richard Lee  
Major Department: Plant Pathology

Citrus tristeza virus (CTV), a member of the family *Closteroviridae*, is the causal agent of one of the most destructive diseases of citrus, causing a diversity of symptoms on various scion and rootstock combinations. The virus is a monopartite, single-stranded, positive-sense RNA virus, with a genome of about 20 kb encapsidated by two capsid proteins. The *Closteroviridae* is the only viral family known to encode a homolog of the HSP70 family of cellular chaperones. The HSP70 homolog (HSP70h) of CTV is a 65 kDa protein (p65) with high homology to cellular chaperones. The carboxyl-end of the p65 protein (3' end of the p65 gene) was chosen for study because of its lesser homology with cellular chaperones, to avoid cross-reactivity of the antibody with host proteins. The 3' end of the p65 gene of CTV was cloned with a histidine tag fusion and expressed in *Escherichia coli*. The purified fusion protein was used to raise a polyclonal antibody in chicken. Using this antibody, the CTV-p65 gene product was specifically detected in CTV-infected but not in healthy citrus plants. The localization pattern of the p65 and the

viral coat protein were similar in direct tissue print studies. The same antibody used for immunogold labeling studies revealed a close association of the HSP70h protein with the virion. This association was later confirmed by co-immuno-precipitation of the virion and the p65 protein. The occurrence of the p65 protein in the inclusion bodies present in CTV infected tissue was studied. Additionally, two different constructs containing a full-length and a frameshift mutant of the HSP70h gene from CTV were transformed into Duncan grapefruit seedlings to test the possibility of inducing pathogen derived resistance against CTV.

CHAPTER 1  
CITRUS TRISTEZA VIRUS: THE DISEASE, THE CAUSAL AGENT AND ITS  
CHARACTERISTICS

Closteroviruses represent a group of emerging and re-emerging economically important plant pathogens. Members of this group affect several crops of major economic importance, such as sugar beet, citrus, tomato, lettuce, potato, sweet potato, grapevine, pineapple, cherry, and some ornamentals (Karasev, 2000).

The family *Closteroviridae* comprises more than 30 plant viruses with filamentous, flexuous virions and includes representatives of either mono or bipartite positive sense single-stranded RNA genomes (Karasev, 2000). Closteroviruses are transmitted semipersistently by insects, i.e. aphids, whiteflies, or mealybugs (Brunt *et al.*, 1996). Based on the virus particle structure, vector transmission, and genome organization, the *Closteroviridae* family has been classified into two genera: Closterovirus, containing monopartite viruses transmitted by aphids, mealybugs and possibly whiteflies (Brunt *et al.*, 1996), and the genus Crinivirus, containing bipartite whitefly-transmitted viruses (Wisler *et al.*, 1998).

**The Disease and Its Causal Agent**

Citrus tristeza virus (CTV), a member of the genus Closterovirus, is the causal agent of one of the most destructive viral diseases of citrus, and it occurs in most of the citrus producing areas of the world (Bar-Joseph, 1989). CTV has a positive-sense single-

stranded RNA genome encapsidated in flexuous particles about 2000 nm in length (Bar-Joseph and Lee, 1989). The virions contain two capsid proteins (CP) arranged in a “rattlesnake” structure: a 25 kDa CP that encapsidates ~95% of the particle and a 27 kDa minor CP that encapsidates ~5% at one terminus. This morphology is considered a hallmark for the closterovirus group (Agranovsky *et al.*, 1995; Febres *et al.*, 1996). CTV occurs as a diverse complex of strains that vary greatly in aphid transmissibility and severity of symptoms in different citrus hosts. The virus is transmitted by grafting, but it is not seed-borne (Bar-Joseph and Lee, 1989). It also has been mechanically transmitted by a knife-cut and slash inoculation but with some difficulty (Garnsey *et al.*, 1977; Garnsey and Muller, 1988). CTV is vectored by several aphid species in a semipersistent manner with the aphid retaining the ability to transmit the virus for up to 24-48 hrs after acquisition (Bar-Joseph, 1989; Racciah *et al.*, 1989). The most efficient vector for CTV is *Toxoptera citricida* Kirkaldy, commonly called brown citrus aphid (Bar-Joseph, 1989; Yokomi *et al.*, 1994). This aphid probably originated in China and now is distributed throughout many regions of the world (Rocha-Peña *et al.*, 1995). In November 1995, the brown citrus aphid was discovered in Florida in the Ft. Lauderdale area (Halbert, 1997) and by the summer of 1997 was widely distributed throughout the South Central and Coastal regions of Florida (Michaud, 1998), threatening the citrus industry of the area.

### **The Disease**

Tristeza, which means “sadness” in Spanish and Portuguese, is best thought of as a family of diseases caused by different strains of CTV. A common tristeza disease is the decline of citrus scion varieties grafted onto sour orange (*C. aurantium* L.) rootstock (Bar-Joseph, 1989). In the field, decline may be rapid or gradual. The most dramatic

symptoms are observed with the combination of sweet orange on sour orange rootstock where sudden wilting and death can occur following CTV infection. In the decline on sour orange symptom, phloem necrosis develops at the bud union causing root starvation. When the starch reserves are finally exhausted, the tree rapidly dies, often leaving a dead tree with fruit hanging but no leaves remaining (Figure 1-1, A) (Lee *et al.*, 1994; Rocha-Peña *et al.*, 1995). The other important disease caused by CTV is stem pitting of the scion regardless of the rootstock, which reduces tree vigor, yield and fruit quality of the tree (Figure 1-1: B, C, G). Stem pitting symptoms of CTV are considered as the most serious disease caused by the virus, because citrus production cannot be continued by just replacing trees on a CTV tolerant rootstock. Other symptoms often associated with stem pitting disease are vein clearing, vein corking and leaf cupping (Figure 1-1, D, E and H) (Lee *et al.*, 1994; Rocha-Peña *et al.*, 1995). Some isolates of CTV induce very mild symptoms or are symptomless, even in the most sensitive citrus species (Bar-Joseph, 1989). Seedling yellows (SY) strains cause chlorosis and stunting in sour orange, acid lemon, and grapefruit indicator plants (Figure 1-1, F) (Rocha-Peña *et al.*, 1995). The seedling yellows reaction is mostly a greenhouse or nursery disorder that is used to detect the presence of the more serious decline inducing or stem pitting strains of CTV (Lee *et al.*, 1994; Rocha-Peña *et al.*, 1995); however seedling yellows can cause problems in the field when infected trees are topworked with susceptible varieties.

### **Cytopathology of CTV-Infected Tissue**

Citrus tristeza virus, as other closteroviruses, is characteristically associated with the phloem which is found most consistently in the phloem companion and parenchyma cells; hence it is called a phloem-limited virus (Karasev, 2000). Cells with active

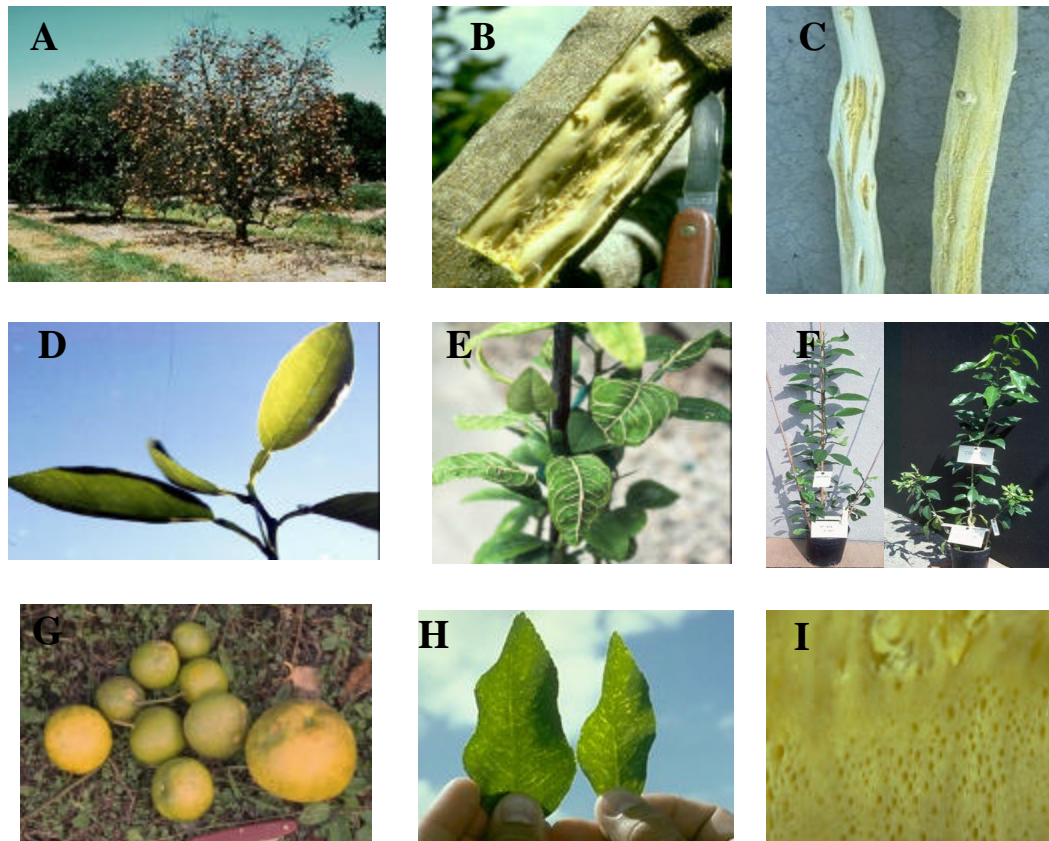


Figure 1-1. Symptoms caused by citrus tristeza virus. (A) Sweet orange tree on sour orange rootstock undergoing tristeza decline (Lee, R.F.); (B) Stem pitting on Pera sweet orange, occurring in Brazil (Lee, R.F.); (C) Stem pitting on grapefruit in Venezuela (Lee, R.F.); (D) Cupping of the leaf in Mexican (Roistacher, C.N.); (E) Vein corking symptoms on leaves of a Mexican lime seedling inoculated with a very severe seedling-yellow tristeza isolate (Roistacher, C.N.); (F) Seedling yellows reaction on grapefruit (left) and sour orange (right) seedlings in the greenhouse (Roistacher, C.N.); (G) Grapefruit collected from a Marsh grapefruit tree on rough lemon rootstock in Colombia which was affected by stem pitting strains of tristeza (Lee, R.F.); (H) Vein-clearing symptoms in the leaf of a Mexican lime seedling (Lee, R.F.); (I) Pinholes in the bark, caused by bristles in the wood, cause honeycombing on the back side of the bark patch over the sour orange rootstock (Lee, R.F.). Photographs presented in this figure were downloaded from [www.ecoport.org](http://www.ecoport.org). The author of the photograph is given in the parenthesis.

closterovirus replication display clusters of vesicles with a diameter of 80-120 nm which show different levels of tonicity and contain a network of fine fibrils (Bar-Joseph *et al.*, 1997). CTV produces inclusion bodies that are confined mostly to the phloem and associated tissue. The inclusion bodies appear to be large aggregates of virus particles mixed with structures of unknown composition which might contain modified cell constituents. The inclusion bodies have been detected by using light microscopy (Brlansky and Lee, 1990; Garnsey *et al.*, 1980), *in situ* immuno-fluorescence (Brlansky *et al.*, 1988), and by transmission electron microscopy (Kitajima and Costa, 1968; Gowda *et al.*, 2000). The detection of CTV inclusions using light microscopy can provide a rapid method for diagnosis of CTV infection (Brlansky, 1987). Studies have shown differences in the number of inclusion bodies caused by mild and severe CTV isolates in the various host species (Brlansky and Lee, 1990). The effect of virus strain or host on the morphology of the various CTV inclusion bodies is not known.

### **Natural Resistance to CTV**

CTV infects all citrus species and varieties, most hybrids and some citrus relatives (Mestre *et al.*, 1997c). Recently, some pummelo (*C. grandis* (L.) Osb.) accessions were found to be resistant to certain CTV strains (Garnsey *et al.*, 1997). There are only three citrus relatives that have been reported to be resistant to CTV (Garnsey *et al.*, 1987; Yoshida *et al.*, 1983): *Severinia buxolia* (Poir.) Tenore, *Swinglea glutinosa* (Blanco) Merr, and *Poncirus trifoliata* (L.) Raf. The resistance found in *P. trifoliata* is conferred by a single dominant gene, designated *Ctv* (Fang *et al.*, 1998; Gmitter *et al.*, 1996), which has been mapped by using molecular markers (Gmitter *et al.*, 1996; Mestre *et al.*, 1997b). Introgression of this resistance into rootstock cultivars has been successful via sexual

hybridization, but the development of CTV-resistant scions has been more difficult due to the introgression of undesirable fruit characteristics from *Poncirus* (Deng *et al.*, 2001b). Molecular cloning of the *Ctv* gene would provide a means to develop resistant scion cultivars using genetic transformation. The region containing this gene has been mapped, and markers flanking and cosegregating with *Ctv* have been developed (Fang *et al.*, 1998).

Recently, Deng *et al.* (2000) identified 22 sequences similar to the NBS-LRR (nucleotide binding site-leucine rich repeat) class resistance gene in the citrus genomic DNA by using PCR amplification with degenerate primers. One of the fragments was closely linked and another seems to co-segregate with *Ctv*, which might facilitate direct landing on the resistance gene (Deng *et al.*, 2001b). Different BAC libraries have been developed to pursue this objective, and some BAC clones and BAC contigs containing R-gene candidates were characterized (Deng *et al.*, 2001b; Yang *et al.*, 2001). The *Ctv* locus was localized within a genomic region of approximately 180 kb, and efforts are being made to assign this locus to a smaller genomic fragment whose function can be confirmed by genetic complementation (Deng *et al.*, 2001a).

Two interesting observations, the fact that the hypersensitive reaction has not been observed in *Ctv*-bearing plants (Mestre *et al.*, 1997b), and that the virus can replicate in protoplasts from CTV-resistant plants (Albiachi-Marti *et al.*, 1999), have raised questions as to whether *Ctv* confers resistance by blocking virus replication or by interfering with virus loading or unloading from the phloem (Mestre *et al.*, 1997b). The same group has suggested that at least two genes are responsible for CTV-resistance in *P. trifoliata* var “Flying Dragon,” based on the short distance accumulation that they

observed in some *Ctv*-Rr progeny segregant plants derived by self-pollination of this resistant genotype. Bulk segregant analysis of this population identified five RAPD-markers linked to a locus (*Ctm*) that is located in a different linkage group from *Ctv* (Mestre *et al.*, 1997a).

## **Molecular Characteristics of CTV**

### **Genomic Organization and Replication Strategies**

CTV is a member of the monopartite genus *Closterovirus* in the family *Closteroviridae* (Bar-Joseph, 1989). The genomic RNA (gRNA) of this virus contains from 19,226 to 19,302 nt, depending on the isolate (Karasev *et al.*, 1995; Mawassi *et al.*, 1996; Suastika *et al.*, 2001; Vives *et al.*, 1999; Yang *et al.*, 1999b), which occur as 12 open reading frames (ORFs), potentially encoding 19 protein products (Karasev, 2000a; Karasev, 2000b; Karasev *et al.*, 1995) (Figure 1-2). These include replication-associated proteins, the homolog of the heat shock proteins 70 (HSP70h), the two coat proteins, and several others products with unknown functions (Bar-Joseph *et al.*, 1997). Computer-assisted sequence analysis has identified two conserved groups or blocks of genes in the genome of CTV and other closteroviruses. The first group (ORF 1a and 1b) includes replication-associated proteins (RNA polymerase, putative helicase, putative methyltransferase, and two accessory processing papain-like proteases (Dolja *et al.*, 1994)). The replication-associated proteins of CTV are translated directly from the gRNA and expressed as a large 400 kDa polyprotein that is further processed by virus-

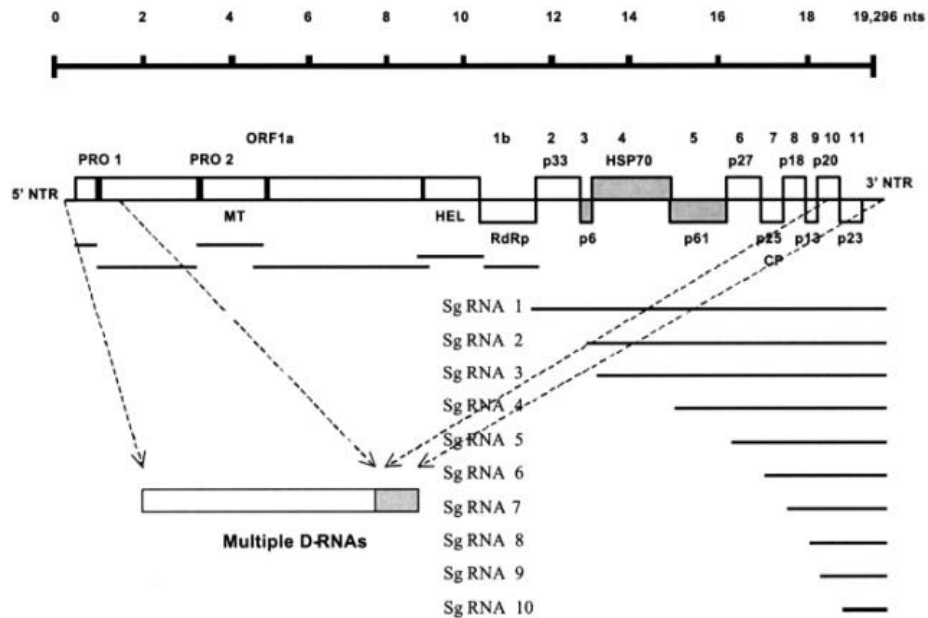


Figure 1-2 . Representation of the gene expression and genome organization of citrus tristeza virus. Open reading frames are shown as boxes and the putative domains on ORF 1a and 1b are separated by lines. PRO: papain-like proteases 1 and 2; RdRp: RNA-dependent polymerase. The genomic and subgenomic RNAs are shown by solid lines, the size, in kilobases, is indicated by the scale at the top. Defective-RNA strategy is shown by dashed lines (Figure reproduced from Ochoa-Corona, 2001).

encoded proteases (Karasev *et al.*, 1995; Mawassi *et al.*, 1995a). ORF1b, which encodes the RNA polymerase, is proposed to be expressed by +1 ribosomal frameshift (Cevik *et al.*, 1999; Cevik, 2001). The second group of genes, ORF 3 to 7, includes a five-gene block unique for closteroviruses. This block encodes a small 6 kDa hydrophobic protein, a 65 kDa homolog of the cellular HSP70 proteins (HSP70h), a 61 kDa protein and a tandem of two structural proteins, a 27 kDa capsid protein (CP) duplicate, and the 25 kDa CP itself (Karasev *et al.*, 1995; Karasev *et al.*, 1994; Pappu *et al.*, 1994; Sekiya *et al.*, 1991). It has been proposed that this unique protein quintet is required for cell-to-cell

movement of a closterovirus, based on the fact that beet yellow closterovirus (BYV) requires this set of proteins for intercellular translocation in leaf epidermis and leaf mesophyll of the local lesion host, *Claytonia perfoliata* (Alzhanova *et al.*, 2000).

The ORFs located at the 3' end potentially encode proteins p18, p13, p20 and p23 the functions of these proteins are not clear yet. It has been reported that p20 gene product accumulated in infected tissue, exhibited a high affinity to itself in a yeast two hybrid system, and was localized mainly in the CTV-infected cells within the amorphous inclusion bodies (Gowda *et al.*, 2000). The p23-kDa protein, encoded by the 3'-terminal gene of CTV, is an RNA-binding protein which contains several basic amino acids and a putative zinc-finger domain between positions 50-86 of its amino acid sequence (Lopez *et al.*, 2000).

### **RNA Populations in Infected Tissue**

CTV-infected plants contain the large double-stranded (ds) replicative form (RF) RNA molecule and a nested set of at least nine smaller 3'-coterminial subgenomic RNAs (sgRNAs) corresponding to the 3'-terminal ORFs 2 to 11. Each sgRNA is present as a single-stranded RNA (ssRNA) molecule and as a corresponding dsRNA species (Hilf *et al.*, 1995; Mawassi *et al.*, 1995a). In addition, the use of 5'-end specific probes demonstrated the presence of a considerable amount of low molecular single-stranded positive-sense RNA fragments, designated Low Molecular Weight Tristeza (LMT) (Mawassi *et al.*, 1995c). Multiple defective RNAs (D-RNA) that vary in size and abundance are associated with a majority of the CTV isolates (Ayllon *et al.*, 1999a; Mawassi *et al.*, 1995b).

Recently an even more complex scenario was described by Gowda *et al.* (2001). They proposed that each controller element in the CTV genome produced three sgRNAs: a 5'-terminal positive-strand and both positive and negative-stranded 3'-terminal RNAs. This implies that theoretically CTV could produce 30-33 different species of RNA in infected cells.

### **LMT RNAs**

The LMT RNAs make up a major proportion of the total virus-associated RNAs (Che *et al.*, 2001; Mawassi *et al.*, 1995c). They mainly consist of a population of RNAs having two modal lengths of 744-746 and 842-854 nucleotides. It has been suggested that these LMT RNAs are produced by termination during the production of genomic RNAs. Additionally, a second class of heterogeneous 5'-coterminal sgRNAs of ~10 Kb, designated Large Molecular Weight Tristeza (LaMT) has been found in infected plants, but in much smaller amounts. LaMT were found less consistently in tissue from chronically infected plants than in RNAs obtained from recent infections (Che *et al.*, 2001). It seems that none of the ten 3' genes encoded by the CTV genome are involved in the synthesis of these 5'-co-terminal sgRNAs, since they appear to be produced normally by a deletion mutant from the virus, CTV-Δ Cla, which has all the 3'-genes deleted (Che *et al.*, 2001; Satyanarayana *et al.*, 1999)

### **Defective RNAs**

When the CTV-VT isolate was cloned and sequenced, the presence of several D-RNAs of various sizes was revealed. The D-RNA were composed of the 5' and 3' termini of the genomic RNA with extensive internal deletions. The size of the termini varied among species, with minimal lengths of 442 nt and 858 nt from the 3' and the 5'

termini, respectively, resulting in different sizes of D-RNAs with different junction sites. The D-RNAs were encapsidated as shorter virions showing the typical heterodimeric encapsidation pattern of CTV (Bar-Joseph *et al.*, 1997; Mawassi *et al.*, 1995b; Mawassi *et al.*, 1995c).

Later, it was found that multiple D-RNAs that vary in size and abundance are present in a majority of CTV isolates (Ayllon *et al.*, 1999a; Mawassi *et al.*, 1995b). The size of the CTV D-RNA species ranges from small (~ 1.6 kb) to nearly genomic full length (> 10 kb) (Bar-Joseph *et al.*, 1997; Mawassi *et al.*, 2000b; Yang *et al.*, 1997). Some isolates have one or two D-RNAs in major abundance, along with multiple minor D-RNAs. Most of the characterized D-RNAs consist of simple fusions of the 5' and 3' genomic termini, but their lengths and junction sites vary among species (Ayllon *et al.*, 1999a; Mawassi *et al.*, 1995c; Yang *et al.*, 1997). Although D-RNAs are usually homologous to the helper, abundant D-RNA with sequences different from that of the major component of the gRNA have been found, suggesting that the CTV-replicase complex might be able to recognize and replicate heterologous sequences *in trans* (Mawassi *et al.*, 2000b).

The variation in abundance of the different D-RNAs in a population suggests selection for those of higher fitness. Using *in vitro* constructed D-RNA, Mawassi *et al.* (2000a) reported that the minimal sequence required for accumulation of the D-RNA was within the genomic 5' proximal ~1 kb, plus the 3' 270 nts, although internal sequences also affect the accumulation. A continuous ORF through most of the sequence derived from the 5' end of the genome was also a requirement for D-RNA amplification,

although its protein product did not affect the amplification of this replicon (Mawassi *et al.*, 2000a).

Defective interfering RNAs are usually found to compete with the non-defective virus genome for the components of the replicase. This interference with viral replication results in a reduced level of virus accumulation and a marked attenuation of viral symptoms in infected plants (Simon and Bujarski, 1994). In contrast, CTV D-RNAs do not noticeably affect levels of accumulation of the genomic or the subgenomic RNAs of the helper virus, suggesting that the D-RNA did not compete for the same pool of replicase as the helper virus (Mawassi *et al.*, 2000b). The only relationship between CTV D-RNAs and biological activity has been reported by Yang *et al.*, (1999) who described an association between the SY reactions of sour orange seedlings and the genomic composition of the D-RNA. They found that among sub-isolates of the VT strain, which were selected from chronically infected Alemow plants, there was an association between the presence of 2.4, 2.7 and 4.5 kb D-RNA, and SY and non-SY reactions, respectively. A similar pattern was obtained with the isolate Mor-T from Israel. This study suggested that the non-SY reaction results either from the absence of SY gene(s) in the genomes of certain CTV strains or through the suppression of the effect of SY gene(s) by D-RNAs with 5' parts larger than 4000 nucleotides (Yang *et al.*, 1999).

The mechanisms suggested to be involved in the generation of the CTV D-RNA are the minus-strand jumping model and the template switching mechanism. The minus-strand jumping model is supported by the finding of an extra C at the junction of the common end D-RNA derived from three different CTV-isolates, and an extra G at the 3'-terminus of the minus strand of the sgRNA for the ORF 11. The second model, the

template switching mechanism, is supported by the presence of direct repeats from two separate genome locations in the virus which have been found flanking or in the vicinity of the junction sites of the CTV D-RNAs (Ayllon *et al.*, 1999a; Bar-Joseph *et al.*, 1997; Yang *et al.*, 1997).

### **Subgenomic RNAs**

RNA viruses employ diverse strategies to express their genomes in their hosts. These include sgRNAs which serve as messenger RNAs for the expression of internal genes. The sgRNAs of CTV, which have been found to be encapsidated in particles, consist of substantial amounts of both negative and positive strands (Mawassi *et al.*, 1995a; Gowda *et al.*, 2001). The sequences involved in their production are known as “controller elements” instead of promoters and the mechanism of their production is not clear yet (Gowda *et al.*, 2001).

Nine sgRNAs were identified when the CTV-specific RNAs from the CTV isolate T36 were extracted from infected tissue and analyzed by Northern blot hybridization using specific probes for the different ORFs. A probe derived from the ORF11 (p23) (Figure 1-2) hybridized with all the sgRNAs, indicating that these were co-terminal. The most abundant species were those corresponding to ORFs 10 and 11 (p20 and p23, respectively), and the number of sgRNAs isolated did not change when the isolate was passed through different hosts (Hilf *et al.*, 1995).

The production of the sgRNA of CTV is regulated both temporally and quantitatively. In studies of the kinetics of accumulation of the CTV-RNAs, it was found that most of the abundant sgRNAs accumulated in parallel to the gRNA, and that the sgRNAs that allow the expression of the 3' genes accumulated to higher levels than those

from the 5' end. The relative order of accumulation of the sgRNAs extracted from CTV-infected tissue was p20>p23>p13>p25>p27>p33>p65>p61>p18, and this pattern of accumulation was maintained either if the RNAs were extracted from CTV-infected citrus tissue or CTV-inoculated *N. bethamiana* protoplasts (Navas-Castillo *et al.*, 1997).

Recently, a new set of sgRNAs which are 5'-co-terminal and positive-stranded has been described to occur in CTV-infected tissue. CTV apparently produces ten or eleven 5'-terminal sgRNAs, one for each sgRNA controller element plus the highly abundant ~800 nt 5'-terminal sgRNA. 5'-terminal sgRNA production was correlated with the ability of the controller element to produce 3'-terminal sgRNAs. It seems that each controller element terminates positive-stranded RNA synthesis from the 5' end as it induces synthesis of the 3'-terminal sgRNA (Gowda *et al.*, 2001). It is not clear whether these 5'-terminal sgRNAs are functional or not.

### **Population Structure and Genetic Diversity of CTV**

CTV field isolates may contain multiple genomic variants, some of which can be separated upon aphid (Tsai *et al.*, 2000) or graft transmission to different host species (Moreno *et al.*, 1993). Uneven distribution of the genomic RNA variants within the infected plant and acquisition of only certain variants by individual aphids may contribute to the population changes during the transmission process (d'Urso *et al.*, 2000). Single-strand conformation polymorphisms (SSCP) and cDNA hybridization analyses have been used to compare genomic populations of CTV isolates (Albiach-Marti *et al.*, 2000a; Ayllon *et al.*, 1999b; d'Urso *et al.*, 2000; Kong *et al.*, 2000). When the population diversity of the California CTV isolates was studied by SSCP, it was found that most of the isolates were composed of a population of genetically related variants (haplotypes),

with one being predominant (usually accounting for 80-90%), and a few haplotypes in very low frequency. In this study, the diversity between different isolates was greater than within isolates (Kong *et al.*, 2000). Ayllon *et al.*(1999b) studied the haplotype distribution of the p20 and p18 genes from CTV after host change and aphid transmission using Spanish and Japanese isolates. They reported that changes in haplotype populations were more drastic for p20 than for p18, and that the variation within the population was more significant than the variation between populations. This suggests that adaptation to a new host (or other environmental conditions) could be as important as the geographical origin at the moment of analyzing population diversities. Albiach-Marti *et al.* (2000a), using hybridization with a panel of cDNA probes to different genomic sequences, also detected changes in the CTV genomic and D-RNA population after aphid transmission.

All these findings provide evidence that changes in the viral population occur during the transmission process, but they do not explain the mechanisms responsible for these changes. Variations observed in SSCP profiles after aphid transmission of CTV isolates would indicate titer increase of certain sequence variants in the aphid transmitted isolate and/or drastic reduction or disappearance of other variants present in the viral population. At least two factors could contribute to the altering of the genomic RNA population in the transmission process: (I) uneven distribution of the genomic RNA variants in different plant parts may result in the aphids acquiring a different viral population, depending on the probing site; and (II) individual aphids might sort some of the variants, even if these are not predominant, and transmit a sub-population different from that of the source isolate (d'Urso *et al.*, 2000). In either case, a minor variant of a

population could become predominant and give rise to a new and different population. Because symptoms caused by CTV are probably dependent on the composition of its viral population, aphid transmission may act as a bottleneck, sorting some genomic RNA variants and giving rise to a different population that may also alter symptom expression (d'Urso *et al.*, 2000). These types of variation have been already reported for CTV. Moreno *et al.* (1993) showed that sub-isolates obtained from mild CTV isolates by various host passages were more severe and express stem pitting. A similar result was reported by Broadbent *et al* (1996), who showed that single aphid transmissions of Australian CTV isolates with the vector *Toxoptera citricida* separated some of the subisolates based on biological indexing on three citrus indicators and the numbers of inclusion bodies produced. Tsai *et al.*(2000) demonstrated the recovery of orange stem pitting strains of CTV after doing single aphid transmissions with *Toxoptera citricida* from a source plant infected with the Florida T66 decline isolate. This sorting of RNA variants of CTV by the aphid could explain the appearance of virulent CTV isolates in areas where they had not been observed before.

Different approaches have been taken to develop molecular techniques for the rapid differentiation of CTV isolates and identification of molecular markers related to the different strains of CTV. Variation in serological reactivity, peptide maps of the CP, dsRNA patterns, hybridizations with cDNA probes, restriction fragment length polymorphism, and SSCP have been described utilized to differentiate CTV isolates and strains (Lee *et al.*, 1988; Moreno and Guerri, 1997; Niblett *et al.*, 2000).

Nucleotide sequence analysis is an accurate procedure for CTV strain differentiation and estimation of molecular genetic variation (Rubio *et al.*, 2001). To

date, the complete sequences of six CTV isolates have been reported: T30 (19,259 nt) and T36 (19,296 nt) from Florida (Albiach-Marti *et al.*, 2000b; Karasev *et al.*, 1995; Pappu *et al.*, 1994), VT (19,226 nt) from Israel (Mawassi *et al.*, 1996), SY568 (19,249 nt) from California (Yang *et al.*, 1999), T385 (19,259 nt) from Spain (Vives *et al.*, 1999) and Nuaga (19,302 nt) from Japan (Suastika *et al.*, 2001). Analysis of these sequences reveals that the genomic organization is similar in all the CTV isolates sequenced so far, although the genomic sequences differ markedly, with as little as 50 to 80% nucleotide identity in much of the genome (Mawassi *et al.*, 1996; Vives *et al.*, 1999). The identity between some sequences is nearly uniform throughout the genome for some isolates (T385 and VT for example), but for other isolates, the sequences are asymmetrical and progressively decrease toward the 5' end, with as little as 42% within the 5'NTR (Lopez *et al.*, 1998). The highest identity between all isolates occurs at the 3' untranslated region (UTR), where the identity is higher than 97% for all isolates (Vives *et al.*, 1999).

Analysis of the polymorphism of the 5'UTRs allowed the classification of CTV sequences into three discrete groups, with intragroup sequence identity higher than 88% and intergroup sequence identity as low as 44%. T36 was the type isolate for group I, VT for group II and various Spanish isolates belong to group III (Lopez *et al.*, 1998). SY568 and T385 belong to group II and III, respectively.

It is not known whether the symptoms induced by CTV isolates in citrus are induced by a predominant genomic sequence, the viral population, a combination of genomic RNA and D-RNA, or other factors (Albiach-Marti *et al.*, 2000b). Two mild isolate sequences, from isolates that do not produce noticeable symptoms in the field (T30 from Florida and T385 from Spain), were compared to determine whether different

isolates inducing similar phenotypes might also have similar sequences (Albiach-Marti *et al.*, 2000b). The RNA genome of both isolates was the same size (19,259 nt), and the nucleotide identity between different ORFs ranged from 98.7 to 100% (Albiach-Marti *et al.*, 2000b; Vives *et al.*, 1999). Because these two isolates were separated in time and geography, this sequence similarity was unexpected. Comparison of additional mild CTV sequences with the T30 isolate showed remarkable sequence similarity, with variability less than 1% (Albiach-Marti *et al.*, 2000b).

Comparison of the sequences of the mild Spanish isolate, T385, and the stem pitting isolate, SY568, from California showed nucleotide identities close to 90% in the 5' and 3' terminal regions of the genome, whereas the central region had over 99% identity. This suggests that the central region of the SY568 genome resulted from RNA recombination between two CTV genomes, one of which was almost identical to the master sequence of a mild isolate (Vives *et al.*, 1999).

Overall, CTV is among the most diverse and complex plant RNA virus. The numerous species of RNA species present in infected tissue, the multiple genomic variants found in field samples, and the unknown function of most of its genes leave open many questions about the virus biology and the infection process.

The main objective of this research was to characterize the HSP70 protein homolog (HSP70h) of CTV, and to study the localization and function of this protein during the process of viral infection. The possibility of generating pathogen-derived resistance, using as transgene the full length HSP70h from CTV or mutated forms of this gene, also was explored. The specific objectives were the following:

1. To develop an antibody for the CTV-HSP70h protein specific enough in its reactivity to enable studies on the function of this viral protein

2. To study the *in vivo* localization and expression of the HSP70h from CTV in infected citrus tissue, as well as the association of this protein with the virion.
3. To study the possible presence of HSP70h in the characteristic inclusion bodies present in CTV-infected tissue.
4. To produce transgenic Duncan grapefruit plants by using *Agrobacterium tumefaciens*-mediated transformation and different constructs of the HSP70h gene from CTV.

CHAPTER 2  
PRODUCTION OF A POLYCLONAL ANTISERUM AGAINST THE CARBOXY-  
TERMINAL END OF THE CTV HEAT SHOCK PROTEIN HOMOLOG (HSP70h)

**Introduction**

Citrus tristeza virus (CTV), a member of the family *Closteroviridae*, causes one of the most economically important diseases of citrus. The CTV symptoms are diverse depending on various scion and/or rootstock combinations (Bar-Joseph and Lee, 1989). The virus has a monopartite, single-stranded, positive-sense RNA genome of about 20 kb encapsidated by two proteins. The CTV genome is organized into 12 open reading frames (ORFs), potentially encoding for at least 19 polypeptides that are expressed through at least three mechanisms: proteolytic processing, translational frameshifting, and production of subgenomic RNAs (Hilf *et al.*, 1995; Karasev *et al.*, 1995).

The *Closteroviridae* is the only viral family encoding for a homolog of the 70-kDa heat shock protein (HSP70) family of cellular chaperones (Agranovsky *et al.*, 1991). The HSP70s are members of a set of proteins which undergo increased synthesis in response to a variety of physical and chemical stresses; and they play diverse roles in successful folding, assembly, intracellular localization, secretion, regulation, and degradation of other proteins (Lindquist and Craig, 1988). These chaperones were originally identified as inducible proteins, but some HSP70s are constitutively expressed and appear to be essential for physiological cell growth (Hartl, 1996; Lindquist and Craig, 1988). They are highly conserved in all domains of life: Archae, eubacteria and

eukaryotes. Eukaryotic genomes encode multiple HSP70 versions that are localized to the various cell compartments (cytosol, endoplasmic reticulum, mitochondria, and chloroplasts) (Karlin and Brocchieri, 1998).

It is thought that the viral HSP70 homolog (HSP70h) was probably acquired by a common ancestor of the closteroviruses by recombination with a host mRNA coding for HSP70 (Dolja *et al.*, 1994). Computer-assisted sequence analysis revealed that the structural elements identified in the N-terminal ATPase domain of cellular HSP70s are conserved in closteroviral homologs, while the more variable C-terminal domain showed limited homology between cellular and closteroviral HSP70s proteins (Agranovsky *et al.*, 1991). Recently, the HSP70h of beet yellows closterovirus (BYV) was shown to be involved in intercellular translocation, representing a new type of plant viral-movement protein (Peremyslov *et al.*, 1999). Additionally, the HSP70h from CTV was shown to be necessary for efficient virion assembly (Satyanarayana *et al.*, 2000).

Information on the possible function of the viral genes from CTV has been inferred by comparative computer assisted and genetic analysis. An alternative way for the functional characterization of a virus protein is to study its intracellular localization in infected tissue. A basic requirement for immunolocalization of a protein is to have an antibody reacting specifically with the target gene product. The objective of this research was to develop an antibody for the CTV-HSP70h protein specific enough in its reactivity to enable further study of the functions of this viral protein in the process of CTV infection.

## Material and Methods

**CTV isolate T3800.** The Florida CTV isolate T3800 was used as a virus source for cloning and expression of the recombinant HSP70h protein. The T3800 source was grapefruit (*Citrus paradisi*; Macf.) plants in greenhouses of the Department of Plant Industry (DPI) and the Plant Pathology Department at University of Florida, both located in Gainesville, FL. CTV isolate T3800 was originated from a lemon tree in a home dooryard in Delray Beach, FL. It causes severe stem pitting in grapefruit, no stem pitting in sweet orange, and causes seedling yellows in sour orange and grapefruit (Manjunath *et al.*, 2000a).

**Reverse transcription and PCR.** The p65 gene from the Florida stem pitting CTV isolate T3800 was reverse transcribed from double-stranded RNA (dsRNA). The dsRNA was purified from infected bark tissue by using non-ionic cellulose (CF-11, Whatman) column chromatography in the presence of 16% ethanol, according to the procedure described by Moreno *et al.*(1990). For the annealing of the primer to the template, 10  $\mu$ l of dsRNA (representing approximately 0.2 g of fresh tissue) and 1  $\mu$ l of primer CN302 (0.1  $\mu$ g/ $\mu$ l) (Table 2-1) were incubated at 70° C for 10 min, then transferred to an ice bucket for a minimum of 5 min. Then, a mixture containing 4  $\mu$ l of 5X first-strand buffer (250 mM Tris-HCl, pH 8.3 at 25°C, 375 mM KCl, 15 mM MgCl<sub>2</sub>), 0.5 mM each dATP, dGTP, dCTP, and dTTP, 10 mM DTT, 1  $\mu$ l RNAsin (20-40 U/ $\mu$ l) (Promega Corp.), and 1  $\mu$ l Superscript II RT (Gibco-Life Technologies) was added to each reaction to give a final volume of 20  $\mu$ l. After one hour incubation at 42°C, the reaction was held at 70°C for 15 minutes, then transferred to ice or stored at -20°C for later use. This cDNA was used as template for the amplification of the full length HSP70h or its carboxy-terminal end.

The PCR reaction was performed in a final volume of 50  $\mu$ l. The mixture contained 5  $\mu$ l of 10X PCR buffer (500mM KCl, 100mM Tris-HCl(pH 9.0 at 25°C) and 1.0% Triton X-100®), 2.5 mM MgCl<sub>2</sub>, 0.4 mM each dNTP (dATP, dGTP, dCTP, and dTTP), 0.1  $\mu$ g each primer (CN 200 and CN 201) (Table 2-1), 2.5 U of Taq DNA polymerase (Promega, Corp), and 2  $\mu$ l of the cDNA template. Thermocycling conditions were 2 min at 94°C, 40 cycles of 45 sec at 94°C, 60 sec at 50°C and 90 sec at 72°C, followed by a final extension of 5 min at 72°C. RT-PCR products (size of approximately 1785 bp) were separated by electrophoresis in agarose gels and photographed using a Fluor-S MAX MultiImager System (Bio-Rad). The RT-PCR amplified fragment was cloned into a pGEM-T vector (Promega) (pGEM-T/HSP70h) and subsequently sequenced at the DNA Sequencing Core Lab, at University of Florida using universal (forward and reverse) M13 primers.

For the amplification of the carboxy-terminal end of the p65 gene from the CTV isolate T3800, either the cDNA template previously described, or a clone of the pGEM-/HSP70h was used as template (0.1  $\mu$ g/  $\mu$ l). The PCR reaction was performed in a final volume of 50  $\mu$ l. The mixture contained 5  $\mu$ l of 10X PCR buffer (500mM KCl, 100mM Tris-HCl(pH 9.0 at 25°C) and 1.0% Triton X-100®), 2.5 mM MgCl<sub>2</sub>, 0.4 mM each dNTP (dATP, dGTP, dCTP, and dTTP), 0.1  $\mu$ g each primer (CN 351 and CN 352) (Table 2-1), 2.5 U of Taq DNA polymerase (Promega, Corp), and 2  $\mu$ l of the cDNA or 1  $\mu$ l of the HSP70h clone as template. Thermocycling conditions were 2 min at 94°C, 40 cycles of 30 sec at 94°C, 30 sec at 50°C and 45 sec at 72°C, followed by a final extension of 5 min at 72°C each. RT-PCR products (442 bp, nucleotides 13382 to 13824 in T36 isolate)

were separated by electrophoresis in agarose gels and photographed using a Fluor-S MAX MultiImager System (Bio-Rad).

Table 2-1: Sequence of the primers used for the RT-PCR and cloning of the HSP70h from CTV

Primer	Sequence	Characteristics
CN302	5'-AGNCGTCANTTCATGGGACGTCA-3'	Sense, alignment near nucleotide 14984 in CTV-T36 isolate. N for degeneracy.
CN351	5'-GAATCCCATATGGCGGCTTCGGTGTCTGTTGTT-3'	Sense, EcoR I and Nde I sites. Alignment at nucleotides 13380 to 13400 in the p65 gene of the CTV-T36 isolate.
CN352	5'-CTCGAGTATTCTTTCCAAATCACTTCCCCG-3'	Antisense, Xho I site, non stop codon. Alignment at nucleotides 13800 to 13824 in p65 gene of the CTV-T36 isolate
CN200	5'-ACATATGGTGCTTTTGGGTTTAG-3'	T36-HSP70h forward, sense primer with NdeI site
CN 201	5'-AGATCTTCAGAGAGGTATTCTTTC C-3'	T36-HSP70h reverse, anti sense with Bgl II site.
CN 468	5'-CATGCCATGGTGCTTTTGGGTTTAGAC -3'	p65 sense, from startcodon, NcoI site at 5'end..

**Cloning in pET-22b(+) and protein expression.** The RT-PCR amplified carboxy-terminal end fragment was cloned into the pGEM-T vector (Promega) and then, subcloned into pET-22b(+) expression vector (Novagen) using the EcoRI and XhoI sites that were incorporated into the primers CN351 and CN352. This cloning produced a fusion of the fragment with a C-terminal His-tag sequence. This new construct was used to transform *Escherichia coli* strain BL21. Induction of the recombinant protein was performed following the pET System Manual instructions (Novagen). Briefly, 500 ml of Luria broth media (LB) (10g Bacto-tryptone, 5g yeast extract, 10g NaCl, adjust pH to 7.5

with NaOH, adjust volume to 1L) were inoculated with an overnight culture of the pET recombinant in BL21. The media was incubated at 37°C with shaking at 220 rpm to an optical density at 600 nm ( $OD_{600}$ ) of approximately 0.5-1.0. After reaching this OD, the protein was induced by adding isopropyl-beta-D-thiogalactopyranoside (IPTG) to a final concentration of 1mM. The culture was then allowed to grow for three hours under the same conditions. The expression of the target protein was assessed by analysis of total cell protein on a SDS-polyacrylamide gel followed by a Coomassie blue or silver staining, according to standard procedures (Sambrook, 1989). A total cell protein sample was also analyzed as described in the pET system Manual (Novagen), to study the localization of the induced protein either in the media, periplasm, soluble cytoplasm or insoluble cytoplasm fraction. The localization of the induced protein defines the purification procedure to follow after the induction.

**Protein purification under denaturing conditions.** The induced culture was harvested by centrifugation at 6,500 x g for 15 min at 4°C. The pellet was then resuspended in 0.1 culture volume of 1X Inclusion Bodies Wash Buffer (IBWB) (20 mM Tris-HCl pH 7.5, 10 mM EDTA, 1% Triton X-100), and lysozyme was added to a final concentration of 100 µg/ml from a freshly prepared stock (10 mg/ml). Additionally, for each gram bacteria harvested, 8 µl of 50 mM phenylmethylsulfonylfluoride (PMSF) was added to the cell suspension. After incubation at 30°C for 15 min, the cells were sonicated on ice (Misonix Inc., Model XL-2000 Microson Ultrasonic) with the power level set between 4-5, at 40%-50% duty, until the cell solution was no longer viscous (15-20 burst). The solution was always kept at 4°C. The pellet was collected by centrifugation at 10,000 x g for 10 min, and washed two times with 0.1 culture volume of

1X IBWB. The insoluble proteins present in the bacterial inclusion bodies were then collected by centrifugation at 10,000 x g for 10 min, and stored overnight at  $-20^{\circ}\text{C}$ .

After thawing the pellet, the insoluble proteins were resuspended in 5 -10 ml of Buffer A (6M guanidium chloride, 0.1 M  $\text{NaH}_2\text{PO}_4$ , 0.01 M Tris-HCl pH 8.0). The lysate was stirred for approximately 1 hour at room temperature, until the solution became translucent. The lysate was then centrifugated at 10,000 x g for 30 min at room temperature to pellet cellular debris. The supernatant was mixed with 50% Ni-NTA resin (Qiagen) at a ratio of 1 ml of resin for each 4 ml of lysate, and shaken for 30 min at room temperature. The lysate-resin mixture was loaded into an empty column with the bottom cap still attached. After removing the bottom cap, the flow-through was collected and saved for later protein analysis. The column was then washed two times with 4 ml of buffer C (8M urea, 0.1 M  $\text{NaH}_2\text{PO}_4$ , 0.01 M Tris-HCl, pH 6.3). The recombinant protein was eluted with 2 ml of buffer D (8M urea, 0.1 M  $\text{NaH}_2\text{PO}_4$ , 0.01 M Tris-HCl, pH 5.9), followed by 2 ml of buffer E (8M urea, 0.1 M  $\text{NaH}_2\text{PO}_4$ , 0.01 M Tris-HCl, pH 4.5). An aliquot of each fraction was analyzed by standard SDS-polyacrylamide gel electrophoresis, followed by a Coomassie blue or silver staining.

Fractions containing the target protein were dialyzed in a multi-step way, against a buffer (0.1 M  $\text{NaH}_2\text{PO}_4$ , 0.01 M Tris-HCl, pH 6.3) that contained decreasing concentrations of urea (6M, 3M, and no urea) in a 24 hour period. Before storage of the induced protein, 10  $\mu\text{l}$  of a broad-spectrum proteinase inhibitor (Sigma) was added to the preparation to inhibit further degradation of the protein.

**Production of the polyclonal antiserum.** The services of Cocalico Biologicals, Inc. (Reamstown, PA) were used for the production of the polyclonal antiserum. Chicken was the host species selected for the project, and two young laying hens were injected with the same immunogen at the same time. The immunogen was supplied as a purified protein stored at  $-20\text{ }^{\circ}\text{C}$ , whose concentration was  $100\text{ }\mu\text{g/ml}$ . The standard Cocalico protocol for immunization was used for the company to raise the polyclonal antiserum in chicken. Briefly it is:

Day 0: Prebleed and collection of pre-egg / initial inoculation.

Day 21: Boost / egg collection.

Day 31: Test bleed.

Day 42: Boost (same as day 21).

Day 52: Test bleed.

Day 63: Boost (same as day 21).

Day 73: Test bleed.

After day 73, a monthly boost followed by a test bleed 10 days later was performed for the following six months. The eggs were collected daily, and evaluated as pools from around the same time of the test bleeds.  $100\text{ }\mu\text{g}$  of antigen were injected into the breast muscle at each time. The first injection was in complete Freund's adjuvant and the remaining in a 1:1 dilution of complete and incomplete Freund's Adjuvants.

Sera collected during test bleeds were evaluated by Western blot analysis according to standard procedures (Sambrook, 1989) using as controls the total cell extract from induced and non-induced *E.coli* strain BL21, as well as bacteria BL21 that did not carry the expression plasmid pET22b(+).

**Extraction and purification of IgY from egg yolks.** Isolation of polyclonal chicken immunoglobulins from pooled eggs was performed using a simple two step procedure (Camenisch *et al.*, 1999). The egg yolks were separated from the egg white, washed with deionized water, and placed in a funnel. The skins of the egg yolk were removed with a forceps, and the yolks collected in a 50 ml screw cap tube. The yolk volume was brought to 25 ml with sodium phosphate buffer (100 mM, pH 7.6), and mixed vigorously. Subsequently, 20 ml of chloroform was added, and the mixture was shaken until a semisolid phase was obtained. After centrifugation at 1,200 x g for 30 min, the supernatant was decanted into a centrifugation tube, and solid polyethylene glycol 6000 was added to a final concentration of 12% (w/v). After centrifugation at 15,700 x g for 10 min, the pellet was suspended and stored at -80°C.

**Cloning and expression of the full length CTV-HSP70h:** The HSP70h gene from CTV was amplified by PCR using as the template the clone pGEM- T/HSP70h from the CTV isolate T3800 previously described, and the primers CN352 and CN468 (Table 2-1). A proofreading polymerase (Vent® polymerase, New England Biolabs) was used for the reaction to generate a blunt-end product following the manufacturer's recommendations. The thermocycling conditions were similar to those previously described for the amplification of the full p65 gene.

The blunt-end PCR product was then cloned in the pCR-BluntII TOPO vector (Invitrogen), and subsequently subcloned in the expression vector pET27b(+) (Novagen), using the NcoI and XhoI restriction sites that were incorporated in the primers. This cloning produced a CTV-HSP70h with a C-terminal HSV·Tag and His·Tag sequences. The HSV·Tag fusion allows the use of a HSV·Tag monoclonal antibody to follow the

expression of the target protein. The induction of the CTV-HSP70h was performed as previously described.

## Results

### Sequence Analysis

The sequence of the HSP70h from the Florida stem pitting CTV isolate T3800 was obtained by sequencing multiple clones of the RT-PCR fragment cloned in the pGEMT vector. The gene was 1785 nt in length (Figure 2-1), and its deduced amino acid sequence contains 594 residues (Figure 2-2), which agreed with the HSP70h previously characterized from CTV (Karasev *et al.*, 1995; Mawassi *et al.*, 1996; Suastika *et al.*, 2001; Vives *et al.*, 1999; Yang *et al.*, 1999b). Analysis of the HSP70h sequences contained in the Genebank indicated some variation occurs in the nucleotide sequences for this gene among the various CTV isolates. The nucleotide sequence identity for the CTV HSP70h ranged from 87 to 99% (Table 2-2), with a conservation of sequence uniformly all along the gene, with randomly scattered variability in the sequence.

At the amino acid level, the identities among the HSP70h from CTV ranged from 90 to 99% (Table 2-3). For the isolate T-3800, the percentage of amino acid identity was 92% with the VT-CTV isolate, and 95% with all the others sequences analyzed. The seedling yellows isolate from Israel (VT) showed the lowest percentage of sequence similarity when compared to the other CTV-HSP70h sequences available in the Genebank database (Table 2-4). The amino acid sequences of the translated p65 gene from CTV (Figure 2-2) were used to construct a cluster dendogram. The clustering of the isolates in this dendogram does not necessarily reflect their biological activities (Figure 2-3, Table 2-4). For example, the two mild isolates included in the analysis (T30 and

T385) do not cluster together and neither do the stem pitting isolates (T3800 and SY385). Only the seedling yellows isolates (VT and Nuaga) shared the same cluster, showing some association between amino acid sequence of the CTV-HSP70h and their biological activity.

Computer assisted analyses have shown that the motifs identified in the ATPase domain of the cellular HSP70s are conserved in the closteroviral HSP70h proteins (Agranovsky *et al.*, 1991) (Figure 2-4 A). If a CD-Search (Conserved Domain Database and Search Service, v1.53) is conducted with the protein sequence of the HSP70h from CTV, two conserved domains are retrieved by the system. These domains are both located at the amino-terminal end of the CTV- HSP70h. One of them is an ATPase domain contained at the N-terminal end of the cellular chaperones (HSP70) that expands 377 aa from the viral chaperone homolog, and the other is a segment of about 167 aa from the FtsA family of prokaryotic cell cycle proteins, which are predicted to contain an ATPase activity (Figure 2-4 B). The C-terminal domain from the CTV-encoded homolog shows limited homology, not only between the closteroviral HSP70h proteins, but also between the closteroviral HSP70h and cellular chaperones. When the PROSITE database of protein families and domains was searched using a chaperone homolog from CTV, two signature sequences of the HSP70h protein family were retrieved. One corresponded to the sequence expanded between amino acid 201 and 214 from the viral homolog (VYDFGGGTFDVSIV), and the other to the sequence included between amino acids 325 and 339 (LVVVGGSSYLPGLLD) from the viral protein. In both cases there is 100% identity between the signature sequence and the amino acid sequence of the CTV-HSP70h (Figure 2-2). Considering these computer assisted analyses, the C-terminal end

of the HSP70h of CTV was chosen to raise a polyclonal antibody because of its lesser homology with cellular chaperones. In this way, it was hoped to avoid cross reactivity with host proteins. The sequence corresponding to the carboxy-terminal end of the HSP70h gene from the Florida stem pitting isolate T3800 (nucleotides 13382 to 13824 in the T36 isolate) was cloned in the pET22b(+) expression vector, producing a fusion protein with a C-terminal histidine-tag sequence

### **Expression and Purification of the Carboxy-Terminal End of the CTV-HSP70h**

The DNA fragment amplified using the primers CN351 and CN352 (Table 2-1) was cloned into the pET22b(+) vector. This fragment of 444 bp corresponds to the sequences spanned by the nucleotides 1333 and 1776 in Figure 2-1. The expression of the cloned fragment produced a protein of 149 amino acids, which corresponds to the amino acids located between positions 445 and 592 at the carboxy-terminal end of the HSP70h protein of the CTV isolate T3800 (Figure 2-2), with a histidine-tag fusion protein (His-tag/HSP70h).

The recombinant protein was expressed in BL21 cells at high levels after induction with 1mM IPTG, and showed the expected size on SDS-polyacrylamide gels (Figure 2-5 a). Using the program “Compute pI / Mw” at the ExPASy server, a theoretical molecular weight of 16,681 Daltons was computed for the target protein. This molecular weight does not consider the extra histidine tag from the carboxy-terminal fusion or the effects of any possible post-translational modifications of the target protein.

The high levels of expression resulted in the formation of insoluble aggregates of proteins (inclusion bodies) where the target protein was localized (Figure 2-5A). Under

Table 2-2. Nucleotide identity<sup>1</sup> among the CTV-HSP70h genes of different isolates of citrus tristeza virus.

	<b>T-3800</b>	<b>T-36</b>	<b>SY-568</b>	<b>T-30</b>	<b>T-385</b>	<b>VT</b>	<b>Nuaga</b>
<b>T-3800</b>	100%	90%	90%	90%	90%	89%	90%
<b>T-36</b>		100%	93%	93%	93%	88%	88%
<b>Sy-568</b>			100%	99%	99%	87%	88%
<b>T-30</b>				100%	99%	87%	88%
<b>T-385</b>					100%	87%	88%
<b>VT</b>						100%	96%
<b>SY-Nuaga</b>							100%

<sup>1</sup> Identity is defined as the extent to which two nucleotide sequences are invariant. This table shows the percentage of identical nucleotides from the total nucleotide sequence (1785 nt).

Table 2-3. Amino acid identity<sup>1</sup> among the CTV-HSP70h proteins expressed by different isolates of citrus tristeza virus

	<b>T-3800</b>	<b>T-36</b>	<b>SY-568</b>	<b>T-30</b>	<b>T-385</b>	<b>VT</b>	<b>Nuaga</b>
<b>T-3800</b>	100%	95%	95%	95%	95%	92%	95%
<b>T-36</b>		100%	95%	95%	95%	90%	93%
<b>Sy-568</b>			100%	99%	99%	91%	94%
<b>T-30</b>				100%	98%	90%	93%
<b>T-385</b>					100%	90%	93%
<b>VT</b>						100%	94%
<b>Nuaga</b>							100%

<sup>1</sup> Identity is defined as the extent to which two amino acid sequences are invariant. The percentage of identity from the total amino acid sequence (594 aa) are shown.

CTV-T3800 Length: 1785 nucleotides

```

1  atgggtgcttt tgggtttaga cttcgggtacc acgttttcaa cagtggctat
51  ggccacgtct tctgagttag ttatactgaa acaatctaat tcgtcgtaca
101 tacctacgtg tttatctctg catgcggatc ctaatagtgt gtcttatggg
151 tacgacgcag aatatttagc ggcttcgggg gaaccagggt cattttacaa
201 agatttgaaa cgggtgggtcg gttgtaccga gaagaactac caaacctact
251 tacacaagtt atcaccttct tataagggtga tagtgaaaga gtttggaact
301 aaaagtgtgc ctgttccgta tttgtcacct ttgaataacg atctcggact
351 cagcatcgct ttacctttac tgatcgcttc atacgctaag tccattttat
401 cggatgcgga acgagtgttt aatgtaagtt gtactggagt tatatgttcg
451 gtacctgctg gttataacac attacagcga gcttttacgc aacagagtat
501 atcgttgctg ggttactctt gcgtgtacat tattaatgaa ccttcagccg
551 ccgcgtactc cactttacct aagttgagtt cggcggataa gtacttagcc
601 gtttacgact tcggtgggtg gacttttgac gtttctatag tgagtgttag
651 gttaccacg ttcgccgta gaagttcagg tggatgatg gacttaggag
701 gtagagacat cgataaaaag ttatcagata aaatatatga gatggccgat
751 tttgtaccgc aaaaagaact gaacgtttct agtttaaagg aagctttatc
801 tcttcaaacc gatccagtca agtacaccgt aactcattac ggaatgagtg
851 aaaccgtatc aatcgatcaa acgacgttaa gggagatagc ttcgacgttc
901 ataactcgaa cgatagacat acttacgcaa gttaagggtta agtctagtat
951 gcctgaatcg caaagtttaa agctgggtgg agtcgggtgga agctcgtact
1001 taccagggct gttggatact ttggcgaccg tgccttttgt gtctgggata
1051 gtaccagtag aagacgcgag aaccgctggt gctagagggt gcgctttata
1101 tagcgagtgt ttggatggta gatccaaggc tctactaata gattgtatca
1151 cgcacatctt gtcagttacg acatttagcg cggattcggg tggtgttgca

```

Figure 2-1. Nucleotide sequence for the HSP70h gene from the grapefruit stem pitting CTV isolate T3800.

1201 gcggccggta gtccaattcc ttttgaagga gaacgaaaac tcacgttgtg  
 1251 caagtgcggt agtacgtcta aatatcaagc aaggatgttc gaaggagatt  
 1301 acgaaaaggt ttttcgaaat gaacgtatat acgctgcttc ggtgtcgttg  
 1351 ttcactttgg gagttaactg gcacgtgcct aacgacgttg agatgactct  
 1401 cgtaactaag gtggactcaa tgggcaaagt ggagttttac cttaaaggtc  
 1451 catctggtga attggtgaac gtgcaaggta cttcgcatta tgattatgct  
 1501 ggtatgcctc accccactag aaagttggtg aggcttagcg attacaaatgt  
 1551 aagctccgcc gctttagttt tagctttgac attaactcgc gaaaaacgag  
 1601 aaaggtttct tttgcggaca ttatttgaca ctttaacagc agacttgcca  
 1651 aagacagcaa gtttaagtga gtactcaaag aagtaccgca tcaactcga  
 1701 cgacatcgat gtcgtctcat cacgtatggg gatcgttggt tcgaaagttt  
 1751 tacggggaag tgatttgga agaatacctc tctga

Figure 2-1 continued.

Table 2-4. Biological properties and origin of the citrus tristeza virus (CTV) isolates included in the alignment of the amino acid sequences of their HSP70h proteins.

CTV isolate	Origin	Symptoms induced
SY568	California	Severe, stem pitting on grapefruit and sweet orange
T385	Spain	Mild
T30	Florida	Mild
T36	Florida	Severe, decline on sour orange
T3800	Florida	Severe, stem pitting on grapefruit
Nuaga	Japan	Seedling yellows
VT	Israel	Seeding Yellows

		*	20	*	
CTV-SY568	:	MVLLGLDFGTTTFSTVAMAT	S	SELVILKQSNS	: 31
CTV-T385	:	MVLLGLDFGTTTFSTVAMAT	S	SELVILKQSNS	: 31
CTV-T30	:	MVLLGLDFGTTTFSTVAMAT	S	SELVILKQSNS	: 31
CTV-T36	:	MVLLGLDFGTTTFSTVAMAT	P	SELVILKQSNS	: 31
CTV-T3800	:	MVLLGLDFGTTTFSTVAMAT	S	SELVILKQSNS	: 31
CTV-Nuaga	:	MVLLGLDFGTTTFSTVAMAT	S	SELVILKQSNS	: 31
CTV-VT	:	MVLLGLDFGTTTFSTVAMAT	S	SELVILKQSNS	: 31

		40	*	60	
CTV-SY568	:	SYIPTCLFLHADPNSVSYGYDAEYLAASGEP			: 62
CTV-T385	:	SYIPTCLFLHADPNSVSYGYDAEYLAASGEP			: 62
CTV-T30	:	SYIPTCLFLHADPNSVSYGYDAEYLAASGEP			: 62
CTV-T36	:	SYIPTCLLLHAE	PNSVSYGYDAEYLAASGES		: 62
CTV-T3800	:	SYIPTCLFLHADPNSVSYGYDAEYLAASGEP			: 62
CTV-Nuaga	:	SYIPTCLFLHADPNSVSYGYDAEYLAASGEP			: 62
CTV-VT	:	SYIPTCLFLHADPNSVSYGYDAEYLAASGEP			: 62

		*	80	*	
CTV-SY568	:	GSFYKDLKRWVGCTAKNYQTYLHKLSP	SYKV		: 93
CTV-T385	:	GSFYKDLKRWVGCTAKNYQTYLHKLSP	PKYKV		: 93
CTV-T30	:	GSFYKDLKRWVGCTAKNYQTYLHKLSP	SYKV		: 93
CTV-T36	:	GSFYKDLKRWVGCTAKNYQTYLHKLSP	SYKV		: 93
CTV-T3800	:	GSFYKDLKRWVGCTEKNYQTYLHKLSP	SYKV		: 93
CTV-Nuaga	:	GSFFKDLKRWVGCTEKNYQSYLHKLSP	SYKV		: 93
CTV-VT	:	GSFYKDLKRWVGCTEKNYQSYLHKLSP	SYKV		: 93

		100	*	120	
CTV-SY568	:	TVEEFGTKSVPVPYLSPLNNDLGLNVALPLL			: 124
CTV-T385	:	TVEKEFGTKSVPVPYLSPLNNDLGLNVALPLL			: 124
CTV-T30	:	TVEEFGTKSVPVPYLSPLNNNLGLNVALPLL			: 124
CTV-T36	:	IVKEFGTKSVPVPYLSPLNNDLGLSVALPSL			: 124
CTV-T3800	:	IVKEFGTKSVPVPYLSPLNNDLGLSIALPLL			: 124
CTV-Nuaga	:	IVKEFGIKSMPVPYLSPLNNDLGLSVALPSL			: 124
CTV-VT	:	IVKEFGIKSMPVPYLSPLNNDLGLSVALPSL			: 124

Figure 2-2. Alignment of the amino acid sequences of HSP70h protein from several CTV isolates. The alignment was generated by the CLUSTAL X (1.8) program. The sequences included were retrieved from the Genebank database, except for that of the CTV T3800 isolate, which was obtained by direct sequencing.

		*	140	*																														
CTV-SY568	:	I	A	S	Y	A	K	S	I	L	S	D	A	E	R	V	F	N	V	S	C	T	G	V	I	C	S	V	P	A	G	Y	:	155
CTV-T385	:	I	A	S	Y	A	K	S	I	L	S	D	A	E	R	V	F	N	V	S	C	T	G	V	I	C	S	V	P	A	G	Y	:	155
CTV-T30	:	I	A	S	Y	A	K	S	I	L	S	D	A	E	R	V	F	N	V	S	C	T	G	V	I	C	S	V	P	A	G	Y	:	155
CTV-T36	:	I	A	S	Y	A	K	S	I	L	S	D	A	E	R	V	F	N	V	S	C	T	G	V	I	C	S	V	P	A	G	Y	:	155
CTV-T3800	:	I	A	S	Y	A	K	S	I	L	S	D	A	E	R	V	F	N	V	S	C	T	G	V	I	C	S	V	P	A	G	Y	:	155
CTV-Nuaga	:	I	A	L	Y	T	K	S	I	L	S	D	A	E	R	V	F	N	V	S	C	T	G	V	I	C	S	V	P	A	G	Y	:	155
CTV-VT	:	I	A	L	Y	T	K	C	I	L	S	D	A	E	R	V	F	N	V	S	C	T	G	V	I	C	S	V	P	A	G	Y	:	155

		160	*	180																														
CTV-SY568	:	N	T	L	Q	R	A	F	T	Q	Q	S	I	S	M	S	G	Y	S	C	V	Y	I	I	N	E	P	S	A	A	A	Y	:	186
CTV-T385	:	N	T	L	Q	R	A	F	T	Q	Q	S	I	S	M	S	G	Y	S	C	V	Y	I	I	N	E	P	S	A	A	A	Y	:	186
CTV-T30	:	N	T	L	Q	R	A	F	T	Q	Q	S	I	S	M	S	G	Y	S	C	V	Y	I	I	N	E	P	S	A	A	A	Y	:	186
CTV-T36	:	N	T	L	Q	R	A	F	T	Q	Q	S	I	S	M	S	G	Y	S	C	V	Y	I	I	N	E	P	S	A	A	A	Y	:	186
CTV-T3800	:	N	T	L	Q	R	A	F	T	Q	Q	S	I	S	L	S	G	Y	S	C	V	Y	I	I	N	E	P	S	A	A	A	Y	:	186
CTV-Nuaga	:	N	T	L	Q	R	A	F	T	Q	Q	S	V	S	L	S	G	Y	T	C	V	Y	I	I	N	E	P	S	A	A	A	Y	:	186
CTV-VT	:	N	T	L	Q	R	A	F	T	Q	Q	S	V	S	L	S	G	I	P	C	V	Y	I	I	N	E	P	S	A	A	A	Y	:	186

		*	200	*																													
CTV-SY568	:	S	T	L	P	K	L	S	S	A	D	K	Y	L	A	V	Y	D	F	G	G	T	F	D	V	S	I	V	S	V	R	:	217
CTV-T385	:	S	T	L	P	K	L	S	S	A	D	K	Y	L	A	V	Y	D	F	G	G	T	F	D	V	S	I	V	S	V	R	:	217
CTV-T30	:	S	T	L	P	K	L	S	S	A	D	K	Y	L	A	V	Y	D	F	G	G	T	F	D	V	S	I	V	S	V	R	:	217
CTV-T36	:	S	T	L	P	K	L	N	S	A	D	K	Y	L	A	V	Y	D	F	G	G	T	F	D	V	S	I	V	S	V	R	:	217
CTV-T3800	:	S	T	L	P	K	L	S	S	A	D	K	Y	L	A	V	Y	D	F	G	G	T	F	D	V	S	I	V	S	V	R	:	217
CTV-Nuaga	:	S	T	L	P	K	L	S	S	A	D	K	Y	L	A	V	Y	D	F	G	G	T	F	D	V	S	I	V	S	V	R	:	217
CTV-VT	:	S	T	L	P	K	L	S	S	A	H	T	Y	L	A	V	Y	D	F	G	G	T	F	D	V	S	I	V	S	V	R	:	217

		220	*	240																													
CTV-SY568	:	L	P	T	F	A	V	R	S	S	G	G	D	M	N	L	G	G	R	I	D	K	K	L	S	D	K	I	Y	E	M	:	248
CTV-T385	:	L	P	T	F	A	V	R	S	S	G	G	D	M	N	L	G	G	R	I	D	K	K	L	S	D	K	I	Y	E	M	:	248
CTV-T30	:	L	P	T	F	A	V	R	S	S	G	G	D	M	N	L	G	G	R	I	D	K	K	L	S	D	K	I	Y	E	M	:	248
CTV-T36	:	L	P	T	F	A	V	R	S	S	G	G	D	M	N	L	G	G	R	I	D	K	K	L	S	D	K	I	Y	E	M	:	248
CTV-T3800	:	L	P	T	F	A	V	R	S	S	G	G	D	M	L	G	G	R	I	D	K	K	L	S	D	K	I	Y	E	M	:	248	
CTV-Nuaga	:	L	P	T	F	A	V	R	S	S	G	G	D	M	N	L	G	G	R	I	D	R	K	L	S	D	K	I	Y	E	L	:	248
CTV-VT	:	L	P	T	F	A	V	R	S	S	G	G	D	M	N	L	G	G	R	I	D	R	K	L	S	D	N	I	C	E	L	:	248

Figure 2-2 continued.

		*	260	28		
CTV-SY568	:	ADFIPQKELNVSSLKEALSLQTDVPKYTVTH			:	279
CTV-T385	:	ADFIPQKELNVSSLKEALSLQTDVPKYTVTH			:	279
CTV-T30	:	ADFIPQKELNVSSLKEALSLQTDVPKYTVTH			:	279
CTV-T36	:	ADFVPQKELNVSSLKEALSLQTDVPKYTVNH			:	279
CTV-T3800	:	ADFVPQKELNVSSLKEALSLQTDVPKYTVTH			:	279
CTV-Nuaga	:	ADFLPQKELNVSSLKEALSLQTDVPKYTVTH			:	279
CTV-VT	:	ADFLPQKELNVSSLKEALSLQTDVPKYTVTH			:	279

		0	*	300	*		
CTV-SY568	:	HGMSETISIDQ TALREIASVFINRTIDILTQ				:	310
CTV-T385	:	HGMSETISIDQ TALREIASVFINRTIDILTQ				:	310
CTV-T30	:	HGMSETISIDQ TALREIASVFINRTIDILTQ				:	310
CTV-T36	:	YGMSETV SIDQ TLREIASVFINRTIDILTQ				:	310
CTV-T3800	:	YGMSETV SIDQ TLREIASV FITRTIDILTQ				:	310
CTV-Nuaga	:	YGMSETV SIDQ TLREIASV FITRTIDILTQ				:	310
CTV-VT	:	FGMSETV SIDQ TLREIASV FITRTIDILTQ				:	310

		320	*	340		
CTV-SY568	:	VKVKS SMPESQSLKLVVVGSSYLPGLLDTL			:	341
CTV-T385	:	VKVKS SMPESQSLKLVVVGSSYLPGLLDTL			:	341
CTV-T30	:	VKVKS SMPESQSLKLVVVGSSYLPGLLDTL			:	341
CTV-T36	:	VKVKS SMPESQSLKLVVVGSSYLPGLLDAL			:	341
CTV-T3800	:	VKVKS SMPESQSLKLVVVGSSYLPGLLDTL			:	341
CTV-Nuaga	:	VKAKS SMPESQSLKLVVVGSSYLPGLLDTL			:	341
CTV-VT	:	VKAKS SMPESQSLKLVVVGSSYLPGLLDTL			:	341

		*	360	*		
CTV-SY568	:	ATVPFVSGIVPVEDARTAVARGCALYSECLD			:	372
CTV-T385	:	ATVPFVSGIVPVEDARTAVARGCALY ECLD			:	372
CTV-T30	:	ATVPFVSGIVPVEDARTAVARGCALYSECLD			:	372
CTV-T36	:	ATVPFVSGIVPVEDARTAVATG CALYSECLD			:	372
CTV-T3800	:	ATVPFVSGIVPVEDARTAVARGCALYSECLD			:	372
CTV-Nuaga	:	ETVPFVSGIVPVEDARTAVARGCALYSECLD			:	372
CTV-VT	:	ETVPFVSGIVPVEDARTAVARGCALYSECLD			:	372

Figure 2-2 continued

		*	260	*	28		
CTV-SY568	:	ADFIPQKELNVSSLKEALSLQTDVPKYTVTH				:	279
CTV-T385	:	ADFIPQKELNVSSLKEALSLQTDVPKYTVTH				:	279
CTV-T30	:	ADFIPQKELNVSSLKEALSLQTDVPKYTVTH				:	279
CTV-T36	:	ADFVPQKELNVSSLKEALSLQTDVPKYTVNH				:	279
CTV-T3800	:	ADFVPQKELNVSSLKEALSLQTDVPKYTVTH				:	279
CTV-Nuaga	:	ADFLPQKELNVSSLKEALSLQTDVPKYTVTH				:	279
CTV-VT	:	ADFLPQKELNVSSLKEALSLQTDVPKYTVTH				:	279

		0	*	300	*		
CTV-SY568	:	HGMSETISIDQ TALREIASVFINRTIDILTQ				:	310
CTV-T385	:	HGMSETISIDQ TALREIASVFINRTIDILTQ				:	310
CTV-T30	:	HGMSETISIDQ TALREIASVFINRTIDILTQ				:	310
CTV-T36	:	YGMSETV SIDQ TVLREIASVFINRTIDILTQ				:	310
CTV-T3800	:	YGMSETV SIDQ T LREIASV FITRTIDILTQ				:	310
CTV-Nuaga	:	YGMSETV SIDQ T LREIASV FITRTIDILTQ				:	310
CTV-VT	:	FGMSETV SIDQ T LREIASV F I I RTIDILTQ				:	310

		320	*	340		
CTV-SY568	:	VKVKS SMPESQSLKLVVVGSSYLPGLLDTL			:	341
CTV-T385	:	VKVKS SMPESQSLKLVVVGSSYLPGLLDTL			:	341
CTV-T30	:	VKVKS SMPESQSLKLVVVGSSYLPGLLDTL			:	341
CTV-T36	:	VKVKS SMPESQSLKLVVVGSSYLPGLLDAL			:	341
CTV-T3800	:	VKVKS SMPESQSLKLVVVGSSYLPGLLDTL			:	341
CTV-Nuaga	:	VKAKS SMPESQSLKLVVVGSSYLPGLLDTL			:	341
CTV-VT	:	VKAKS SMPESQSLKLVVVGSSYLPGLLDTL			:	341

		*	360	*		
CTV-SY568	:	ATVPFVSGIVPVEDARTAVARGCALYSECLD			:	372
CTV-T385	:	ATVPFVSGIVPVEDARTAVARGCALYSECLD			:	372
CTV-T30	:	ATVPFVSGIVPVEDARTAVARGCALYSECLD			:	372
CTV-T36	:	ATVPFVSGIVPVEDARTAVATG CALYSECLD			:	372
CTV-T3800	:	ATVPFVSGIVPVEDARTAVARGCALYSECLD			:	372
CTV-Nuaga	:	ETVPFVSGIVPVEDARTAVARGCALYSECLD			:	372
CTV-VT	:	ETVPFVSGIVPVEDARTAVARGCALYSECLD			:	372

Figure 2-2 continued

	380	*	400	
CTV-SY568	: GRSKALLIDCITHHLSVTT	FSADSVVVAAG	: 403	
CTV-T385	: GRSKALLIDCITHHLSVTT	FSADSVVVAAG	: 403	
CTV-T30	: GRSKALLIDCITHHLSVTT	FSADSVVVAAG	: 403	
CTV-T36	: GRSKALLIDCITHHLSVTT	FSADSVVVAAG	: 403	
CTV-T3800	: GRSKALLIDCITHHLSVTT	FSADSVVVAAG	: 403	
CTV-Nuaga	: GRSKALLIDCITHHLSVTT	FSADSVVVAAG	: 403	
CTV-VT	: GRTKALLIDCITHHLSVTQ	FSADSVVVAAG	: 403	

	*	420	*	
CTV-SY568	: SPIPFEGE	RKLTLRKC	VSTSNYQ	ARMFEGDY : 434
CTV-T385	: SPIPFEGE	QKLTLRKC	VSTSNYQ	ARMFEGDY : 434
CTV-T30	: SPIPFEGE	QKLTLRKC	VSTSNYQ	ARMFEGDY : 434
CTV-T36	: SPIPFEGE	QKLTLRKC	VSTSNYQ	ARMFEGDY : 434
CTV-T3800	: SPIPFEGE	RKLTLRKC	VSTSKYQ	ARMFEGDY : 434
CTV-Nuaga	: SPIPFEGE	RKLTLRKC	VSTSNYQ	ARMFEGDY : 434
CTV-VT	: TPIPFEGE	RKLTLRKC	VSTSNYQ	ARMFEGDY : 434

	440	*	460	
CTV-SY568	: EKVFRNERIYAASVSLFTLGVNWR	V	PNDVEM	: 465
CTV-T385	: EKVFRNERIYAASVSLFTLGVNWH	V	PNDVEM	: 465
CTV-T30	: EKVFRNERIYAASVSLFTLGVNWR	V	PTD	VEM : 465
CTV-T36	: EKVFRNERIYAASISLFTLGVNWS	V	PNDVEM	: 465
CTV-T3800	: EKVFRNERIYAASVSLFTLGVNWH	V	PNDVEM	: 465
CTV-Nuaga	: EKVFRNERIYAASVSLFTLGVNWR	V	PNDVEM	: 465
CTV-VT	: EKVFRNERIYAASVSLFTLGVNWR	V	PNDVEM	: 465

	*	480	*	
CTV-SY568	: TLVTKVDSMGKVEFY	LKGPSGELVNV	QGT	SR : 496
CTV-T385	: TLVTKVDSMGKVEFY	LKGPSGELVNV	QGT	SR : 496
CTV-T30	: TLVTKVDSMGKVEFY	LKGPSGELVNV	QGT	SY : 496
CTV-T36	: TLVTKVDSMGKVEFY	LKGPSGELVNV	QGT	SH : 496
CTV-T3800	: TLVTKVDSMGKVEFY	LKGPSGELVNV	QGT	SH : 496
CTV-Nuaga	: TLVTKVDSMGKVEFY	LKGPSGELVNV	QGT	SH : 496
CTV-VT	: TLVTKVDSMGKVEFY	LKGPSGELVNV	QGT	SH : 496

Figure 2-2 continued

		500		*		520		
CTV-SY568	:	YDYTGMPHPTRN	LVKLS	DY	NVNSAALVLALT	:	527	
CTV-T385	:	YDYTGMPHPTRN	LVKLS	DY	NVNSAALVLALT	:	527	
CTV-T30	:	YDYTGMPRPTRN	LVKLS	DY	NVNSAALVLALT	:	527	
CTV-T36	:	YDYAGMPHPTRK	LVRLS	DY	NVNSAALVLALT	:	527	
CTV-T3800	:	YDYAGMPHPTRK	LLRLS	DY	NVSSAALVLALT	:	527	
CTV-Nuaga	:	YDYVGMPPHTRK	LLRLS	DY	NVNSAALVLALT	:	527	
CTV-VT	:	YDYVGMPPRPTRK	LLRLS	AYK	VNSAALVLALT	:	527	

		*		540		*		5
CTV-SY568	:	LTREKREKFLLR	TLFD	TLLADLRRTAS	LS	SEY	:	558
CTV-T385	:	LTREKREKFLLR	TLFD	TLLADLRRTAS	LS	SEY	:	558
CTV-T30	:	LTREKREKFLLR	TLFD	TLLADLRRTAS	LS	SEY	:	558
CTV-T36	:	LTREKREKFLLR	TLFD	TLLADLRKTAS	LG	EY	:	558
CTV-T3800	:	LTREKRERFLLR	TLFD	TLLADLRKTAS	LS	SEY	:	558
CTV-Nuaga	:	LTREKREKFLLR	TLFD	ALLADLRKTEI	LS	SEY	:	558
CTV-VT	:	LTREKRERFLLR	TLFD	TLLADLRKTAS	LS	SDI	:	558

		60		*		580		
CTV-SY568	:	SKKYP	ITRNDIDVV	SSRMGIVVSKVLR	GS	SDL	:	589
CTV-T385	:	SKKYP	ITRNDIDVV	SSRMGIVVSKVLR	GS	SDL	:	589
CTV-T30	:	SKKYP	ITRNDIDVV	SSRMGIVVSKVLR	GS	SDL	:	589
CTV-T36	:	SKKYP	ITRNDIDVV	SSRMGIVVSKVLR	GS	SDL	:	589
CTV-T3800	:	SKKYP	ITRNDIDVV	SSRMGIVVSKVLR	GS	SDL	:	589
CTV-Nuaga	:	SKKYP	ITRNDIDV	SSRMGIVVSKVLR	GS	SDL	:	589
CTV-VT	:	LR	YIR	ITRNDIDVV	SSRMGIVVSKVLR	AS	SDL	589

		*		
CTV-SY568	:	ER	IPL	: 594
CTV-T385	:	ER	IPL	: 594
CTV-T30	:	ER	IPL	: 594
CTV-T36	:	ER	IPL	: 594
CTV-T3800	:	ER	IPL	: 594
CTV-Nuaga	:	ER	VPL	: 594
CTV-VT	:	ER	VPL	: 594

Figure 2-2 continued

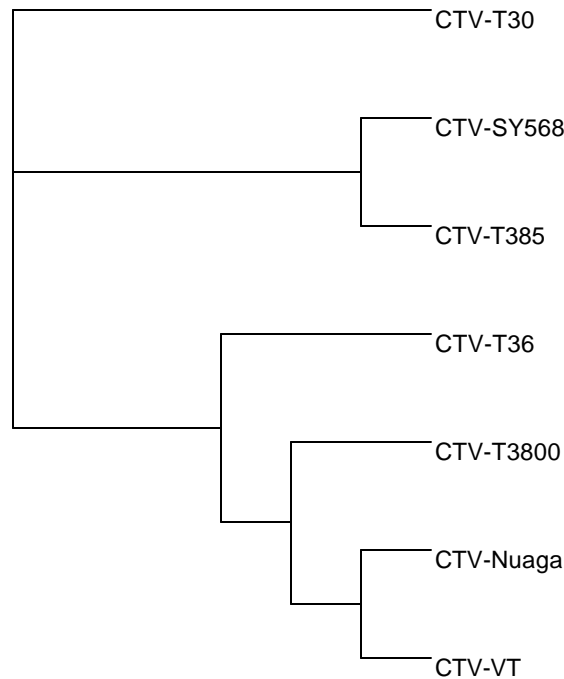


Figure 2-3. Cluster dendrogram based on the amino acid sequences of the translated p65 gene for the various CTV isolates. The biological characteristics of the isolates are summarized in Table 2-4.

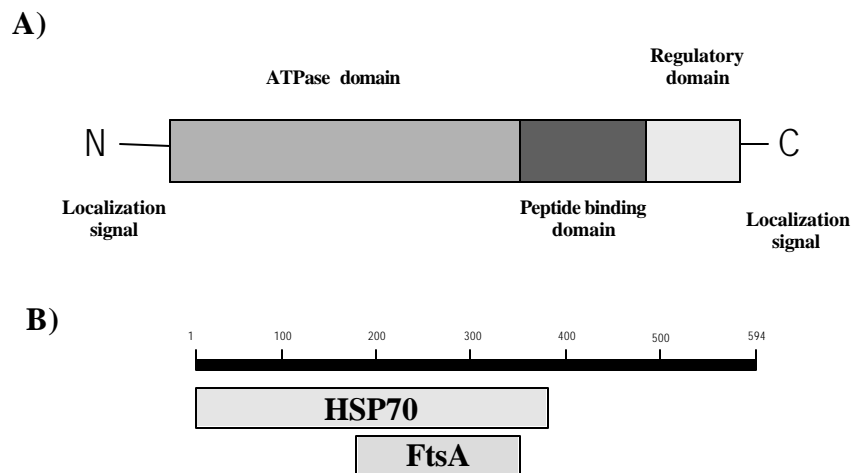


Figure 2-4. Domain conservation between HSP70s and HSP70h proteins. (A) Representation of the domain structure of members of the 70kDa stress proteins. (B). Graphical overview of the putative conserved domains detected in the HSP70h of CTV, using CD-Search. The numbers 1 to 594 represent the amino acid sequence of this protein. HSP70 represents the conservation with the ATPase domain contained in the family of cellular chaperones, and FtsA represents the conservation with the family of prokaryotic cell cycle proteins

the same expression conditions, bacteria carrying only the vector pET22b(+) did not express any exogenous protein with a size similar to the target protein (not shown).

After removing soluble proteins from the inclusion bodies by using sonication and washes with Triton X-100 as described in the Materials and Methods section, the inclusion bodies were solubilized in a buffer containing 6M guanidium chloride and 8M urea. This solution was applied to a Ni-NTA resin (Qiagen) and purified by elution using

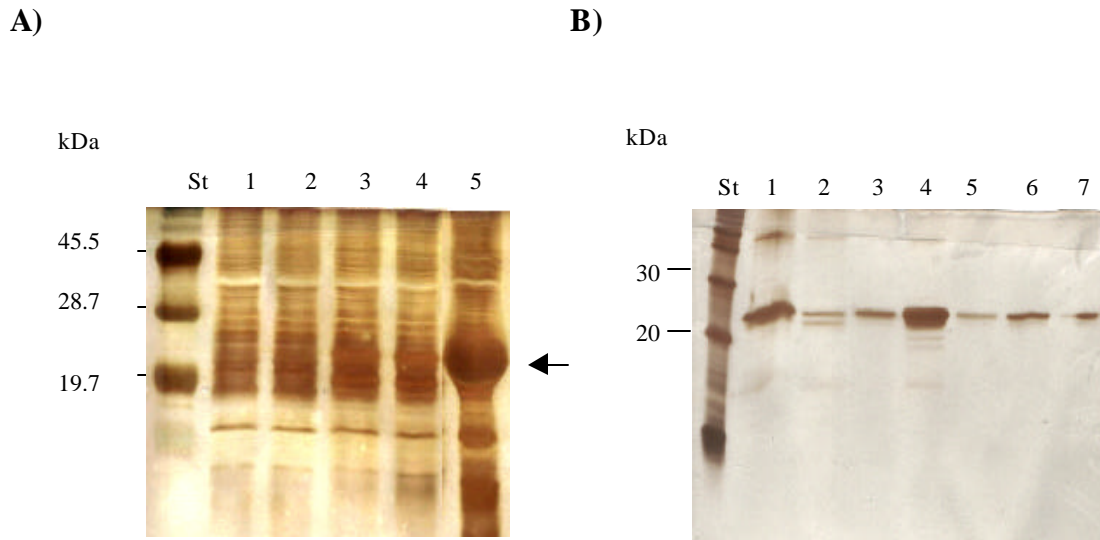


Figure 2-5. Silver stained SDS-polyacrylamide gel electrophoresis (PAGE) showing the over-expression of the 149 amino acid fragment fusion protein in *E.coli* BL21 cells. (A) Protein expression at 37°C: Lanes 1 and 2, non-induced bacteria; lanes 3 and 4, IPTG-induced bacteria; lane 5, insoluble fraction containing the induced protein (inclusion bodies). The arrow indicates the position of the induced protein in the gel. (B) Purification of the fusion protein: Lanes 1 to 4 show different fractions eluted from the Ni<sup>2+</sup>-NTI column after solubilization of the inclusion bodies. Lanes 5 to 7 show proteins obtained after dialysis of fractions shown in lanes 1, 3, and 4, respectively.

a pH gradient (Figure 2-5 B). The purified protein was then dialyzed in a multi-step way, against a buffer (0.1 M NaH<sub>2</sub>PO<sub>4</sub>, 0.01 M Tris-HCl, pH 6.3) that contained decreasing concentrations of urea (6M, 3M, and no urea) over a 24 hour period. This procedure allows the refolding of the protein by removing the denaturing agent from the medium. The target protein obtained after dialysis (Figure 2-5 B) was used as antigen to raise polyclonal antibody in chicken.

### **Production of the Polyclonal Antiserum**

The purified His-tag/HSP70h fusion protein was injected into two young laying hens for six months, according to the protocol described in Material and Methods section. Sera collected during test bleeds were evaluated by Western blot analysis for their reactivity against the recombinant protein used to raise the antiserum, against non-induced bacteria, and against bacteria without the expression vector. Each of the sera tested was diluted 1:1000.

A reaction of the antibody with the induced fusion protein was observed after day 73 (according to the scheme presented in the Material and Methods). The reactivity increased with the new booster immunizations until it reached a plateau after the fourth test bleed. The serum did not react with non-induced bacteria, or bacteria without the plasmid pET22b(+) (Figure 2-6). The reactivity pattern of the antibody was similar for the test bleeds obtained from the two hens immunized, although there was a slightly stronger and more specific reaction with one of the hens (UF-C17).

After six months of immunizations, there was no further improvement in the reactivity of the antibody. Therefore, it was decided to finish the booster immunizations

and proceed with the IgY purification from the eggs that were collected and pooled from around the same time as the test bleeds from months three to six .

To further characterize this antibody, the full length CTV-HSP70h was over-expressed as an HSV·Tag- HIS ·Tag fusion protein in BL21 cells (Figure 2-7). The induced protein was detected by a HSV·Tag monoclonal antibody, which has high affinity and specificity for the 11 amino acid peptide derived from Herpes Simplex Virus glycoprotein D. This antibody recognized a specific band that corresponds with the expected size of the fusion protein (65kDa plus fusion peptides) after induction of the bacterial cells with IPTG (Figure 2-7).

When similar western blots containing the lysate from induced and non-induced bacteria were probed, either with the HSV·Tag monoclonal antibody, or the chicken antibody raised for the carboxyl-terminal end of the viral chaperone (UF-C17), a similar pattern of the reactivity of the proteins bands was observed (not shown). There also was some non-specific reaction of the chicken antibody UF-C17 with other expressed bacterial proteins. These were probably proteins that were co-purified with the viral chaperone, or cellular chaperones from the bacteria that share homology with the viral protein. In order to reduce non-specific reactions with plant tissue, the chicken antibody was pre-adsorbed with healthy citrus tissue extract. This pre-adsorption reduced the number of bands visualized after performing a Western blot with induced and non-induced bacterial lysate (Figure 2-8 A, B).

When this pre-adsorbed antibody was used to probe the bacterial-expressed CTV-HSP70h, a single prominent protein was detected from the induced culture. By Western blot analysis, this protein corresponded in size with the protein detected by the HSV·Tag

monoclonal antibody (Figure 2-8 B). This confirms that the chicken antibody was able to recognize the full-length protein of the viral chaperone analog expressed in BL21 cells.

### Discussion

The sequences of the HSP70s are highly conserved throughout a wide range of organisms, from bacteria to mammals (Agranovsky *et al.*, 1991). The cellular HSP70 sequences are more highly conserved in their N-terminal region, with the C-terminal end being more variable (Craig *et al.*, 1993). Computer-assisted analysis shows that the N-terminal domain of the 65kDa protein from CTV has high levels of similarity to the HSP70 ATPases, while the C-terminal portion shows no homology with the equivalent domain in the cellular HSP70s. The C-terminal region of the HSP70h from CTV also shows moderate homology among the closteroviral chaperones (Agranovsky *et al.*, 1991; Pappu *et al.*, 1994).

The sequences available for the CTV-HSP70h protein have an amino acid identity that ranges from 90 to 99%. When these sequences were arranged into a dendrogram, the clustering obtained did not result in the clustering of isolates having similar biological properties. This suggests that p65 probably is not involved in determining the symptomatology of a particular CTV isolate. Relationships between sequence data and biological properties have been found in the case of CP (Pappu *et al.*, 1993a; Pappu *et al.*, 1993b), p27 (Febres *et al.*, 1994) and p23 (Pappu *et al.*, 1997) genes from this virus.

Previously there were attempts to produce an antibody to the p65 protein from CTV by expressing the full sized recombinant protein in bacterial cells (C.L.Niblett,

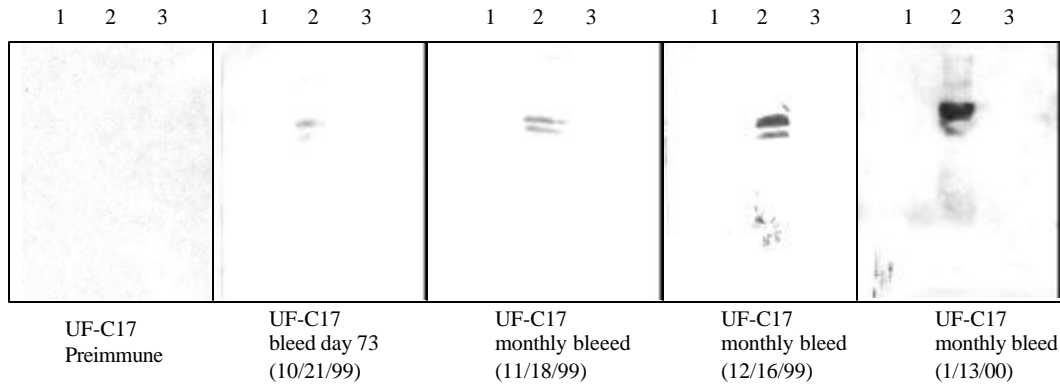


Figure 2-6. Western blots showing the reactivity of the test bleeds. The serum used in each blot is indicated at the bottom of the figure for all tests. Lane 1: non-induced BL21 cells; Lane 2: IPTG-induced BL21 cells carrying the plasmid with the carboxyl-terminal end of the CTV-HSP70h; lane 3: induced BL21 cells not carrying the plasmid.

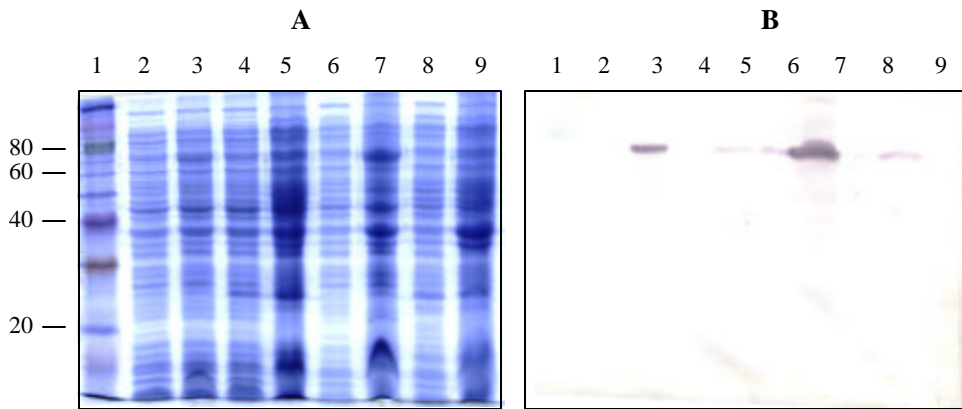


Figure 2-7. Expression and analysis of the CTV-HSP70h induction in BL21 cells. (A) Coomassie blue-staining of a 10% SDS PAGE- gel. The total bacterial lysate was analyzed before (lanes 2 and 4) and after (lanes 3 and 5) induction of protein expression. The induced lysate from lanes 3 and 5 was fractionated in soluble (lanes 6 and 8) and insoluble fractions (lanes 7 and 9) to localize the target protein. The positions of the molecular weight markers (10kDa protein ladder standard, Gibco-BRL) are indicated at the left. (B) Western blot analysis of the induced CTV-HSP70h protein. A gel identical to the one shown in (A) was transferred to a nitrocellulose membrane and probed with a HSV-Tag monoclonal antibody conjugated with alkaline phosphatase. The blot was developed using the NBT-BCIP substrate.

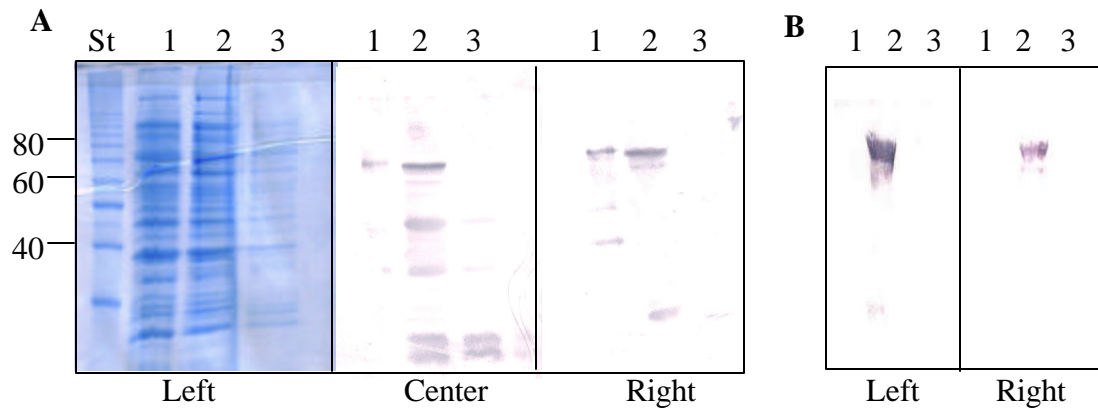


Figure 2-8: Western blot showing the reaction of the bacterial-expressed CTV-HSP70h protein with the HSV-Tag monoclonal or chicken polyclonal antibody.

(A) Left: Coomassie blue staining of a 10% PAGE-SDS gel. Center: Western blot using the polyclonal antibody raised against HSP70h non-adsorbed and pre-adsorbed (right) with healthy citrus extracts.

(B) Western blot showing the reaction of the bacterial expressed HSP70h (full length protein), using monoclonal HSV-Tag (left) or the pre-adsorbed chicken antibody (right). For figures in A and B, lane 1: non-induced bacterial lysates; lane 2: IPTG-induced bacterial lysate; and lane 3: healthy citrus tissue. The positions of the molecular weight (10kDa protein ladder standard, Gibco- BRL) are indicated at the left.

personal communication). The antisera raised using this protein gave non-specific reactions with healthy citrus tissue, as well as some other bacterial-expressed proteins. This suggests that the p65 homolog from CTV has sequence similarity with the cellular chaperones, and also structural similarities with them. These preliminary results suggested that the C-terminal end of the chaperone homolog from CTV may be a better candidate to raise an antibody for specific detection of this protein, due to its lower homology with cellular chaperones. Utilization of the more conserved N-terminal domain would more likely result in cross-reactivity of the serum with host heat shock proteins. A fragment of 149 aa from the carboxyl-terminal end of the protein was expressed in bacterial cells and used as antigen for chicken immunization. The polyclonal antiserum obtained reacted specifically with the cognate antigen, and also with a full-size recombinant CTV-p65 protein on Western blot analysis.

Using this antibody, it should be possible to study the immuno-localization of the viral protein in CTV-infected tissue, and in this way, improve the understanding of the function of this gene product in the process of viral infection as well as its interaction with cell components.

CHAPTER 3  
*IN VIVO* LOCALIZATION OF THE HSP70 PROTEIN HOMOLOG (HSP70h) IN  
CITRUS TRISTEZA CLOSTEROVIRUS INFECTED PLANTS

**Introduction**

Citrus tristeza virus (CTV), the causal agent of the most economically important virus disease of citrus, is a closterovirus with filamentous particles of about 2000 x 11 nm in size. CTV is transmitted by man via infected buds and locally spread by various aphid species (Bar-Joseph and Lee, 1989). *Toxoptera citricida* and *Aphis gossypii* are the most efficient vectors, transmitting the virus in a semipersistent manner. The virus causes different disease syndromes depending on the isolate and the scion/rootstock combination of the citrus tree. Some CTV isolates cause decline and death of trees on the most desirable horticultural rootstock, sour orange (*Citrus aurantium*). Other isolates induce the stem pitting disease on the scion, which results in reduced vigor and small fruit on infected trees. There also are some mild isolates, which do not elicit symptoms on infected citrus plants (Bar Joseph, 1989; Bar-Joseph and Lee, 1989; Roistacher, 1991).

The CTV-genome is a single-stranded, positive sense RNA molecule of 19226-19302 nt, organized into 12 open reading frames (ORFs), potentially encoding at least 19 protein products (Figure 3-1) (Albiach-Marti *et al.*, 2000; Karasev *et al.*, 1995; Mawassi *et al.*, 1996; Pappu *et al.*, 1994; Vives *et al.*, 1999). CTV also contains two untranslated regions (UTRs) of about 105-108 and 273 nt at the 5' and 3' termini, respectively. ORF 1a encodes a 349-kDa polyprotein with two protease-like domains, followed by a

methyltransferase-like and helicase-like domains. ORF1b contains an RNA-dependent RNA polymerase-like domain that is thought to be expressed by a +1 translational frameshift (Cevik *et al.*, 1999; Karasev *et al.*, 1995). ORFs 1a and 1b are translated directly from the genomic RNA, whereas ORFs 2 through 11 are expressed via sub-genomic RNAs (sgRNAs) that are 3' co-terminal (Hilf *et al.*, 1995; Karasev *et al.*, 1995).

There is limited information available about the function of the CTV encoded proteins (Manjuntah *et al.*, 2000). Early reports about function established that the product of the ORF6 and ORF7, which are the minor capsid protein (CPm) and the capsid protein (CP), respectively, encapsidate the virion (Febres *et al.*, 1996; Sekiya *et al.*, 1991). More recently, it was reported that the p23 (ORF11) is an RNA binding protein (Lopez *et al.*, 2000), p20 (ORF10) accumulates in the amorphous inclusion bodies (Gowda *et al.*, 2000), and that p65 (ORF4) and p61 (ORF5) in addition to both CPs are necessary for efficient virion assembly (Satyanarayana *et al.*, 2000). Computer analysis and *in vitro* translation experiments have shown that at least five proteolytic products are predicted to be processed from the polyprotein product (ORF1a) in CTV infected plants (Erokhina *et al.*, 2000; Karasev *et al.*, 1995; Vazquez, 2001). Some of the CTV-encoded proteins have been detected *in vivo* using antibodies developed against bacterial expressed proteins. Using this strategy, the CP (Manjunath *et al.*, 1993; Nikolaeva *et al.*, 1995), CPm (Febres *et al.*, 1994), p20 (Price *et al.*, 1996), RdRp (Cevik *et al.*, 1999) and p23 (Pappu *et al.*, 1997) have been detected in CTV-infected but not in healthy tissue .

So far the CTV-HSP70h, the product of the ORF4, has not been detected *in vivo*. The purpose of this research was to study the *in vivo* localization and expression of the HSP70h from CTV infected citrus tissue, as well as the association of this protein with

the virion. A polyclonal antibody previously developed against this protein was used in tissue printing, co-precipitation and immunogold labelling experiments. The results obtained confirm that this protein is expressed upon virus infection, and that there is a close association between the HSP70h and the filamentous virion of CTV.

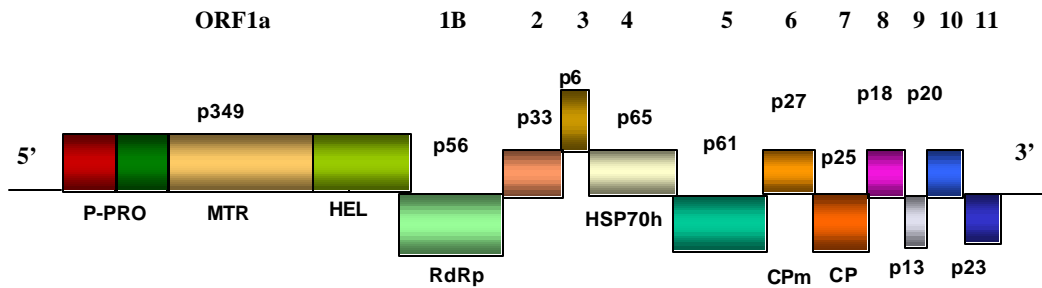


Figure 3-1. Representation of the citrus tristeza closterovirus genome. Open reading frames are shown as boxes. Putative domains in the ORF1a are separated by lines. P-Pro: Papain-like proteases 1 and 2; MTR: putative methyltransferase; HEL: putative helicase; RdRp: RNA-dependent RNA polymerase; HSP70h: heat shock protein homolog; CPm: minor coat protein; CP: coat protein.

## Material and Methods

**Tissue printing.** Tissue blots were prepared as described Garnsey *et al.* (1993). They were prepared from stem or petiole pieces from healthy or CTV-infected citrus tissue. A smooth fresh cut was made with a razor blade, and the cut surface was pressed gently and evenly to a nitrocellulose membrane. After drying the membrane for 10-30 minutes, it was blocked with phosphate-buffered saline (PBS) buffer (0.02 M sodium phosphate buffer with 0.15 M sodium chloride, pH 7.4.) plus 1% bovine serum albumin (BSA) for one hour. After three washes, the membrane was incubated with the primary antibody overnight at room temperature (CREC 35 for CTV-CP, dilution 1:10,000; UF-C17 for CTV-HSP70h, dilution 1:1000). The membrane was washed again, and then incubated with the corresponding secondary antibody that was conjugated with alkaline phosphatase (dilution 1:30,000) for four hours at 37°C. After washing the membrane three times, it was developed with the alkaline phosphatase substrate (NBT-BCIP). All washes were done with PBS-Tween 20 (PBS + 0.5 ml Tween 20 per liter) (PBST), for 5 minutes with gentle agitation.

**Immunoprecipitation.** CTV particles were immunoprecipitated using paramagnetic beads (Dyna Co.) coated with sheep anti-rabbit IgG and CTV specific antibodies (CREC35, produced in rabbit), or goat-anti-chicken and HSP70h specific antibodies (UF-C17, produced in chicken). The Dynabeads-CTV virion complexes were resuspended in 50  $\mu$ l of Western blot extraction buffer (0.125 M Tris HCl, pH6.8, plus 4% SDS, 20% glycerol, and 10% mercaptoethanol), and then boiled for three minutes. Ten  $\mu$ l of the resuspended virions were loaded and run in a 10% PAGE, electrophoresed at 120 V for 2 hours, blotted to a nitrocellulose membrane, and then the membrane was

analyzed by Western blot using the polyclonal antisera raised against CTV-HSP70h (UF-C17) or CTV-CP (CREC35) at a dilution of 1:1,000 and 1:5,000 , respectively.

**Serologically specific electron microscopy (SSEM).** Adsorption of the CTV particles to the grids was done following the SSEM procedure described by Derrick and Brlansky (1976). Briefly, crude extracts from bark, stems or petioles from healthy or CTV-infected citrus plants were obtained by chopping the tissue in extraction buffer (0.05M Tris-HCl, pH 7.2, plus 0.15 M NaCl, 0.4M sucrose). CTV particles were adsorbed to carbon-formvar coated copper grids using a CTV-CP specific antibody (1052 IgG, diluted 1:500) by floating the grid on drops of the crude extract for 1h. After rinsing the grids first in 0.05M Tris-HCl buffer, pH 7.2, and then with water, they were positively stained with a 5% solution of uranyl acetate in 50% ethanol for 5 min, and washed in 95% ethanol. The grids were viewed with a Philips 201 transmission electron microscope at different magnifications.

**SSEM-immunogold labeling.** Adsorption of the CTV-particles to the grids was done following the SSEM procedure described by Derrick and Brlansky (1976), and outlined in the previous paragraph. Briefly, after adsorption of the particles to the grid, they were first washed with 3 drops of buffer (0.05M Tris-HCl, pH 7.2) for three minutes each, then in 2 drops of blocking buffer (0.05M Tris HCl, pH 7.2, with 0.1% BSA) for 3 min each, and finally one extra drop of blocking buffer for 30 minutes. The grids were then transferred to drops of primary antibody [UF-C17 (from chicken) and chicken pre-immune antiserum were diluted 1:100, for the CTV-CP antibody (1052, from rabbit) the dilution was 1:500 in blocking buffer]. The grids were rinsed with three drops of blocking buffer for three minutes each, and then transferred to a drop of the secondary

antibody. For detection, a 10 nm gold-conjugated goat anti chicken IgG or a 15 nm gold-conjugated goat anti rabbit IgG were used at a dilution 1:100 in blocking buffer. The grids were rinsed first in blocking buffer, then in three drops of water, and finally stained with 5% uranyl acetate in 50% ethanol and rinsed in 95% ethanol.

## Results

### *In Vivo* Detection of the HSP70h by Tissue Printing.

An antibody raised against the carboxy-terminal end of the CTV-HSP70h was previously produced in chicken (Chapter 2). This antibody showed a specific reaction with the bacterial-expressed protein antigen (149 aa), as well as the full length bacterial expressed chaperone homolog from CTV. To study whether the HSP70h protein was expressed in infected plants, tissue-printing studies were conducted using this antibody and a CP-specific antibody.

When the blots were treated with the CP antiserum, the imprint of the stem was clearly visible with deep purple staining. The purple stained area was the phloem of CTV-infected stems (Figure 3.2; row C, columns 2, 3 and 4). The healthy tissue imprint showed a faint pink coloration that was easily distinguished from the intense purple stained areas in the phloem of the CTV-infected samples (Figure 3.1; column 1, rows A, B, C).

When the antibody raised against the CTV-HSP70h protein (UF-C17) was used to probe the blot, the chaperone homolog was specifically detected in CTV-infected but not in uninfected citrus plants (Fig.3.2, membranes in row A and B, columns 2, 3, 4, as compared to column 1). The localization pattern of the CTV-HSP70h and the CTV-CPs were similar in the direct tissue printing studies, and this corresponded to the phloem

tissue. The amount of purple staining was less for the HSP70h than for the CP suggesting a much lower level of expression for the CTV-HSP70h than for the CTV-CP. The chicken antibody, UF-C17, did not react with healthy tissue, and only a faint pink color similar to the reaction obtained with the CP antiserum against healthy tissue was observed in the membrane (Figure 3-2, column 1, rows A and B).

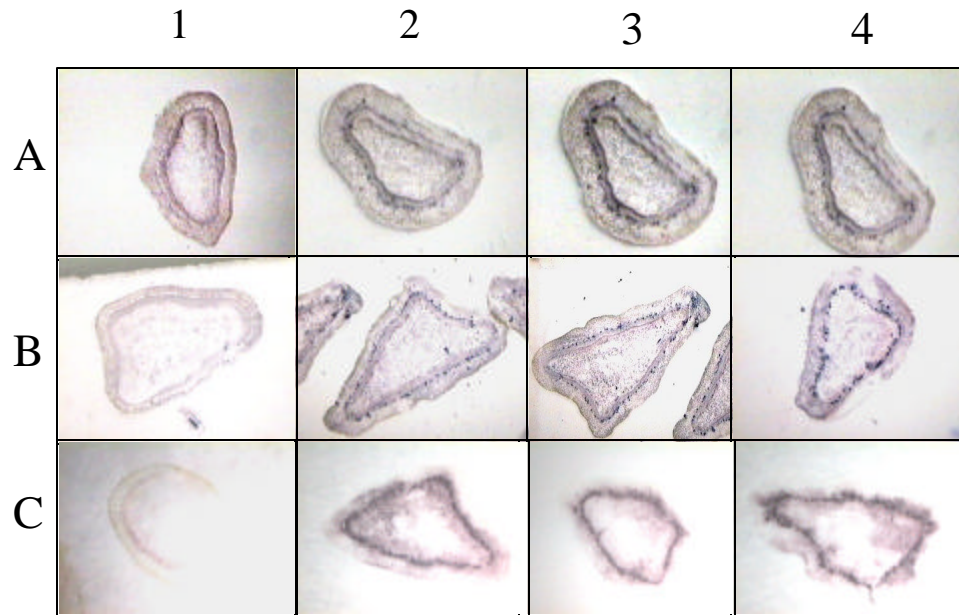


Figure 3.2. Tissue prints of infected and healthy citrus stems after incubation with HSP70h and coat protein specific antibodies. Column 1 healthy citrus tissue; columns 2, 3 and 4 CTV-infected tissue. Membranes in rows A and B were incubated with antibody raised against the CTV-HSP70h (UF-C17). Membranes in row C, were incubated with antibody raised against the CTV-CP (CREC35).

### **Immunoprecipitation of an HSP70h-CP Complex From CTV-Infected Plants.**

Immunoprecipitation was used to determine whether the CTV-HSP70h could interact with the CP in extracts of CTV infected plants. When the CTV-CP antibody (CREC-35) was used to produce the precipitate, immunoblotting of the precipitated proteins with anti-CP antibody revealed the presence of CP in CTV-infected plants (Figure 3.3 A, bottom, lanes 2 and 3), but not in the uninfected plants (Figure 3.2 A, bottom, lanes 1). Furthermore, the HSP70h was also present in that precipitate. Its presence was revealed by using the chicken antibody against the chaperone homolog in the immunoblot. A unique band, absent in extracts from uninfected plants, was detected in extracts from CTV-infected tissue (Figure 3.3 A, top, lanes 2 and 3). This band has an apparent molecular weight of 65 kDa. The antibody also showed a weak reaction with some host proteins (probably cellular HSP70s) of greater molecular weight than the closteroviral chaperone protein (Figure 3.3 A, top, lanes 1, 2 and 3).

When the extracts from CTV-infected plants were immunoprecipitated with the CTV-HSP70h antibody, immunoblotting of the precipitated proteins with CP antibody revealed the presence of the CP in the precipitate. In the left portion of Figure 3.3 B, the proteins precipitated with the CP antibody and the proteins precipitated with the HSP70h antibody are shown in a silver stained SDS-PAGE gel. An equivalent gel was transferred to a membrane and blotted with the CP antibody (Figure 3.3 B, right portion). A comparison of the intensity of the bands obtained with each antibody (right portion, lanes 2 and 3) demonstrates that the CP antibody was more efficient in the precipitation of the complex than the CTV-HSP70h antibody. When the chicken preimmune serum was used to immunoprecipitate proteins from healthy and CTV-infected citrus tissue, the CTV-CP antibody did not react with any proteins transferred to the membrane.

**SSEM-Immunogold labeling.**

To further examine the association between the HSP70h and the CP of CTV, immunogold labeling of CTV particles was performed with the same antibody used in the co-precipitation experiments. Before doing the decoration of the virus particles, the relative amount of CTV virions present in the extracts was determined by SSEM (Figure 3.4). The decoration was performed only if enough particles were present. All the CTV isolates used for this experiment, T3, T4, T36 and T3800 showed high virus titer and, subsequently, there were sufficient virions on the grids for decoration. Labeling of the virions using the CP antibody (1052) was done as a positive control to ensure that the technique was working properly. Figure 3.5 shows the gold particles concentrated along almost the entire length of the virion when these were labeled with the CP antiserum. The number of gold particles were variable, but there were usually more than 13 for each full length CTV-particle.

When the chicken antibody produced against the CTV-HSP70h was used to decorate the trapped particles, the HSP70h protein was detected in close association with the virions. There were a variable number of gold particles associated with each virion, ranging from 2 to 11 (Figure 3.6). Most of the gold label was associated with full length virions or with virion fragments. This can be better seen in Figure 3.6 E where the virion is labeled with eleven gold particles and there also are some gold particles associated with fragmented CTV virions. Thus, the CTV-HSP70h protein was detected in close association with the virions and virion fragments.

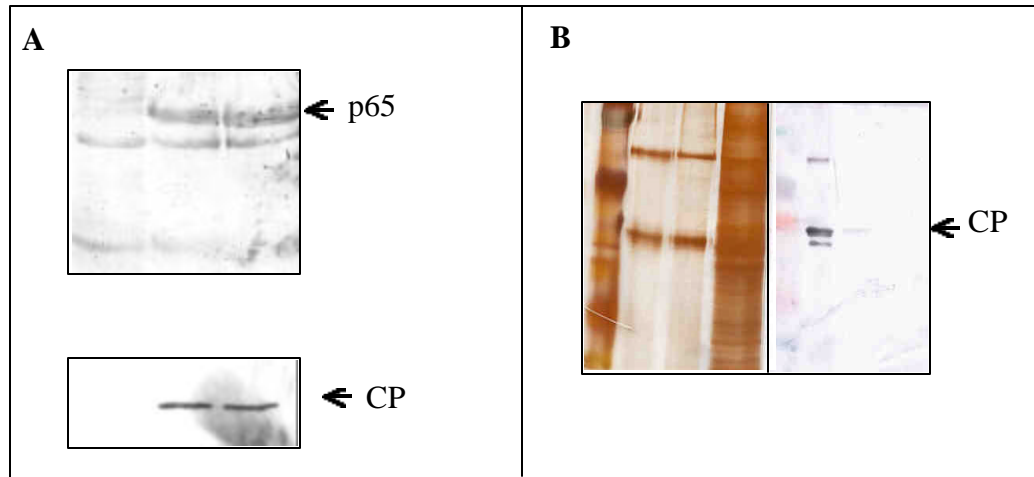


Figure 3.3. Interaction of CTV-HSP70h and CTV-CP in CTV infected tissue.

Extracts from CTV-infected and uninfected citrus plants were incubated with paramagnetic beads either coated with anti-CP or anti-HSP70h antibody. The precipitated proteins were analyzed by immunoblotting of the PAGE-separated proteins with either anti-HSP70h or anti-CP antibody. (A). Top: Precipitated proteins obtained with the CP antibody, and then the membrane probed with the antibody to the CTV-HSP70h. Bottom: The same precipitates probed with the anti-CP antibody. Lane 1: healthy tissue, lanes 2 and 3, immunoprecipitated virions from CTV infected tissue (B). Left half: Silver stained PAGE of the immunoprecipitated proteins. Right half: Immunoblotting of the PAGE-separated proteins using the CTV CP antibody. Lane 1: protein standard, lane 2: precipitate obtained from CTV-infected tissue with the CTV CP antibody, lane 3: precipitate obtained with the CTV HSP70h antibody, and lane 4: healthy citrus tissue.

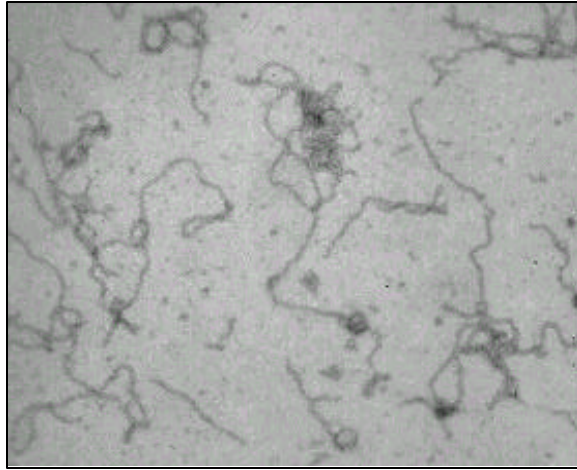


Figure 3.4. Serologically specific electron microscopy (SSEM) of trapped citrus tristeza virus (CTV) particles. The CTV coat protein specific antibody was used for trapping the particles on the grid. The magnification of the micrograph is 30,000x.

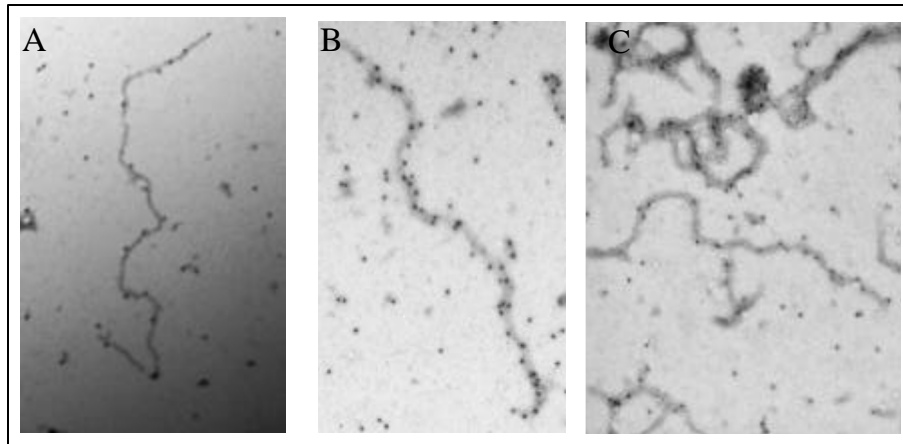


Figure 3.5. Immunogold labeling of citrus tristeza virus trapped particles using the coat protein specific antibody. The CTV-CP specific antiserum 1052 was used for trapping of the particles to the grid. The magnification of the micrograph is 45,000x

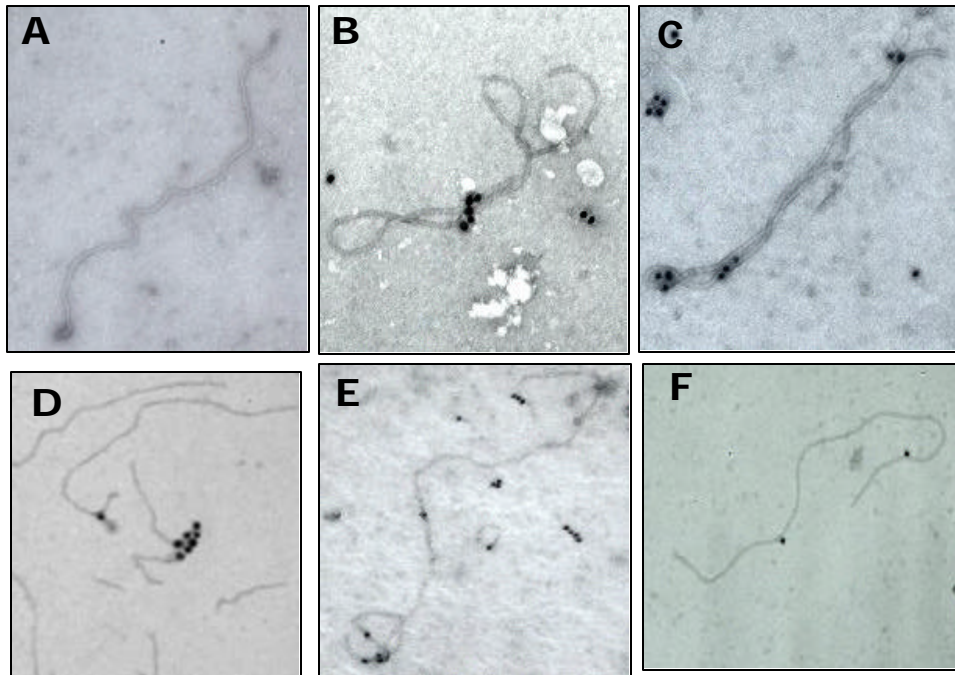


Figure 3.6. Immunogold labeling of citrus tristeza virus particles using the CTV-HSP70h-specific antibody. (A) CTV particles labeled with the preimmune serum. (B) to (F). Decoration of CTV virions with the gold particles conjugated to the CTV-HSP70h specific antibody. All of the micrographs are at 45,000X magnification.

### Discussion

The proteins from the HSP70 family of molecular chaperones are conserved among unicellular and multicellular organisms (Chervitz *et al.*, 1998; Guy and Li, 1998; Tatusov *et al.*, 1997). The major known functions of the HSP70 proteins are to mediate the correct folding, assembly, intracellular localization, secretion, regulation and degradation of other proteins (Gething, 1997). *Closteroviridae* members are the only viruses known to encode an HSP70 homolog of cellular molecular chaperones-like proteins (Karasev, 2000).

The purpose of this research was to study the *in vivo* expression of the CTV-HSP70h and its possible association with CTV virions. Using an antibody specific for

this protein, it was possible to identify the presence of the CTV- HSP70h in infected citrus tissue but not in non-infected tissue, using tissue printing studies. The localization pattern of the CTV-HSP70h and the viral CP were similar in direct tissue printing, and they corresponded with the location of the phloem tissue. Additionally using two different experimental approaches, SSEM-immunogold labelling and immunoprecipitation from plant extracts , provide strong evidence for the existence of HSP70h-virion complexes in CTV-infected plants.

Co-localization of the HSP70h with virions, as reported in beet yellow virus (BYV)-infected cells (Medina *et al.*, 1999), and the detection of HSP70h in partially purified preparations of lettuce infectious yellows virus (LIYV) (Tian *et al.*, 1999), suggest a physical association between the viral chaperones and the virions (Alzhanova *et al.*, 2000). It also was shown for BYV that the HSP70h-virion complex is stable at high salt concentrations, but the use of other dissociating agents, such as sodium dodecyl sulfate, lithium chloride, or alkaline pH, resulted in at least partial virion disassembly. The formation of the HSP70h-virion complex apparently does not involve covalent bonds with any of the virion components (Napuli *et al.*, 2000). These authors estimated the number of viral chaperones bound to each virion. They separated virions and associated proteins by SDS-PAGE, and the approximate amount of BYV-HSP70h was determined by comparison with standardized dilutions of a marker protein. By this approach, it was found that each virion binds an average of 10 molecules of HSP70h protein. In this present study, direct immunogold labeling of the CTV-HSP70h showed that there are a variable number of molecules associated with each virion, ranging from 2 to 11. This variation may result from the manipulations of the plant extracts during the process of

extraction and decoration of the particles, or to the fact that all the chaperone-specific antibody binding sites were not saturated.

Complexes between the HSP70 and CP during viral infection have been reported for viruses such as Sindbis virus (Garry *et al.*, 1983), vesicular stomatitis virus (Garry *et al.*, 1983), adenovirus type 5 (Macejak and Luftig, 1991), poliovirus and coxsackievirus (Macejak and Sarnow, 1992). The association of constitutively expressed cellular chaperones and mature virions of animal RNA viruses has been reported for rabies virus, vesicular stomatitis virus, Newcastle disease virus, influenza A virus (Sagara and Kawai, 1992) and canine distemper virus (Oglesbee *et al.*, 1990). Because of the diverse functions of the cellular chaperones and their increased expression and association with viral proteins during viral infections, it is likely that HSP70 proteins assist in some aspects of virion assembly as a cellular chaperone protein (Cripe *et al.*, 1995).

Satyanarayana *et al.* (2000) have reported that the CTV-HSP70h appears to be required for efficient virion formation, since mutations in the HSP70h gene resulted in large decreases of the ability of the virus to be serially passaged in *Nicotiana benthamiana* protoplasts, as well as reductions in the proportions of full length particles. Peremyslov *et al.* (1999) described that the chaperone homolog of BYV functions in intracellular translocation and represents an additional type of plant viral movement protein.

There are numerous possible functions that are feasible for the association of the CTV-encoded chaperone with its virion during viral infection. It may be required not only for virion formation, but also for virion disassembly during the process of viral infection. The viral chaperone may play a role in aphid transmission, as has been

reported for some other plant viruses which require virus-encoded proteins other than those on the virion for vector transmission (Harrison and Murrant, 1984; Pirone, 1991). CTV-HSP70h also can mediate the intercellular translocation of the virion as has been reported for BYV. Finally, the CTV-HSP70h protein as a molecular chaperone could play a role in preventing aggregation or assisting in the proper folding of the viral proteins during the process of infection.

In summary, the data presented here confirm that the HSP70 chaperone homolog encoded by CTV is expressed in CTV-infected plants and not in non-infected plants, and that it forms a complex with the CTV virion or with the individual capsid proteins during the process of CTV-infection.

CHAPTER 4  
THE CTV-HSP70h AS A COMPONENT OF CTV INCLUSION BODIES

**Introduction**

The family *Closteroviridae* is comprised of more than 30 plant viruses with flexuous, filamentous virions and includes representatives with either mono- or bipartite positive sense single stranded RNA genomes. The Closteroviruses, a member of this family, are a large and diverse group of viruses affecting several crops of major economic importance, e.g. sugarbeet, citrus, tomato, sweet potato, grapevine, pineapple, cherry, and some ornamentals (Karasev, 2000). Studies have shown that closterovirus infections induce characteristic inclusion bodies (IB) within phloem associated cells, including phloem parenchyma and companion cells (Lesemann, 1988). These IB include cytoplasmic vesiculated membranous areas within infected cells, referred to as beet yellow virus (BYV)-type vesicles, surrounded by lipid droplets (Medina *et al.*, 1998).

Citrus tristeza virus (CTV) has been shown to produce IB that are confined mostly to the phloem. The detection of CTV inclusions using light microscopy or *in situ* immuno-fluorescence can provide a rapid method for diagnosis of CTV infection (Brlansky, 1987; Brlansky *et al.*, 1988). Early reports on CTV-infected tissue revealed the presence of chromogenic bodies in the phloem parenchyma cells adjacent to sieve tubes with strands of dark staining masses and needle-like structures (Kitajima and Costa, 1968; Schneider, 1959; Shneider and Sasaki, 1972). Schneider suggested that the chromatic cells were the primary cytological symptoms from CTV infection, and that

they were involved in the development of wood pitting, vein clearing, and seedling yellows symptoms. Staining of the inclusions with magenta and azure A suggested the presence of nucleoproteins in fibrous and banded inclusions (Christie and Edwarson, 1977; Garnsey *et al.*, 1980). Electron microscopic observations of thin sections revealed the presence of large numbers of CTV particles packed in paracrystalline arrays in the phloem of sieve elements (Bar-Joseph *et al.*, 1979).

Studies have shown higher numbers of IB in various host species infected by severe CTV isolates as compared to mild isolates (Brlansky and Lee, 1990). The effect of virus strains or host on the morphology of the various CTV IB is not known. Recently, Gowda *et al.* (2000) reported the immunolocalization of the p20 protein (ORF 10) from CTV with the amorphous IB present in CTV-infected tissue, suggesting that the p20 protein is a major component of this type of inclusion.

The purpose of this research was to determine if the CTV heat shock protein analog (CTV-HSP70h) occurs in the characteristic IB present in CTV-infected tissue.

## **Material and Methods**

**Virus isolates and plant material.** Florida CTV isolates T3, T66, T36, T30, T55 and T4, were used throughout the study. T3 causes severe decline on sweet orange grafted on sour orange, and severe stem pitting and vein clearing on Mexican lime. Isolate T36 produces mild seedling yellows and decline on sour orange, T66 produces strong reaction on Mexican lime and decline on sour orange, and T30 and T55 isolates produce mild symptoms on Mexican lime, and no noticeable symptoms on commercial citrus trees. T4 isolate produces a strong reaction on Mexican lime, but it is negative for seedling yellows and decline on sour orange. The host selected for inclusion body

purification was Mexican lime. Healthy Mexican lime tissue control was included for comparison.

**Light microscopy.** Petiole samples approximately 0.5 cm long were excised from the leaves at the abscission zone. Transverse sections were prepared using a Harris WRC cryostat-microtome (Harris Manufacturing, Inc). Sections were stained according to the method described by Garnsey *et al* (1980). Briefly, sections were stained for approximately 15 minutes in 0.05% Azure A in 2-methoxyethanol and buffered with 0.2M Na<sub>2</sub>HPO<sub>4</sub>. Stained sections were washed sequentially in 95% ethanol and 2-methoxy ethyl acetate, mounted in Euparal and observed under the light microscope.

**Inclusion body purification.** A protocol based on the purification procedure described by Lee *et al.*, (1982) was used in this study. Briefly, tender bark tissue was homogenized in TSM buffer (0.05M Tris-HCl, pH 8.0, 10% sucrose, 0.5% β-mercaptoethanol), using 1g of fresh weight tissue and 15 ml of TSM buffer, and then centrifuged at 10,000 x g for 15 min at 4°C. The pellet was homogenized in 15 ml of TSM buffer using a Polytron type homogeneizer and filtered through two layers of cheesecloth. The filtrate was centrifuged at 4,000 x g for 15 min through a 5 ml pad of 20% sucrose made in TSM buffer. The pellet was resuspended in 5 ml of buffer (0.05M Tris HCl, pH 8.0 plus 5% Triton X-100), let set for 30 min at room temperature, and then centrifuged at 2,500 x g for 10 min. The resultant pellet was resuspended in 2 ml of TSM buffer and layered onto a cesium sulfate step gradient prepared by layering 3 ml of 1.5 molal CsSO<sub>4</sub>, 3 ml 1.0 molal CsSO<sub>4</sub>, and 3.0 ml 0.5 molal CsSO<sub>4</sub>. All the CsSO<sub>4</sub> solutions were prepared in 0.05M Tris HCl, pH 8.0 plus 30% sucrose. The step gradient was centrifuged at 36,000 rpm for 3.5 hours at 12°C using a SW41 Beckman rotor.

Following centrifugation in the cesium sulfate gradient, the IB (IB) were localized about  $\frac{1}{2}$  to  $\frac{3}{4}$  through the gradient. The bands containing the IB were collected, washed with TSM buffer, and loaded into a new step centrifugation gradient, this time prepared by layering 1.5 ml 1.5 molal CsSO<sub>4</sub>, 4 ml 1molal CsSO<sub>4</sub>, and 4 ml 0.5 molal CsSO<sub>4</sub>. This step gradient was centrifuged at 36,000 rpm for 12 hours at 12°C using a SW41 Beckman rotor. The IB appeared as compact greenish bands located in the lower half of the gradient.

**Fluorescent antibody microscopy.** Antibodies raised against the following CTV proteins were used as primary antibody : coat protein (CP), minor coat protein (p27), p20 and HSP70h (p65). A volume of 100  $\mu$ l from the fractions containing the partially purified IB was pipetted onto a black polycarbonate membrane (0.2 micron, Poretics Corp). The membrane was overlaid with 3 drops of the primary antibody diluted 1:20 in the antibody buffer (0.02M Tris-HCl pH 8.2, 0.9% NaCl, 1% gelatin, 0.1% BSA) for 30 minutes at room temperature. The membrane was then washed by flooding with a pipette full (approximately 1 ml) of antibody buffer, let set for 1 minute and the buffer pipetted off. The membrane was overlaid with 3-4 drops of goat anti-chicken antibody- (for detection of HSP70h) or goat anti-rabbit antibody (for detection of CP, p27 and p20 proteins)- tetramethyl-rhodamine (TRITC) labeled IgG diluted 1:20 with antibody buffer and incubated for another 30 min. The membrane was washed, and then mounted on a glass microscope slide with the sample side up using 1-2 drops of Aqua Mount mounting media (Lerner Laboratories) and covered with a cover slip. The samples were observed using a Zeiss Dialux fluorescence microscope, at 40X magnification.

**SDS- polyacrylamide gel electrophoresis (SDS-PAGE).** An aliquot of 100  $\mu$ l from the fraction contained the IB was resuspended in 500  $\mu$ l of ESB buffer (9M urea, 4.5% SDS, 7.5%  $\beta$ -mercaptoethanol and 75 mM Tris-HCl, pH 6.8) and gently agitated. The samples were then boiled for 10 minutes and loaded onto a 10 or 12% SDS-PAGE gel that was prepared following standard protocols (Sambrook, 1989). The gels were electrophoresed at 120 Volts for 2 hours.

**Protein silver staining.** After electrophoresis, the gel was fixed in a solution 50% methanol, 5% acetic acid (v/v) in water for 30 minutes. Then the gel was washed first in 50% methanol for 10 min, and then in water for other ten minutes. The gel was sensitized by one minute incubation in 0.02% sodium thiosulfate, and rinsed with two changes of distilled water for 1 minute each. After rinsing, the gel was submerged in a chilled 0.1% silver nitrate solution and incubated for 30 minutes at 4°C. After incubation, the gel was rinsed twice with water for 1 minute and developed in 0.04% formalin in 2% sodium carbonate with gentle shaking. After the desired staining intensity was achieved, the development of the gel was stopped by decanting the reagent and washing the gel with 5% acetic acid (v/v).

**Western blot analysis.** The protein samples were loaded onto a 10% SDS-PAGE gel, and electrophoresed at 120 Volts for 2 hours. The proteins were then blotted to a nitrocellulose membrane and blocked with 3% BSA in TBST buffer (25 mM Tris-HCl, pH 8.0, 125 mM NaCl, 0.1% Tween 20). After, overnight incubation with the primary antibody (UF-C17, a chicken antibody against the CTV- HSP70h, diluted 1:1000 in blocking solution, or CP antibody, 1052 raised in rabbit against purified virus, at the same dilution) and 4 hours with the secondary antibody (alkaline phosphatase conjugated

goat antichickens IgG or goat anti rabbit, diluted 1:30,000 in blocking buffer), the membrane was developed using the NBT-BCIP substrate.

## Results

### Light Microscopy and Inclusion Body Purification

The Azure A staining procedure was used to observe the IB in CTV-infected tissue. Inclusions were observed in the phloem, phloem fiber and parenchyma cells of CTV-infected tissue, but not in sections taken from healthy plants (Figure 4-1). Those plants showing staining of IB by Azure A were selected for the IB purification procedure. As previously reported by Bransky *et al.* (1990), more IB were observed in tissue infected with severe CTV isolates than in tissue infected with mild isolates.

A protocol for purification of IB based on the previous procedure described by Lee *et al.* (1982) was used with an additional gradient centrifugation step added. Extracts from healthy Mexican lime were included as a negative control to enable comparison of the bands obtained from infected and healthy citrus tissue. After the first step gradient centrifugation, the starch granules were pelleted at the bottom of the tube in all the samples, but the bands containing the IB were not easily differentiated from the host proteins when compared with the gradient loaded with healthy tissue extracts (Figure 4-2; A throughout E). A second step gradient centrifugation allowed a more compacted banding of the IB, with these bands located at different positions in the gradient compared to the proteins present in the healthy tissue, which formed a band near the bottom of the tube (Figure 4-2, F throughout J). The bands located in the lower half of the cesium sulfate gradient were collected, and in cases where there was not a clear differentiation between the IB and the host proteins (as for example, isolates T30 and T55

in Figure 4-2), the bottom fraction was split into two fractions. All fractions collected were enumerated from top to bottom for further analysis. An estimation of the density at the different fractions was calculated by weighing 100  $\mu$ l of volume collected for each fraction. The band present in the cesium sulfate gradient loaded with healthy tissue had a density (g/ml) of 1.63, and the densities for the fractions containing the CTV IB ranged from 1.28 to 1.47 (Figure 4-2).

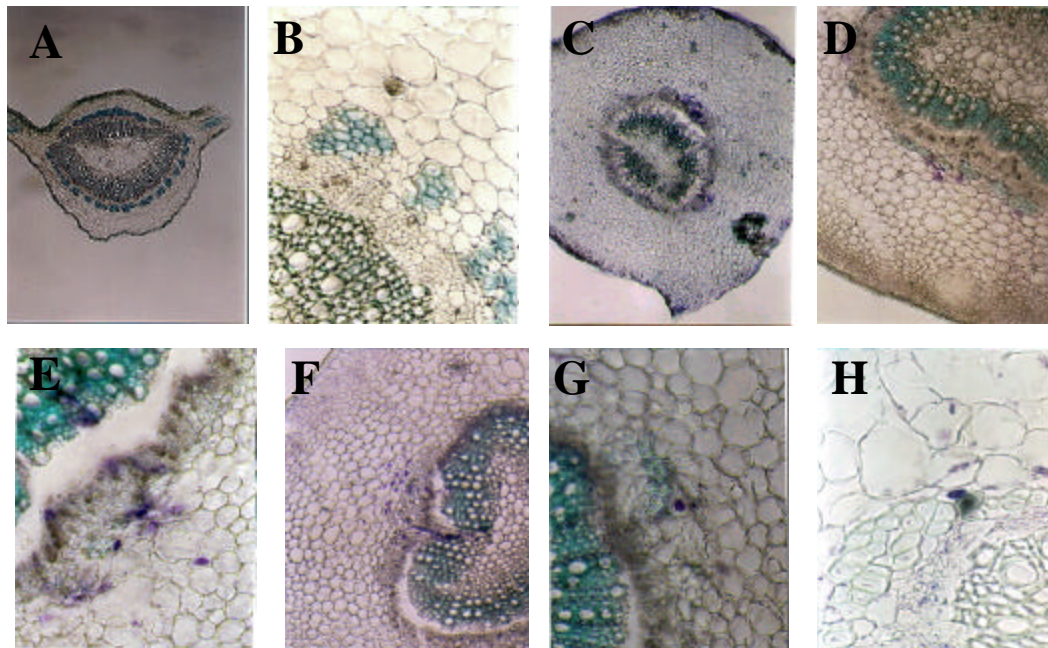


Figure 4-1. Azure A staining and light microscopy of leaf petiole sections of healthy and CTV infected tissue. A and B, sections of healthy citrus tissue at a magnification of 13.2 X and 80X respectively. From C throughout H, sections of CTV-infected tissue at different magnifications. 25X in C, 40X in D and F, 80X in E and G, and 160X in H. The isolates shown in the figure are T4 (C), T3 (D through G) and T4 (H).

### Fluorescent Antibody Microscopy

In an attempt to look for the presence of the HSP70h in the partially purified IB, an aliquot of the IB was incubated with the UF-C17 antibody or the preimmune chicken antiserum, and then with the secondary antibody (goat anti-chicken) labeled with TRITC. Because the preimmune chicken antiserum showed reactivity with the proteins contained in the IB fractions, the fluorescence observed when the antibody UF-C17 was used as primary antibody could not be attributed to the presence of the CTV-HSP70h in the IB. The secondary antibody, by itself, did not react with the IB. When a rabbit preimmune serum

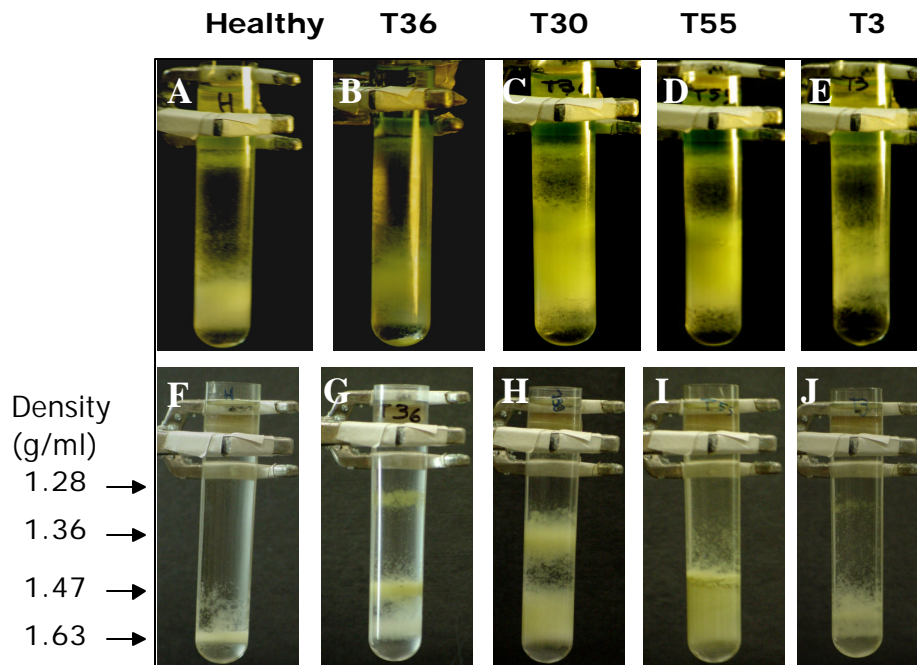


Figure 4-2. Inclusion body purification. The procedure consisted of two consecutive cesium sulfate step gradients. From A through E the bands obtained after the first gradient are shown, and from F through J, the pattern obtained after the second step gradient. The tissue loaded onto each gradient is shown at the top of the figure. Densities (g/ml) calculated for the bands isolated from the gradient are shown at the left.

was used as primary antibody, there was no fluorescence associated with the IB (Figure 4-3, A). Antiserum raised against the p20 (ORF12), the CP (ORF7), and the p27 (ORF6), previously developed in C.L. Niblett's lab, were used to study the composition of the proteins isolated from the gradient centrifugation. The antibody reacting with the CP (antibody 1052) showed a strong red-orange fluorescence when used with the IB (Figure 4-3, B and C). The antibody reacting with the p27 also showed some fluorescence when it was used as primary antibody, but the number of foci were considerably smaller in number and size than the fluorescence foci obtained with the CP antiserum (Figure 4-3, D). When the antibody raised against the p20 protein was used as primary antibody, there was no fluorescence associated with IB.

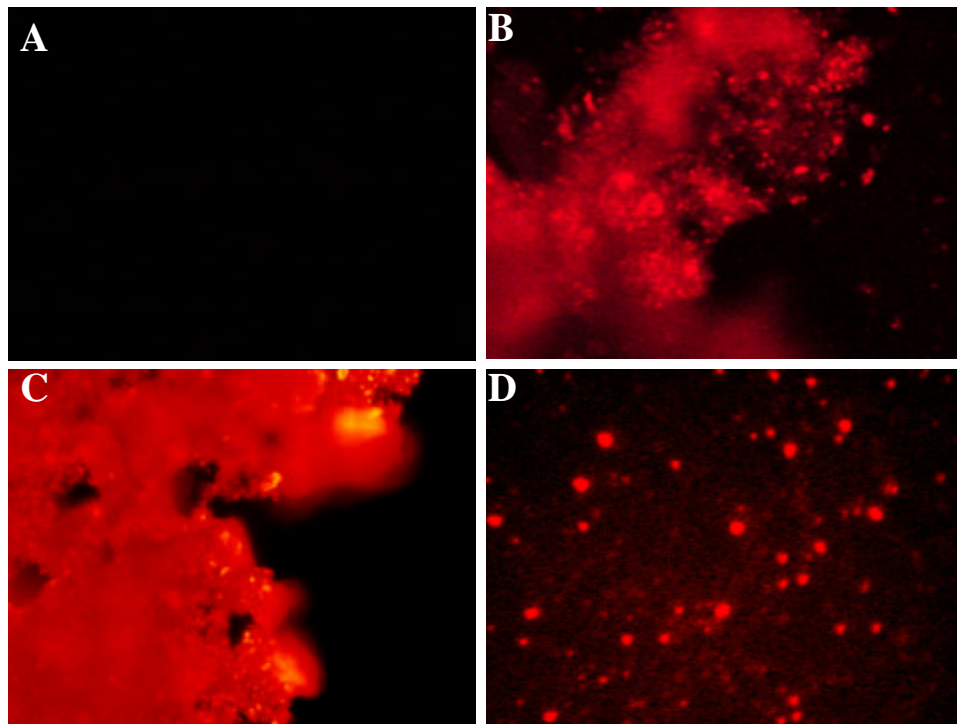


Figure 4-3. Immunofluorescence of proteins contained in the CTV inclusions using a TRITC-labeled conjugate. The inclusion bodies were incubated with the rabbit preimmune serum (A), the antibody (1052) raised against the CP-CTV (B and C), or the p27 antibody (D). All pictures are shown at 40X magnification.

### **Analysis by SDS-Polyacrylamide Gel Electrophoresis (SDS-PAGE)**

The different fractions collected from the cesium sulfate step gradient centrifugation were loaded onto a 10 or 12% SDS-PAGE gel. Proteins collected from healthy tissue fractions were used to detect the presence of host proteins in the fractions collected from CTV-infected bark. Three size groups of proteins were stained in the gels. One group around 15 kDa, other group around 25 kDa, and the last group had a molecular mass higher than 55 kDa (Figure 4-4).

The proteins present in the fractions collected from healthy tissue were also detected in the fractions collected from CTV-infected plants. This was unexpected since the bands occurred at different positions in the cesium sulfate gradient. However, several proteins were present only in IB fractions from extract from infected tissue. These may be virus-encoded proteins, or proteins from the host expressed as a response to virus infection.

To ensure the reproducibility of the proteins patterns obtained, several IB extractions were performed from plants infected with the different CTV isolates. The proteins obtained were reproducible and consistent for the different extractions. Interestingly, there was similarity in the pattern of the proteins obtained for the top fractions from the severe isolates T36 and T66, and the mild isolates T55 and T30, respectively (Figure 4-4).

The SDS-PAGE using a 10% gel enabled a better resolution of the proteins having molecular masses higher than 55 kDa. In this size group of proteins there were proteins which were exclusively present in the CTV-inclusions, as well as other proteins that also were present in the healthy tissue. In general, less variation between isolates,

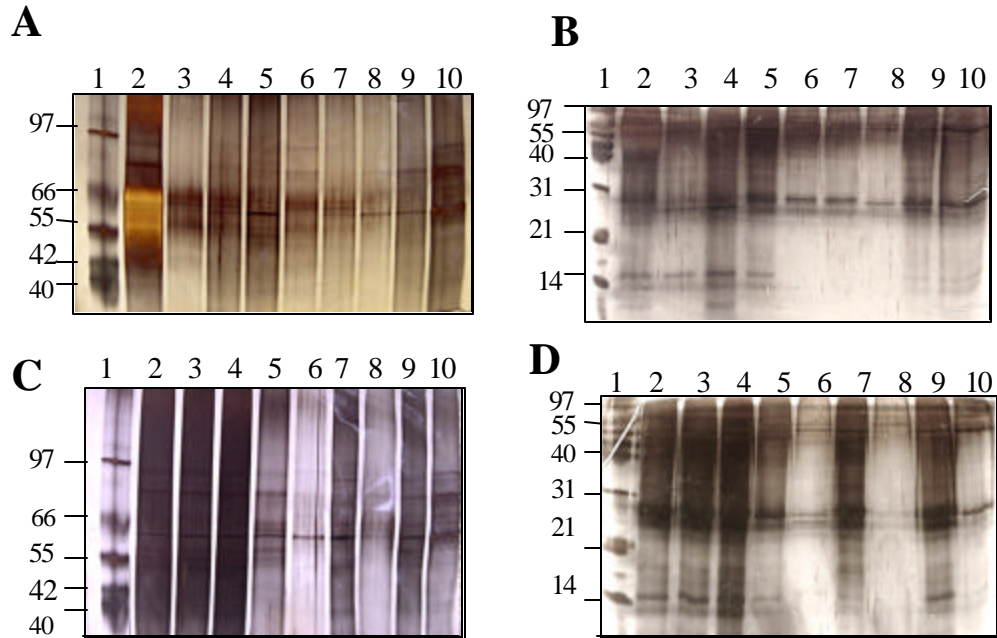


Figure 4-4. Silver staining of SDS-PAGE gels containing proteins from partially purified CTV inclusion bodies (IB) from citrus tristeza virus (CTV) infected and healthy bark tissue

Gels of 10% (B and D) and 12% (A and C) were loaded with a fraction of the purified and ESB-solubilized IB proteins. Gels A and B: Lane 1: protein standard; lane 2: fraction 1 from T66; lanes 3, 4 and 5: fractions 1, 2 and 3 from T36; lanes 6 and 7: fraction 1 and 2 from T4; lanes 8 and 9: fractions 1 and 2 from T3; lane 10: proteins from healthy tissue. Gels C and D: Lane 1: protein standard; lanes 2 and 3: fractions 1 and 2 from T55; lane 4: fraction 1 from T30, lane 5: fraction 2 from T66; lane 6: fraction 4 from T36; lane 7: fraction 3 from T4; lane 8: fraction 3 from T3, lane 9: fraction 3 from T55, lane 10: proteins from healthy tissue. The numbers to the left indicate the molecular masses of the standards run in lane 1

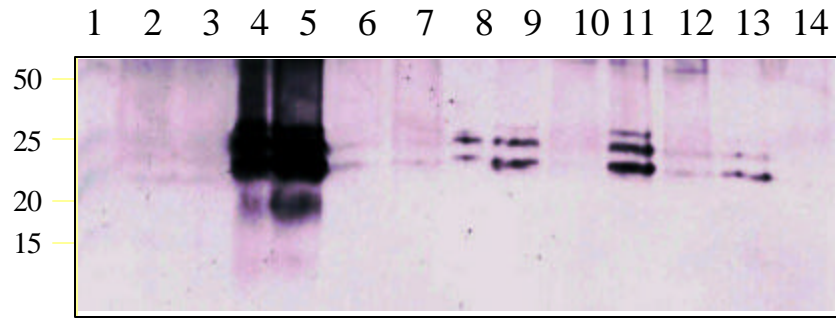


Figure 4-5. Western blot detection of the CTV-CP in the purified inclusion bodies. Lane 1: protein standard; lanes 2 and 3: fractions 1 and 2 from T55; lanes 4, 5, and 6: fractions 1, 2, and 3 from T36; lane 7: fraction 1 from T30; lanes 8 and 9: fractions 1 and 2 from T3; lane 10: fraction 3 from T55; lane 11: fraction 4 from T36; lane 12: fraction 2 from T30; lane 13: fraction 3 from T3; lane 14: proteins from healthy tissue.

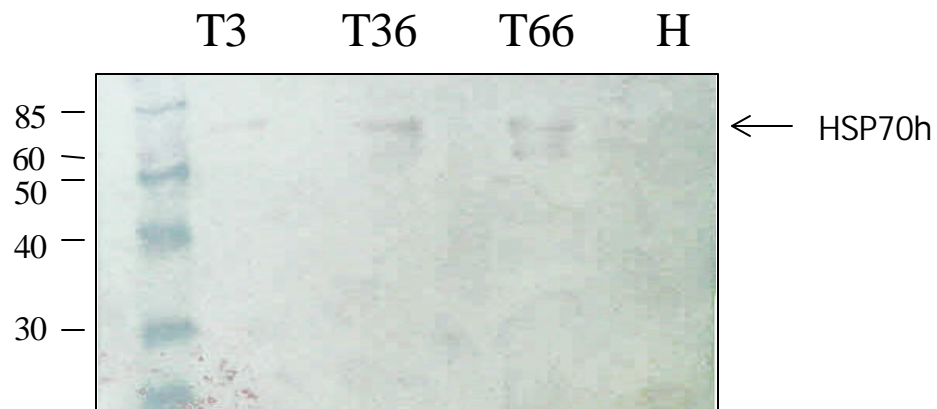


Figure 4-6. Western blot detection of the CTV-HSP70h in the purified inclusion bodies (IB). The IB-proteins loaded in each lane are shown at the top of the figure.

and the presence of more host proteins was found in this size group of proteins than in the proteins of lower molecular mass, as detected by the silver staining.

### **Western Blot Analysis**

Western blot analysis was performed with the proteins from fractions from the cesium sulfate gradient. When the CP antibody was used to probe the membrane, the CP was found at different concentrations in all fractions collected for the different isolates used in this study. This band was absent in the proteins from fractions from healthy citrus tissue (Figure 4-5)

The chicken antibody raised against the CTV HSP70h protein was used for immunodetection of the HSP70h in the virus IB. The Western blots revealed a band with a molecular mass higher than 60 kDa present in the viral IB fractions that was absent in the fractions isolated from healthy tissue extracts. A membrane containing the solubilized IB from the top fractions for isolates T36, T66 and T3 is shown in Figure 4-6. Isolate T66 also contains an extra band of lower molecular weight, which may correspond to a some proteolysis product of the HSP70h. No bands of similar molecular mass were observed from fractions collected from healthy tissues (Fig. 4-6).

When the blots were treated with antibodies raised against the p20, p23, RdRp, and p18 proteins, there was not detection of bands of the expected sizes associated with the CTV IB. Only the p27 antibody gave a weak reaction when used for immunodetection of the minor coat protein in the viral inclusions (not shown).

## Discussion

A protocol for purification of the IB present in CTV infected tissue was optimized based on the previously reported procedure (Lee *et al.*,1982). This protocol, based on two step gradient centrifugations, enabled recovery of fractions containing IB from the CTV-infected tissue which sedimented at different positions in the gradient than the proteins present in healthy citrus tissue extracts.

When these proteins were analyzed by fluorescent labeled antibody microscopy, only the CP and p27 proteins were detected in the CTV inclusions. The non-specific reaction by the chicken preimmune serum with the IB proteins precluded the use of this technique to analyze the presence of the HSP70h in these structures.

The SDS-PAGE showed that there is no great variability in the protein composition of the viral IB. Although there were not enough isolates included in this study to associate a protein pattern with specific biological activity, there was similarity in the patterns obtained between the top fractions of the severe isolates T36 and T66, and the mild isolates T55 and T30, respectively. The silver stained gels also demonstrated that the fractions containing the CTV IB also contained numerous host proteins, despite their different locations following the step gradient centrifugation.

Western blot analysis indicated the presence of the HSP70h in the IB fractions from CTV-infected tissue but present in low amounts. Therefore, it is necessary to complement the present study with immunogold labeling analysis of ultrathin sections of CTV-infected tissue to gain additional evidence about the presence of these proteins in the viral IB.

The p20 protein from CTV was reported to be the major constituent of the amorphous IB (Gowda *et al*, 2000). In that study, ultrathin sections from CTV-infected

tissue were examined by TEM, and the p20 antibody associated primarily with the amorphous IB, while the CP-specific antibody associated primarily with the crystalline IB which are thought to be composed of aggregates of virions.

We did not find evidence of the p20 protein in the purified CTV-IB. We do not know if the purification procedure used in this study allowed the purification of both the amorphous and crystalline inclusions which are associated with closterovirus infected tissue. One possibility is that our procedure enhances the purification of the crystalline inclusions, and not the amorphous structures, which could explain the absence of the p20 antibody reaction.

For many positive-stranded RNA viruses, replication is associated with cell membranes (Buck, 1996). For assembly of the replicative complexes, some viruses employ the use of pre-existing membrane organelles, whereas others induce their own modification, leading to the formation of cytopathic ultrastructures. In closterovirus-infected tissue, two types of IB have been described in phloem associated cells. These are the amorphous and vesiculated inclusions, and the crystalline aggregates. The proteins encoded by the first ORF from BYV, p63 (methyltransferase-like) and p100 (helicase-like), have been localized in the membranous-structures induced by the virus and are referred as BYV-type vesicles. This ORF is known to encode the principal viral products involved in RNA-replication and transcription *in vivo*. These results led to the suggestion that the BYV-type of vesicle membranes are the specific sites of closterovirus replication (Erokhina *et al.*, 2000). However, Gowda *et al.* (2000) concluded that the amorphous IB of CTV do not appear to be involved in virus assembly, since antibody

localization experiments showed little CP to be associated with these amorphous inclusions.

The viral chaperone appears to be required for efficient virion formation (Satyanarayana *et al.*, 2000). Results from Chapter 3 indicate that the viral chaperone protein (HSP70h) is expressed, and that it forms a complex with the CTV virion or with the individual capsid proteins during the process of infection by CTV. In our study, abundant CP was found in the purified IB, and the Western blot analysis also indicated that the HSP70h was present in these structures. We do not know if the IB isolated using the purification procedure described in this chapter are the site of CTV-replication, or if the presence of the HSP70h in the inclusions is simply the result of the protein association with the virion.

Further detailed ultrastructural analysis is necessary to provide information on the specific localization of the HSP70h at the cellular level, and the types of IB purified by the protocol described here.

CHAPTER 5  
AGROBACTERIUM-MEDIATED TRANSFORMATION OF DUNCAN GRAPEFRUIT  
(*Citrus paradisi*; Macf)

**Introduction**

Viral diseases cause serious losses worldwide in horticultural and agricultural crops. Conventional breeding programs to develop resistance are effective, but the time needed to release a new variety, and the possibility of integration of undesirable traits make plant transformation technology an important approach for cultivar improvement. The powerful combination of genetic engineering and conventional breeding programs permits useful traits encoded by transgenes to be introduced into commercial crops within a viable time frame (Hansen and Wright, 1999).

An alternative approach to engineering resistance was proposed by Sanford and Johnson (1985); they suggested the possibility of engineering resistance by transforming a susceptible plant with genes derived from the pathogen itself. This was named “parasite-derived resistance”, but subsequently the term “pathogen-derived resistance” (PDR) became more commonly used. The PDR concept states that the expression of a viral gene at either an inappropriate time or in inappropriate amounts or in an inappropriate form during the infection cycle can perturb the ability of the pathogen to sustain an infection. Therefore, plant viral transgenes can protect plants from infection by the virus from which the transgene was derived.

Transgenic plants carrying plant virus-derived nucleotide sequences can exhibit increased resistance to the viral diseases. Many viral sequences confer some level of either resistance to infection or suppression of disease symptoms, which is better known as tolerance (Fitchen and Beachy, 1993). The viral sequences used to developed PDR include those encoding capsid or coat proteins (CP), viral replicase, movement proteins, non- translatable sequences, defective interfering or satellite viruses, etc (Baulcombe, 1996).

In 1986, Powell *et al.* first demonstrated that transgenic tobacco plants expressing the CP gene from tobacco mosaic virus (TMV) had an increased level of resistance to TMV infection. Since then, numerous crop species have been genetically modified by transformation with the viral CP with the intent of producing virus-resistant varieties (Fitchen and Beachy, 1993). The majority of viruses for which PDR has been successfully developed have positive-stranded RNA genomes. These include members of the tobamo-, cucumo-, potex-, poty-, luteo-, carla-, ilar-, tobra-, nepo-, and alfalfa mosaic groups (Lomonosoff, 1995).

The resistance mechanism(s) are not yet completely understood, but it is known that transgene products (RNA or protein) are involved (Jacquet *et al.*, 1998). Evidence that the accumulation of CP itself is responsible for at least some cases of coat protein mediated resistance (CPMR) has been provided for both TMV (Nejidat and Beachy, 1989) and cucumber mosaic virus (CMV) (Okuno *et al.*, 1993). Additionally, for transgenic plants with heterologous or defective versions of movement proteins, there is some evidence that the protein itself is responsible for the resistant phenotype (Lapidot *et al.*, 1993; Zhang *et al.*, 1999). It also has been shown that only a dysfunctional form of

the movement protein can give rise to resistance, whereas the presence of wild type protein may actually potentiate virus infection (Lomonossoff, 1995; Zhang *et al.*, 1999). Thus, the defect in the movement protein has the properties of a dominant negative mutation (Herskovitz, 1987).

On the other hand, indications that the expression of a protein was not a requisite for resistance came from the finding of the lack of correlation between protein levels and resistance in plants containing CP genes from potato leafroll virus (PLRV), potato virus Y (PVY) (Kawchuk *et al.*, 1990), and tobacco etch virus (TEV) (Lindbo and Dougherty, 1992a; Lindbo and Dougherty, 1992b). In these cases, resistance did not require the synthesis of any virus-derived protein, or protein fragment, but instead the expressed RNA. This phenomenon became known as RNA-mediated resistance and was characterized by a high level of resistance not easy to overcome by a high inoculum dose, as compared to protein-mediated resistance (Lomonossoff, 1995). Its high sequence specificity is another characteristic of RNA-mediated resistance, since this resistance seems to be effective only against closely related viruses (Baulcombe, 1996; Lomonossoff, 1995; Marano and Baulcombe, 1998). A possible mechanism to explain the RNA-mediated resistance was proposed: the presence of the virus or the viral homologous endogenous plant transcript is able to trigger a resistance mechanism active in the cytoplasm which prevents virus replication in the cell (Dougherty *et al.*, 1994; Lindbo *et al.*, 1993).

Recently it was proposed that the RNA-mediated virus resistance appears to induce a form of post-transcriptional gene silencing (PTGS) (Baulcombe, 1996). The PTGS mechanism is typified by the highly specific degradation of both the transgene

mRNA and the target RNA, which contains either the same or complementary nucleotide sequences. If the transgene contains viral sequences, then virus genomic RNA cannot accumulate in the plant (Lindbo and Dougherty, 1992a). In addition, it also was proposed that PTGS is a manifestation of a natural virus resistance mechanism in plants (Baulcombe, 1996; Pruss *et al.*, 1997) since gene silencing can be induced by plant virus infection in the absence of any known homology of the viral genome to host genes, and because viruses can be initiators and targets of the gene silencing (Ratcliff *et al.*, 1997).

Citrus tristeza virus (CTV) is a member of the *Closteroviridae* family. Since the outbreak of decline in sour orange in the early thirties, CTV has caused widespread and important economic losses because it kills citrus trees on sour orange rootstock or as a result of stem pitting on the scion (Bar Joseph *et al.*, 1989). Measures to control losses caused by CTV include quarantine to avoid the introduction of exotic isolates, certification schemes to prevent CTV spread and cross protection with mild isolates (Cervera *et al.*, 1998a; Rocha-Pena *et al.*, 1995). Genetically engineered mild-strain cross protection and RNA-mediated resistance are two strategies currently being considered for management of CTV (Albiach-Marti *et al.*, 2000b).

Genetic transformation and recovery of transgenic citrus trees has been achieved in various species, hybrids and *Citrus* relatives such as sweet orange (*Citrus sinensis* (L) Osbeck) varieties pineapple (Cervera *et al.*, 1998a; Pena *et al.*, 1995a) and Navel (Bond and Roose, 1998), Carrizo citrange (*Citrus sinensis* L.Osbeck x *Poncirus trifoliata*) (Cervera *et al.*, 1998b; Gutierrez *et al.*, 1997; Moore *et al.*, 1992; Peña *et al.*, 1995b), grapefruit (*Citrus paradisi* Macf.) (Luth and Moore, 1999; Yang *et al.*, 2000), *Poncirus trifoliata* (Kaneyoshi *et al.*, 1994) and Mexican lime (*Citrus aurantifolia* Swing.)

(Gutierrez *et al.*, 1997; Peña *et al.*, 1997). Citrus transformation procedures are often inefficient due to the growth of non-transgenic or chimeric shoots during selection, low frequencies of transformation and difficulties in rooting of transgenic shoots (Gutierrez *et al.*, 1997; Peña *et al.*, 1997).

There are some reports of the integration and/or expression of foreign genes other than markers, in *Citrus* or its relatives. Among them, a chemically synthesized gene of the human epidermal growth factor was transformed into *Poncirus trifoliata* under the control of the cauliflower mosaic virus 35S RNA gene promoter, and the introduced gene(s) were expressed in the young leaves of the regenerated plants (Kobayashi *et al.*, 1996). Constitutive expression of the *Arabidopsis* genes LEAFY and APETALA1 obtained by genetic transformation of citrange plants was associated with an appreciable shortening of the juvenile phase of the citrus transformed plants (Peña *et al.*, 2001).

Attempts to develop PDR against CTV have been reported in the literature. Gutierrez *et al.*, (1997) produced transgenic Carrizo citrange, sour orange (*C. aurantium* L.) and key lime plants expressing the CP gene from CTV. Later, Dominguez *et al* (2000) reported the introduction of the CTV-CP into Mexican lime plants by using an improved transformation protocol. This methodology used internodal stem segments from greenhouse-grown seedlings as explant material for transformation. Similarly, Ghorbel *et al.* (2000) showed an enhancement of the transformation frequency of sour orange by using explants from 4-month old seedlings grown in the greenhouse. This method allowed them to introduce the CP-CTV gene into sour orange plants with an efficiency of  $3.6 \pm 1$  %. The p23 gene from CTV was also transformed into Mexican lime plants to study whether the over-expression of this gene, or its truncated form, could

affect the normal CTV-infection process. Interestingly, the constitutive expression of p23 induced a phenotype that resembled the CTV symptoms, whereas the plants containing the truncated form of this gene were normal. They suggested that p23 gene product is involved in symptom development and has a role in CTV pathogenesis (Ghorbel *et al.*, 2001b). None of the reports have shown data for evaluation for CTV-resistance.

The *Closteoviridae* is the only virus family that encodes a protein with similarity to the cellular chaperones, a 70-kDa heat-shock protein homolog (HSP70h). Satyanarayana *et al.* (2000) reported the involvement of HSP70h protein in CTV-assembly. Mutations in the HSP70h-CTV gene resulted in a large decrease in the ability of the virus to be passaged in crude sap and in substantial reductions in the proportion of full length particles. Recently, the HSP70h of BYV, a member of the *Closteroviridae* family, was shown to be involved in intercellular translocation, representing a new type of plant viral-movement protein (Peremyslov *et al.*, 1999).

In this study, two different constructs (full-length and a frameshift mutant) of the HSP70h gene from CTV were transformed into Duncan grapefruit seedlings to test the possibility of inducing PDR, either by over expression of the CTV HSP70h protein or by the expression of a truncated form of this protein.

## **Materials and Methods**

**Cloning and frameshift mutation of the CTV-HSP70h.** The Florida CTV-isolate T3800 was used as a virus source for the process of cloning the HSP70h gene. The biological properties of this isolate have been described in the Material and Methods in Chapter 2. The clone pGEM-T/HSP70h described in Chapter 2 was used as template

for the generation of the constructs described here. The restriction sites *ApaI* and *XhoI* were introduced at the 5' and 3' end of the CTV-HSP70h by PCR amplification, using the primers CN394 (5'-GGGCCCATGGTGCTTTTAGGTTTAG-3') and CN401 (5'-CTCGAGTCAGAGAGGT ATTCTTTCC-3'). Thermocycling conditions were 2 min at 94°C, 40 cycles of 45 sec at 94°C, 60 sec at 50°C and 90 sec at 72°C, followed for a final extension of 5 min at 72°C. The amplified product was cloned into the pGEMT vector, generating the plasmid pGEM-T/HSP70h-1.

For the generation of the frameshift (FS) mutant, the vector pGEM-T/HSP70h-1 was digested with the restriction enzyme *HindIII*. After that, the linearized plasmid was gel-purified using the Genclean II kit (Bio101, Inc.) following the manufacturer instructions; blunt-ended with Klenow fragment and religated to give pGEM-T/HSP70h-1-*HindIII* using standard procedures (Sambrook, 1989). To confirm the frameshift mutation, the plasmid was sequenced at the DNA Sequencing Core Lab, University of Florida, using universal (forward and reverse) M13 primers.

A pUC118-based plasmid vector containing the cauliflower mosaic virus 35S promoter and termination signal (pUC118-35S Poly 2-9) kindly provided by Dr. V. Febres was used for the generation of the plant transformation constructs. First, the full length and frameshift mutant of the CTV-HSP70h were subcloned into the *ApaI*-*XhoI* cloning sites of the pUC118-35S Poly 2-9 vector. This was done by consecutive digestions of the plasmid vectors pGEM-T/HSP70h-1 and pGEM-T/HSP70h-1-*HindIII* with the restriction enzymes *NcoI*, *XhoI*, and *ApaI*. This cloning located the sequence of interest between the 35S promoter and the termination signal. These fragments were then cloned into the *PstI* sites of the binary plant transformation vectors pCambia-2201

and pCambia-2202, both containing the NPT-II gene as a selectable marker and GUS or GFP as reporter genes, respectively. These modified pCambia vectors were then introduced into *Agrobacterium tumefaciens* strain Ag11 using the cold shock transformation method.

***Agrobacterium* co-culture, plant transformation and regeneration.** A protocol previously described for transformation of epicotyl segments of Carrizo citrange and key lime (Moore *et al.*, 1992), and subsequently modified for transformation of etiolated grapefruit seedling (Luth and Moore, 1999) was used for most of the transformation and regeneration steps. A modification that involved an extra step in a shoot elongation medium was included before grafting of the regenerated shoots, according to Yang *et al.* (2000).

**Seed germination.** *Citrus paradisi* cv. Duncan seeds were peeled and sterilized, first with 70% ethanol for 5 min and 0.525% hypochlorite solution plus 0.05% Tween-20 for 10 min, then they were rinsed five times with sterile distilled water. The seeds were placed individually into 150 X 25 mm tubes containing half-strength MS medium (2.13 g/l MS salts, 50 mg/l myo-inositol, 15 g/l sucrose and, pH 5.7) with 7 g/l agar. The tubes were kept in the dark at 28 °C or at room temperature until the germinated seedlings were used for transformation, approximately 4–6 weeks after planting (Figure 5-1).

**Transformation of epicotyl segments.** *Agrobacterium tumefaciens* strain Ag11 containing the binary plasmid pCambia2201 or 2202, with either the CTV-HSP70h full length or the mutant construct, was inoculated into YEP medium (10 g/l Bactopeptone, 10 g/l yeast extract and 5 g/l NaCl, pH 7.0) containing the appropriate antibiotics. They were grown overnight to log phase ( $OD_{600nm} = 0.5-1.0$ ) at 280 rpm and 28°C. The cultures

were centrifuged at 4°C and 5,000 rpm for 5 min, and the pellets were resuspended to a final concentration of  $5 \times 10^8$  cfu/ml in MS medium containing 100 mM acetosyringone.

The epicotyl portions of the etiolated seedlings were cut into 1 cm segments and soaked in the *Agrobacterium* inoculum for 1 min. Then, the inoculated segments were placed horizontally in petri plates containing co-cultivation medium (MS medium plus 7 g/l agar, and 100 mM acetosyringone), the plates were sealed and kept in the dark at room temperature for 2–3 days (Figure 5-1).

**Selection and regeneration of transgenic shoots.** After 2-3 days of co-cultivation, the epicotyl segments were transferred to a shoot induction medium (MS medium with 0.5mg/l benzyl adenine (BA) and 7g/l Bacto-agar) supplemented with 500 mg/l Claforan to inhibit further growth of *Agrobacterium* and with 100 mg/l kanamycin sulfate for selection of transgenic shoots. The plates were maintained at 28°C with a 16-hour photo-period provided by cool-white fluorescent light for 6-8 weeks. Transfers to fresh medium were made at 4 week intervals.

**Rooting of transgenic shoots.** When shoots appeared and reached about 5-10 mm in length, they were removed from the explants and placed on rooting medium (MS medium with 0.5 mg/l naphthalene acetic acid). Shoots remained on this medium for approximately 6 weeks (Figure 5-1). Because after this time there was no evident root formation in any of the shoots, they were transferred to a shoot elongation medium [BG medium composed of MS salts and B5 vitamins, 0.2 mg /l 6-benzylaminopurine (BAP), 0.5 mg/l gibbereic acid (GA3) , 2.5% sucrose, pH 5.8 solidified with 8% agar] containing 500 mg/l Claforan before proceeding with the grafting.

**Grafting of regenerated shoots.** Two month old Carrizo citrange greenhouse-grown seedlings were used as rootstocks for grafting *ex vitro*. The seedlings were decapitated, and a vertical excision was made 3-5 mm deep. The shoots were grafted by cutting them into a V-shape, and inserting them into the incisions on the rootstock. Leaves of the transformed shoots were removed. A standard 200  $\mu$ l pipet tip was used to hold the graft in place. After 2-4 weeks, the scion had grown new leaves, and the pipet tip was removed.

**Analysis of regenerated shoots.** Epicotyl segments transformed with the different constructs previously described were examined periodically for the expression of GFP and GUS, depending on the vector used. The expression of GFP in the regenerated shoots was analyzed by using a dissecting microscope (Zeiss) with a fluorescent light source with a 515 nm long pass emission filter transmitting red and green light and a 450-490 nm excitation filter. GUS expression was analyzed by histochemical staining. The leaves were placed in ELISA plates or 2-ml eppendorf tubes containing the GUS staining solution (50 mM NaPO<sub>4</sub>, pH 7.2, 0.5% Triton X-100, 1mM 5-bromo-4-chloro-3-indolyl- D-glucuronide (X-Gluc)) that was diluted from a 20mM stock made in dimethylformamide). Vacuum was applied for 5 min to infiltrate the leaves with the substrate, and then the tubes or plates were incubated overnight at 37°C with gentle agitation. The staining solution was removed, and the chlorophyll was removed from the leaves with several washes in 70% ethanol.

**PCR amplification assay.** The regenerated shoots were analyzed for the presence of GUS, GFP and HSP70h or HSP70h-*HindIII*. Two or three leaves from the putative transgenic leaves (fresh weight 10-30 mg) were frozen in liquid nitrogen and then homogenized using a micro-pestle in a microcentrifuge tube. Before the sample was thawed, 300  $\mu$ l of extraction buffer (100 mM Tris-HCl, pH 8.0; 50mM EDTA, pH 8.0; 500 mM NaCl, and 0.07%  $\beta$ -mercaptoethanol) were added, and the sample was vortexed vigorously. Then 90  $\mu$ l of 5M potassium acetate were added, and after mixing, the sample was incubated on ice for 30 min. After centrifugation at 7,000 rpm for 5 min at room temperature in a microcentrifuge, the supernatant was transferred to a new microcentrifuge tube. Three volumes of 6M NaI from the GeneClean kit were added to supernatant and mixed, followed by 5  $\mu$ l of the glass milk from the same kit. The tube was incubated at room temperature for 10 min. After three washes with the washing solution from the kit (following the manufacturer instructions), the tubes were dried, and the DNA was eluted in 20  $\mu$ l of water by incubation at 65°C for 10 minutes, and then a centrifugation (2 min) to recover the supernatant.

For PCR detection of the transgene, the DNA was digested with *PstI*, and 5  $\mu$ l of the digest was used for the amplification reaction. The PCR reaction was performed in a final volume of 25  $\mu$ l. The mixture contained 2.5  $\mu$ l of 10X PCR buffer (500mM KCl, 100mM Tris-HCl, pH 9.0 at 25°C and 1.0% Triton X-100), 2.5 mM MgCl<sub>2</sub>, 0.4 mM each dNTP (dATP, dGTP, dCTP, and dTTP), 0.1  $\mu$ g each primer (See Table 5-1 for each set), 2.5 U of Taq DNA polymerase (Promega, Corp), and 5  $\mu$ l of the DNA template.

Thermocycling conditions for all sets of primers were 2 min at 94°C, 35 cycles of 30 sec at 94°C, 30 sec at 52°C and 45 sec at 72°C, followed for a final extension of 5 min at

72°C. PCR products were separated by electrophoresis in 1% agarose gels and photographed using a Fluor-S MAX MultiImager System (Bio-Rad).

Table 5-1. Set of primers used for PCR assay of the putative transgenic plants.

Gene	Sequence	Expected product (bp)
GUS	IPG 25+ 5'- ACCACGCCGAACACCTG-3'	310
	IPG 82- 5'- CTTCACTGCCACTGACC-3'	
GFP	CN 462 5'-ATGGTGAGCAAGGGCGAGGAG-3'	717
	CN 463 5'- CTTGTACAGCTCGTCCATGCC-3'	
HSP70h and FS mutant	CN 466 5'- GATGTTCGAAGGAGATTACG-3'	501
	CN 401 5'- CTCGAGTCAGAGAGGTATCTTTCC-3'	

## Results

### Constructs Used in the Transformation Experiments

The full length and a frameshift mutant of the HSP70h from CTV were selected to genetically engineer grapefruit plants. The frameshift mutant conserved 332 residues (55.9%) from the amino-terminal portion of the total of 594 amino acids of this protein. Several stop codons were introduced at that location, producing a truncated form of the CTV-HSP70h (Figure 5-2). These 332 amino acids contain almost all the motifs identified in the ATPase domain of cellular chaperones that are conserved in the closteroviral chaperon homologs, as indicated in Chapter 2.

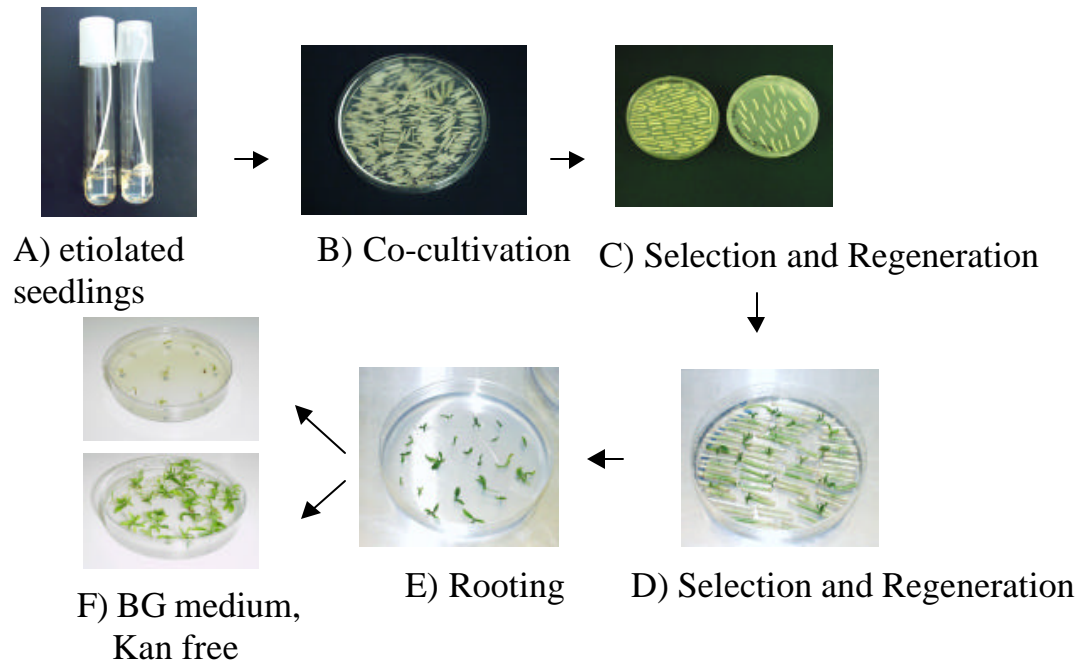


Figure 5-1. *Agrobacterium*-mediated transformation of grapefruit epicotyl segments. (A) *In vitro* grown etiolated seedlings. (B) Co-cultivation of epicotyl segments with the *Agrobacterium* strain AgL1 that contains the binary plasmid with the CTV-HSP70h. (C) and (D) Regeneration of shoots using the antibiotic kanamycin (Kan) for selection. (E) Shoots after transfer to a rooting medium. (F) Shoots after transfer to an elongation medium. Top: shoots that were transformed with the *Agrobacterium* strain AgL1, bottom: non-transformed shoots.

## HSP70h, 5'→3'; Frame 1

atgggtgcttttgggttttagacttcggtaccacgttttcaacagtggctatggccacgtct  
 M V L L G L D F G T T F S T V A M A T S  
 tctgagttagttatactgaaacaatctaattcgtcgtacatacctacgtgtttatcttg  
 S E L V I L K Q S N S S Y I P T C L F L  
 catgcggtatcctaatagtgtgtcttatggttacgacgcagaatatttagcggcttcgggg  
 H A D P N S V S Y G Y D A E Y L A A S G  
 gaaccagggttcattttacaaagatttgaaacgggtgggtcgggtgtaccgagaagaactac  
 E P G S F Y K D L K R W V G C T E K N Y  
 caaacctacttacacaagttatcaccttcttataaggtgatagtgaaagagtttggaact  
 Q T Y L H K L S P S Y K V I V K E F G T  
 aaaagtgtgctgttccgtatgtgtcacctttgaataacgatctcggactcagcatcgct  
 K S V P V P Y L S P L N N D L G L S I A  
 ttacctttactgactcgtttcatacgttaagtcatttttatcggatgcggaacgagtgttt  
 L P L L I A S Y A K S I L S D A E R V F  
 aatgtaagttgtactggagttatatgttcggtacctgctgggttataaacacattacagcga  
 N V S C T G V I C S V P A G Y N T L Q R  
 gcttttacgcaacagagtatatcgttgtcgggttactcttgctgtacattattaatgaa  
 A F T Q Q S I S L S G Y S C V Y I I N E  
 ccttcagccgcccgcgtactccactttacctaagttgagttcggcgggataagtacttagcc  
 P S A A A Y S T L P K L S S A D K Y L A  
 gtttacgacttcgggtgggtgggacttttgacgtttctatagtgagtggttaggttaccacg  
 V Y D F G G G T F D V S I V S V R L P T  
 ttcgccggttagaagttcaggtggtgatatggacttaggcggttagagacatcgataaaaag  
 F A V R S S G G D M D L G G R D I D K K  
 ttatcagataaaaatatatgagatggccgattttgtaccgcaaaaagaactgaacgtttct  
 L S D K I Y E M A D F V P Q K E L N V S  
 agtttaaaggaagctttatctcttcaaaccgatccagtcaggtacaccgtaactcattac  
 S L K E A L S L Q T D P V K Y T V T H Y  
 ggaatgagtgaaaccgatcaatcgatcaaaccgacggttaagggagatagcttcgacgttc  
 G M S E T V S I D Q T T L R E I A S T F  
 ataactcgaacgatagacatacttacgcaagtttaaggttaagtcctagtagctcgaatcg  
 I T R T I D I L T Q V K V K S S M P E S  
 caaagtttaaagctgggtggttagtcggtggaagctcgtacttaccagggctggtggatact  
 Q S L K L V V V G G S S Y L P G L L D T  
 ttggcgaccgtgccttttgtgtctgggatagtagaccagtagaagacgcgagaaccgctggt  
 L A T V P F V S G I V P V E D A R T A V  
 gctagaggggtgctctttatatagcgagtggttggatggttagatccaaggctctactaata  
 A R G C A L Y S E C L D G R S K A L L I  
 gattgtatcacgcacatctttgtcagttacgacatttagcgcggattcgggttggttgca  
 D C I T H H L S V T T F S A D S V V V A  
 gcgccgggtagtcctaattccttttgaaggagaacgaaaactcacgttgtgcaagtgctgtt  
 A A G S P I P F E G E R K L T L C K C V  
 agtacgtctaaatatcaagcaaggatggttcgaaggagattacgaaaagggtttttcgaaat  
 S T S K Y Q A R M F E G D Y E K V F R N  
 gaacgtatatacgtgcttcgggtgtcgttggttcactttgggagtttaactggcagctgctt  
 E R I Y A A S V S L F T L G V N W H V P

Figure 5-2. Nucleotide and amino acid sequences of the CTV-HSP70h and the frameshift mutant cloned in the binary vectors used for transformation. The sequences are shown from 5' to 3' and, the *Hind* III restriction site used to generate the frameshift mutant is underlined. Stop codons are shown as “-“ in the sequence of the generated mutant.

aacgacgttgagatgactctcgtaactaaggtggactcaatgggcaaagtggagttttac  
 N D V E M T L V T K V D S M G K V E F Y  
 cttaaaggtccatctgggtgaattgggtgaacgtgcaaggtacttcgcattatgattatgct  
 L K G P S G E L V N V Q G T S H Y D Y A  
 ggtatgcctcaccctactagaaaagttggtgaggttagcgttagcattacaatgtaagctccgcc  
 G M P H P T R K L L R L S D Y N V S S A  
 gcttttagtttttagctttgacattaactcgcgaaaaacgagaaaggtttcttttgccggaca  
 A L V L A L T L T R E K R E R F L L R T  
 ttatttgacactttaacagcagacttgcgaaagacagcaagtttaagtgagtactcaaag  
 L F D T L T A D L R K T A S L S E Y S K  
 aagtaccgatcactcgaaacgacatcgatgctcgtctcatcacgtatggggatcgttggtt  
 K Y P I T R N D I D V V S S R M G I V V  
 tcgaaagttttacggggaagtgatttggaaagaatacctctctga  
 S K V L R G S D L E R I P L -

HSP70h-*Hind* III (frameshift mutant), 5'→3'; Frame 1

atggtgcttttgggttttagacttcggtaccacgttttcaacagtggttatggccacgtct  
 M V L L G L D F G T T F S T V A M A T S  
 tctgagttagttatactgaaacaatctaattcgtcgtacatacctacgtgtttatctctg  
 S E L V I L K Q S N S S Y I P T C L F L  
 catgcccgatcctaatagtgtgtcttatggttacgacgcagaaatatttagcggcttcgggg  
 H A D P N S V S Y G Y D A E Y L A A S G  
 gaaccaggttcattttacaaagatttgaacgggtgggtcgggtgtaccgagaagaactac  
 E P G S F Y K D L K R W V G C T E K N Y  
 caaacctacttacacaagttatcaccttcttataaggtgatagtgaaagagtttggaaact  
 Q T Y L H K L S P S Y K V I V K E F G T  
 aaaagtgtgcctgtttccgtatattgtcacctttgaataacgatctcggactcagcatcgct  
 K S V P V P Y L S P L N N D L G L S I A  
 ttacctttactgatcgttccatacgttaagtcattttatcgggatgcggaacgagtgttt  
 L P L L I A S Y A K S I L S D A E R V F  
 aatgtaagttgtactggagttatatgttcgggtacctgctgggtataacacattacagcga  
 N V S C T G V I C S V P A G Y N T L Q R  
 gcttttacgcaacagagtatatcgttgtcgggttactcttgctgtgtacattattaatgaa  
 A F T Q Q S I S L S G Y S C V Y I I N E  
 ccttcagccgcccgcgtactccactttacctaagttgagttcggcggataagttacttagcc  
 P S A A A Y S T L P K L S S A D K Y L A  
 gtttacgacttcgggtgggtgggacttttgacgtttctatagtgagtggttaggttaccacg  
 V Y D F G G G T F D V S I V S V R L P T  
 ttccgcttagaagttcaggtggtgatatggacttaggcggtagagacatcgataaaaaag  
 F A V R S S G G D M D L G G R D I D K K  
 ttatcagataaaaatatatgagatggccgattttgtaccgcaaaaagaactgaacgtttct  
 L S D K I Y E M A D F V P Q K E L N V S  
 agtttaaagggaagctagctttatctcttcaaaccgatccagtcaggtacacccgtaactca  
 S L K E A S F I S S N R S S Q V H R N S  
 ttacggaatgagtgaaaccgtatcaatcgatcaaaccgacgttaagggagatagcttcgac  
 L R N E - N R I N R S N D V K G D S F D

Figure 5-2. Continued



with no evident differences in the regeneration rates among the constructs used during the experiments.

During the regeneration process, the new shoots were examined for the expression of GFP, to detect transformation with the vector pCambia 2202 or any of its derivatives. The expression of GFP was never observed under the dissecting fluorescent microscope. Similarly, the regenerated shoots obtained from segments transformed with the vector pCambia 2201, or its derivatives, tested negative for GUS expression when the shoots were transferred to the rooting medium. When tested later in a second assay for GUS activity, six of those shoots surviving in the elongation medium showed positive GUS staining (Table 5-2 and Figure 5-4). Most of the shoots showed chimeric staining patterns, ranging from a few dots to almost completely blue (Figure 5-4).

In the past, our laboratory has experienced some inconsistency with the expression of reporter genes when evaluating transgenic shoots. Therefore, all the regenerated shoots were transferred to rooting medium, and then further evaluations were made. The segments were kept in this medium for more than five weeks, and no roots ever developed. Additionally, the shoots did not show any further growth, and many of them died during this time.

Grafting of transgenic shoots of different citrus species has been reported as a successful alternative to rooting in media (Peña *et al.*, 1995; Yang *et al.*, 2000). The protocol of Yang *et al.* (2000) for grafting of regenerated shoots *ex vitro* was used after invigorization of the regenerated shoots on a non-selective medium. This protocol allowed some growth in some of the shoots, although most of the small regenerated plants continued to die.

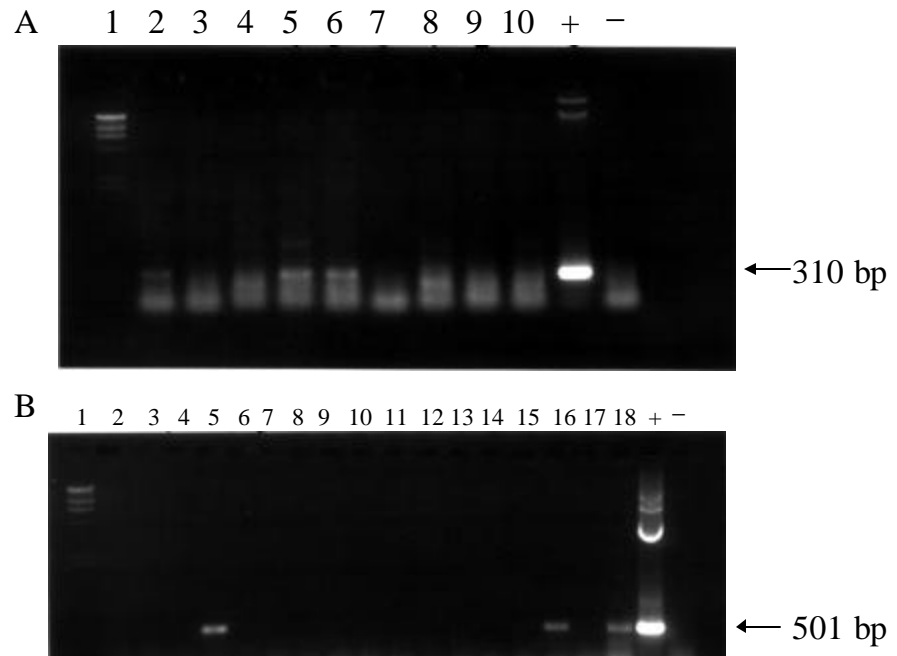


Figure 5-3. Analysis of the putative transgenic Duncan grapefruit plants by PCR. (A) Amplification products obtained using the primer set IPG25 and IPG82, to detect the presence of GUS gene in the plants. . The arrow at the right shows the expected product size Lane 1: Lambda/*Hind* III marker, lanes 2 to 10: PCR amplification using DNA extracted from individual plants transformed with the vector pCambia 2201. In the positive control (+) the template used in the PCR reaction was the vector pCambia 2201, and the template for the negative control (-) was DNA extracted from non-transformed plants. (B). Amplification products obtained using the primer set CN466 and CN401 to detect the presence of the HSP70h or its frameshift mutant in the regenerated plants. The arrow at the right shows the expected size (501 bp). Lane 1: Lambda/*Hind* III marker, lanes 2 to 10: PCR amplification using DNA extracted from plants transformed with the frameshift construct, lanes 11-18: DNA extracted from plants transformed with the full length CTV-HSP70h construct. In the positive control (+), the template used in the PCR reaction was the vector pGEM-T/HSP70h, and the template for the negative control (-) was DNA extracted from non-transformed plants.

Table 5-2. Summary of the results of Duncan grapefruit transformation experiments performed with the constructs containing the CTV-HSP70h, the frameshift mutant (HSP70h-HindIII), or the binary vector by itself.

Vector	N° of segments	Regenerated shoots <sup>1</sup>	N° of survivors <sup>2</sup>	PCR positives <sup>3</sup>	Reporter positives <sup>4</sup>
pCambia-2201	420	96 (23%)	23	4/9	3
pCambia-2201/HSP70h	730	150 (21%)	16	2/8	3
pCambia-2201/HSP70h-HindIII	780	180 (23%)	50	1/9	0
pCambia-2202	550	115 (21%)	13	4/10	0
pCambia-2202/HSP70h	850	203 (24%)	32	0/13	0
pCambia-2201/HSP70h-HindIII	904	230 (25%)	14	1/7	0

<sup>1</sup> The percentage of shoots was calculated based on the number of segments used for each construct.

<sup>2</sup> Number of shoots growing in the elongation medium.

<sup>3</sup> The constructs containing the CTV-HSP70h or the frameshift mutant of this gene were amplified with the primer set CN466-CN401. To assay for the presence of the vectors pCambia 2201 or 2202, the GUS and GFP primers were used in the PCR reactions, respectively.

<sup>4</sup> The reporter for the vector pCambia 2201 is the GUS gene, and for vector pCambia 2202 it is the GFP gene.

### PCR Assay of the Putative Transgenic Plants

After one month in the shoot elongation medium, plants showing at least two developing leaves were selected for PCR analysis for the presence of the transgene. The expected amplification product was obtained from seven of the regenerated plants transformed with the binary vector pCambia 2201 and from five of the plants transformed with the vector pCambia 2202 (Table 5-2, Figure 5-3). The primer set CN462-CN463, which amplifies the GFP gene, produced faint bands (not shown). This may be due to the

low amount of DNA obtained from the samples, or possibly due to the presence of some residual *Agrobacterium* that survived from the initial co-culture step. Further analysis is needed when more green tissue is available.

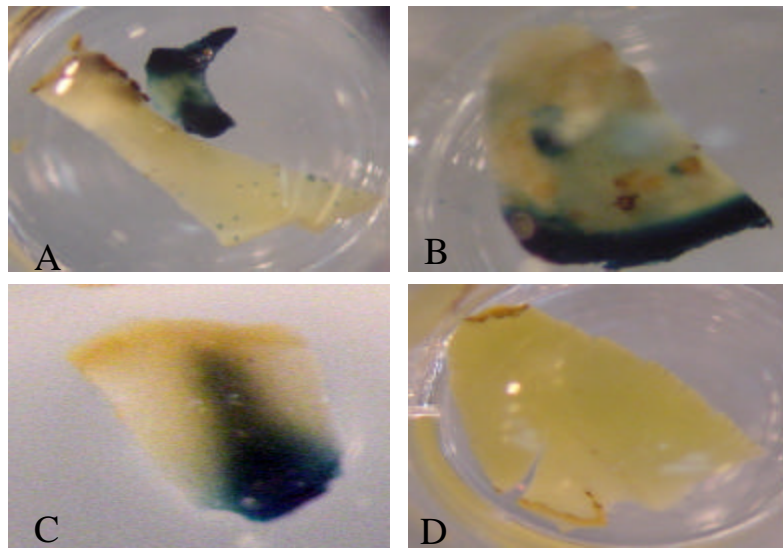


Figure 5-4. Histochemical GUS-staining of the regenerated shoots. (A) through (C) show shoots regenerated from epicotyl segments transformed with *Agrobacterium tumefaciens* carrying derivatives of the binary vector pCambia 2201. A shoot regenerated from a non-transformed epicotyl segment is shown in (D).

## Conclusions

In an attempt to obtain PDR against CTV, *Agrobacterium*-mediated transformation of Duncan grapefruit was conducted using two different constructs, one with a full length CTV-HSP70h gene and the second using a truncated form of the HSP70h. From approximately 3000 epicotyl segments that were transformed with these constructs, only six plants have been positively scored as transgenic by histochemical GUS staining. The expression of the GFP reporter gene was not detected in the regenerated plants. This could be due to an unsuccessful transformation process, or due to problems with the expression of the GFP gene in citrus.

The use of epicotyl explants for agro-transformation of Duncan grapefruit has been previously reported with success (Luth and Moore, 1999). In these experiments, the same citrus cultivar and transformation techniques were used. However, factors such as the type of *Agrobacterium* strain, size of the T-DNA and characteristics of the transgene could influence the efficiency of the transformation process.

The two main components for successful *Agrobacterium*-mediated gene transfer are the T-DNA and the vir gene region. The modern binary vectors take advantage of the fact that these two components can reside in different plasmids (Hellens *et al.*, 2000), so these functions are provided by the binary vectors and the disarmed Ti plasmids, respectively. The strain AgL1 used in the transformation process described here contains the Ti-plasmid “pTiBo542ΔT-DNA” (Hellens *et al.*, 2000), which is equivalent to the plasmid present in the supervirulent strain A281. A disarmed derivative of this strain, EHA105, showed super-transformation ability in citrus (Ghorbel *et al.*, 2001). The

binary vector used by Ghorbel *et al.* (2001) , and the co-cultivation in a medium rich in auxins may account of the better results that they obtained.

In addition we can not rule out that the presence of the transgene interfered with the normal development of the regenerated plants. The CTV-HSP70h shows high homology to the cellular chaperones, proteins whose expression seems to be tightly regulated. The constitutive expression of the CTV-HSP70h under the control of the 35S promoter may have been detrimental to the new regenerated transgenic plants, negatively affecting the number of plants recovered.

At present, the plants which have been scored GUS positive have been grafted onto Carrizo citrange rootstock, along with several plants which scored GFP negative. We are awaiting development of new shoots to conduct further evaluations including Northern blot hybridization to detect levels of synthesis of the CTVHSP70h transcript and the number copies of the transgene in those plants.

## LIST OF REFERENCES

- Agranovsky, A. A., Boyko, V. P., Karasev, A. V., Koonin, E. V., and Dolja, V. V. (1991). Putative 65 kDa protein of beet yellows closterovirus is a homologue of HSP70 heat shock proteins. *J Mol Biol* **217**, 603-610
- Agranovsky, A. A., Lesemann, D. E., Maiss, E., Hull, R., and Atabekov, J. G. (1995). "Rattlesnake" structure of a filamentous plant RNA virus built of two capsid proteins. *Proc Natl Acad Sci U S A* **92**, 2470-2473.
- Albiach-Marti, M., Grosser, J. W., Hilf, M., Gowda, S., Mawassi, M., Satynarayana, T., Garnsey, S., and Dawson, W. (1999). CTV resistant plants are not immune at the cellular level. *Abstract of the 18<sup>th</sup> Annual Meeting of the American Society for Virology*. University of Massachusetts, Amherst, Mass., July 10-14, 1999, p 192.
- Albiach-Marti, M. R., Guerri, J., de Mendoza, A. H., Laigret, F., Ballester-Olmos, J. F., and Moreno, P. (2000a). Aphid transmission alters the genomic and defective RNA populations of citrus tristeza virus isolates. *Phytopathology* **90**, 134-138.
- Albiach-Marti, M. R., Mawassi, M., Gowda, S., Satyanarayana, T., Hilf, M. E., Shanker, S., Almira, E. C., Vives, M. C., Lopez, C., Guerri, J., Flores, R., Moreno, P., Garnsey, S. M., and Dawson, W. O. (2000b). Sequences of citrus tristeza virus separated in time and space are essentially identical. *J Virol* **74**, 6856-65.
- Alzhanova, D. V., Hagiwara, Y., Peremyslov, V. V., and Dolja, V. V. (2000). Genetic analysis of the cell-to-cell movement of beet yellows closterovirus. *Virology* **268**, 192-200.
- Ayllon, M. A., Lopez, C., Navas-Castillo, J., Mawassi, M., Dawson, W. O., Guerri, J., Flores, R., and Moreno, P. (1999a). New defective RNAs from citrus tristeza virus: evidence for a replicase-driven template switching mechanism in their generation. *J Gen Virol* **80**, 817-21.
- Ayllon, M. A., Rubio, L., Moya, A., Guerri, J., and Moreno, P. (1999b). The haplotype distribution of two genes of citrus tristeza virus is altered after host change or aphid transmission. *Virology* **255**, 32-9.
- Bar-Joseph, M., Garnsey, S. M., and Gonsalves, D. (1979). Closteroviruses: A distinct group of elongated plant viruses. *Adv. Virus Res.* **25**, 93-168.
- Bar-Joseph, M., and Lee, R. (1989). Citrus tristeza virus. *CMI/AAB Descriptions Plant Viruses* **353**. Assoc. Appl. Biol., Wellesbourne, UK. p7

- Bar-Joseph, M., Marcus, R., and Lee, R.F. (1989). The continuous challenge of citrus tristeza virus control. *Annu. Rev. Phytopathol.* **27**, 291-316.
- Bar-Joseph, M., Yang, G., Gafny, R., and Mawassi, M. (1997). Subgenomic RNAs: The possible building blocks for modular recombination of *Closteroviridae* genomes. *Semin Virol* **8**, 113-119.
- Baulcombe, D. C. (1996). Mechanisms of pathogen-derived resistance to viruses in transgenic plants. *Plant Cell* **8**, 1833-1844
- Bond, J. E., and Roose, M. L. (1998). *Agrobacterium*-mediated transformation of the commercially important citrus cultivar Washington navel orange. *Plant Cell Rep* **18**, 229-234
- Brlansky, R. H. (1987). Inclusion bodies produced in *Citrus* spp. by citrus tristeza virus. *Phytophylactica* **19**, 211-214.
- Brlansky, R. H., Lee, R. F., and Garnsey, S. M. (1988). *In situ* immunofluorescence for the detection of citrus tristeza inclusion bodies. *Plant Dis* **72**, 1039-1041.
- Brlansky, R. H., and Lee, R. F. (1990). Numbers of inclusion bodies produced by mild and severe strains of citrus tristeza virus in seven citrus hosts. *Plant Dis* **74**, 297-299.
- Broadbent, P., Brlansky, R. H., and Indsto, J. (1996). Biological characterization of Australian isolates of citrus tristeza virus and separation of subisolates by single aphid transmissions. *Plant Disease* **80**, 329-333.
- Brunt, A. A., Crabtree, K., Dallwitz, M.J., Gibbs, A.J., Watson, L. and Zurcher, E.J. (eds.) (1996). *Plant viruses online: descriptions and lists from the VIDE database*. Version: 20th August 1996. 18<sup>th</sup> September 2001 <http://image.fs.uidaho.edu/vide/refs.htm>.
- Buck, K. (1996). Comparison of the replication of positive-stranded RNA viruses of plants and animals. *AdvVirus Res.* **47**, 159-251.
- Camenisch, G., Tini, M., Chilov, D., Kvietikova, I., Srinivas, V., Caro, J., Spielmann, P., Wenger, R. H., and Gassmann, M. (1999). General applicability of chicken egg yolk antibodies: the performance of IgY immunoglobulins raised against the hypoxia-inducible factor 1alpha. *Faseb J* **13**, 81-8.
- Cervera, M., Juarez, J., Navarro, A., Pina, J. A., Duran-Vila, N., Navarro, L., and Peña, L. (1998a). Genetic transformation and regeneration of mature tissues of woody fruit plants bypassing the juvenile stage. *Transgenic Res* **7**, 51-59.
- Cervera, M., Pina, J. A., Juarez, J., Navarro, L., and Peña, L. (1998b). *Agrobacterium*-mediated transformation of citrange: factors affecting transformation and regeneration. *Plant Cell Rep* **18**, 271-278.

- Cevik, B., Chandrika, R., Manjunath, K. L., Lee, R. F., and Niblett, C. L. (1999). Characterization of the ribosomal +1 frameshift in the RNA-dependent RNA polymerase gene of citrus tristeza closterovirus. *Phytopathology* **89**, 13.
- Cevik, B. (2001). Characterization of the RNA-dependent RNA polymerase gene of citrus tristeza closterovirus. PhD. Dissertation. University of Florida, Gainesville
- Che, X., Piestun, D., Mawassi, M., Yang, G., Satyanarayana, T., Gowda, S., Dawson, W. O., and Bar\_Joseph, M. (2001). 5'-coterminal subgenomic RNAs in citrus tristeza virus-infected cells. *Virology* **283**, 374-381.
- Chervitz, S. A., Aravind, L., Sherlock, G., Ball, C. A., Koonin, E. V., Dwight, S. S., Harris, M. A., Dolinski, K., Mohr, S., Smith, T., Weng, S., Cherry, J. M., and Botstein, D. (1998). Comparison of the complete protein sets of worm and yeast: orthology and divergence. *Science* **282**, 2022-2028.
- Christie, R. G., and Edwarson, J. R. (1977). *Light and electron microcopy of plant virus inclusions*. Florida agricultural experimental station monograph series 9.
- Craig, E. A., Gambill, B. D., and Nelson, R. J. (1993). Heat shock proteins: molecular chaperones of protein biogenesis. *Microbiol Rev* **57**, 402-414.
- Cripe, T. P., Delos, S. E., Estes, P. A., and Garcea, R. L. (1995). *In vivo* and *in vitro* association of hsc70 with polyomavirus capsid proteins. *J Virol* **69**, 7807-7813
- Deng, Z., Huang, S., Ling, P., Chen, C., Yu, C., Weber, C. A., Moore, G. A., and Gmitter, F. G. (2000). Cloning and characterization of NBS-LRR class resistance-gene candidate sequences in citrus. *Theor Appl Genet* **101**, 814-822.
- Deng, Z., Huang, S., Ling, P., Yu, C., Tao, Q., Chen, C., Wendell, M. K., Zhang, H. B., and Gmitter, F. G. (2001a). Fine genetic mapping and BAC contig development for the citrus tristeza virus resistance gene locus in *Poncirus trifoliata* (Raf.). *Mol Gen Genomics* **265**, 739-747.
- Deng, Z., Tao, Q., Chang, Y. L., Huang, S., Ling, P., Yu, C., Chen, C., Gmitter, F. G., and Zhang, H. B. (2001b). Construction of a bacterial artificial chromosome (BAC) library for citrus and identification of BAC contigs containing resistance gene candidates. *Theor App Genet* **102**, 1177-1184.
- Derrick, K. S., and Brlansky, R. H. (1976). Assay for viruses and mycoplasmas using serologically specific electron microscopy. *Phytopathology* **66**, 815-820.
- Dolja, V. V., Karasev, A. V., and Koonin, E. V. (1994). Molecular biology and evolution of closteroviruses: Sophisticated build-up of large RNA genomes. *Annu Rev of Phytopathol* **32**, 261-285.

- Dominguez, A., Guerri, J., Cambra, M., Navarro, L., Moreno, P., and Pena, L. (2000). Efficient production of transgenic citrus plants expressing the coat protein gene of citrus tristeza virus. *Plant Cell Rep* **19**, 427-433.
- Dougherty, W. G., Lindbo, J. A., Smith, H. A., Parks, T. D., Swaney, S., and Proebsting, W. M. (1994). RNA-mediated virus-resistance in transgenic plants - exploitation of a cellular pathway possibly involved in RNA degradation. *Mol Plant Microbe Interact* **7**, 544-552.
- d'Urso, F., Ayllon, M. A., Rubio, L., Sambade, A., de Mendoza, A. H., Guerri, J., Moreno, P., and Moreno, P. (2000). Contribution of uneven distribution of genomic RNA variants of citrus tristeza virus (CTV) within the plant to changes in the viral population following aphid transmission. *Plant Pathol* **49**, 288-294.
- Erokhina, T. N., Zinovkin, R. A., Vitushkina, M. V., Jelkmann, W., and Agranovsky, A. A. (2000). Detection of beet yellows closterovirus methyltransferase-like and helicase-like proteins *in vivo* using monoclonal antibodies. *J Gen Virol* **81**, 597-603.
- Fang, D. Q., Federici, C. T., and Roose, M. L. (1998). A high-resolution linkage map of the citrus tristeza virus resistance gene region in *Poncirus trifoliata* (L.) Raf. *Genetics* **150**, 883-890.
- Febres, V. J., Pappu, H. R., Anderson, E. J., Pappu, S. S., Lee, R. F., and Niblett, C. L. (1994). The diverged copy of the citrus tristeza virus coat protein is expressed *in vivo*. *Virology* **201**, 178-181.
- Febres, V. J., Ashoulin, L., Mawassi, M., Frank, A., Bar-Joseph, M., Manjunath, K. L., Lee, R. F., and Niblett, C. L. (1996). The p27 protein is present at one end of citrus tristeza virus particles. *Phytopathology* **86**, 1331-1335.
- Fitchen, J. H., and Beachy, R. N. (1993). Genetically-engineered protection against viruses in transgenic plants. *Annu Rev Microbiol* **47**, 739-763.
- Garnsey, S. M., Gonsalves, D., and Purcifull, D. E. (1977). Mechanical transmission of citrus tristeza virus. *Phytopathology* **67**, 965-968.
- Garnsey, S. M., Christie, R. G., and Derrick, K. S. (1980). Detection of citrus tristeza virus II . Light and electron microscopy of inclusions and virus particles. . *In: 8<sup>th</sup> Conf. Int. Organ. Citrus Virol.* (E. C. Calavan, S. M. Garnsey, and L. W. Timmer, Eds.), pp. 9-16. Riverside, California.
- Garnsey, S. M., Barret, H., and Hutchison, D. (1987). Identification of citrus tristeza virus resistance in *Citrus* relatives and its potential applications. *Phytophytolactica* **19**, 187-191.

- Garnsey, S. M., and Muller, G. W. (1988). Efficiency of mechanical transmission of citrus tristeza virus. *In: 10<sup>th</sup> Proc. Conf. Intl. Org. Citrus Virol.* (L. W. Timmer, S. M. Garnsey, and L. Navarro, Eds.), pp. 46-54, Riverside, California.
- Garnsey, S. M., Permar, T. A., Cambra, M., and Henderson, C. T. (1993). Direct tissue blot immunoassay (DTBIA) for detection of citrus tristeza virus. *In: 12<sup>th</sup> Proc. Conf. Intl. Org. Citrus Virol* (IOCV, Ed.), pp. 39-50, Riverside, California.
- Garnsey, S. M., Su, H., and Tsai, M. (1997). Differential susceptibility of pummelo and Swingle citrumelo to isolates of citrus tristeza virus. *In: 13<sup>th</sup> Proc. Conf. Intl. Org. Citrus Virol.* (J. Da Graca, P. Moreno, and R. Yokomi, Eds.), pp. 138-146, Riverside, California.
- Garry, R. F., Ulug, E. T., and Bose, H. R., Jr. (1983). Induction of stress proteins in Sindbis virus- and vesicular stomatitis virus-infected cells. *Virology* **129**, 319-332.
- Gething, M. J. E. (1997). *Guidebook to Molecular Chaperones and Protein Folding Catalyst*. Oxford Univ. Press, Oxford, UK.
- Ghorbel, R., Dominguez, A., Navarro, L., and Peña, L. (2000). High efficiency genetic transformation of sour orange (*Citrus aurantium*) and production of transgenic trees containing the coat protein gene of citrus tristeza virus. *Tree Physiol* **20**, 1183-1189.
- Ghorbel, R., La-Malfa, S., Lopez, M. M., Petit, A., Navarro, L., and Pena, L. (2001a). Additional copies of virG from pTiBo542 provide a super-transformation ability to *Agrobacterium tumefaciens* in citrus. *Physiol Mol Plant Pathol* **58**, 103-110
- Ghorbel, R., Lopez, C., Fagoaga, C., Moreno, P., Navarro, A., Flores, R., and Pena, L. (2001b). Transgenic citrus plants expressing the citrus tristeza virus p23 protein exhibit viral-like symptoms. *Mol Plant Pathol* **2**, 27-36.
- Gmitter, F. G., Xiao, S. Y., Huang, S., Hu, X. L., Garnsey, S. M., and Deng, Z. (1996). A localized linkage map of the citrus tristeza virus resistance gene region. *Theor App Genet* **92**, 688-695.
- Gowda, S., Satyanarayana, T., Davis, C. L., Navas-Castillo, J., Albiach-Marti, M. R., Mawassi, M., Valkov, N., Bar-Joseph, M., Moreno, P., and Dawson, W. O. (2000). The p20 gene product of citrus tristeza virus accumulates in the amorphous inclusion bodies. *Virology* **274**, 246-254.
- Gowda, S., Satyanarayana, T., Ayllon, M. A., Albiach-Marti, M. R., Mawassi, M., Rabindran, S., Garnsey, S. M., and Dawson, W. O. (2001). Characterization of the cis-acting elements controlling subgenomic mRNAs of citrus tristeza virus: Production of positive- and negative-stranded 3'-terminal and positive-stranded 5'-terminal RNAs. *Virology* **286**, 134-151.

- Gutierrez, M. A., Luth, D., and Moore, G. A. (1997). Factors affecting *Agrobacterium*-mediated transformation in *Citrus* and production of sour orange (*Citrus aurantium* L.) plants expressing the coat protein gene of citrus tristeza virus. *Plant Cell Rep* **16**, 745-753.
- Guy, C. L., and Li, Q. B. (1998). The organization and evolution of the spinach stress 70 molecular chaperone gene family. *Plant Cell* **10**, 539-56.
- Halbert, S. E. (1997). Brown citrus aphid: Current situation and prognosis. *Cit. Ind.*, April Issue.
- Hansen, G., and Wright, M. S. (1999). Recent advances in the transformation of plants. *Trends Plant Sci* **4**, 226-231.
- Harrison, B. D., and Murrant, A. F. (1984). Involvement of virus-coded proteins in transmission of plant viruses by vectors. *In: Vectors in Virus Biology*, pp. 1-36. Academic Press, London.
- Hartl, F. U. (1996). Molecular chaperones in cellular protein folding. *Nature* **381**, 571-579.
- Hellens, R., Mullineaux, P., and Klee, H. (2000). A guide to *Agrobacterium* binary Ti vectors. *Trends Plant Sci* **5**, 446-451.
- Herskovitz (1987). Functional inactivation of genes by dominant negative mutations. *Nature* **229**, 219-222.
- Hilf, M. E., Karasev, A. V., Pappu, H. R., Gumpf, D. J., Niblett, C. L., and Garnsey, S. M. (1995). Characterization of citrus tristeza virus subgenomic RNAs in infected tissue. *Virology* **208**, 576-82.
- Jacquet, C., Ravelonandro, M., Bachelier, J. C., and Dunez, J. (1998). High resistance to plum pox virus (PPV) in transgenic plants containing modified and truncated forms of PPV coat protein gene. *Transgenic Res* **7**, 29-39.
- Kaneyoshi, J., Kobayashi, S., Nakamura, Y., Shigemoto, N., and Doi, Y. (1994). A simple and efficient gene-transfer system of trifoliolate orange (*Poncirus-Trifoliata* Raf). *Plant Cell Rep* **13**, 541-545.
- Karasev, A. V., Nikolaeva, O. V., Koonin, E. V., Gumpf, D. J., and Garnsey, S. M. (1994). Screening of the closterovirus genome by degenerate primer-mediated polymerase chain reaction. *J Gen Virol* **75**, 1415-1422.
- Karasev, A. V., Boyko, V. P., Gowda, S., Nikolaeva, O. V., Hilf, M. E., Koonin, E. V., Niblett, C. L., Cline, K., Gumpf, D. J., Lee, R. F., and et al. (1995). Complete sequence of the citrus tristeza virus RNA genome. *Virology* **208**, 511-520.

- Karasev, A. V. (2000). Genetic diversity, and evolution of closteroviruses. *Annu. Rev. Phytopathol.* **38**, 293-324.
- Karlin, S., and Brocchieri, L. (1998). Heat shock protein 70 family : Multiple sequence comparisons, function, and evolution. *J Mol Evol* **47**, 565-577.
- Kawchuk, L. M., Martin, R. R., and Mcpherson, J. (1990). Resistance in transgenic potato expressing the potato leafroll virus coat protein gene. *Mol Plant Microbe Interact* **3**, 301-307.
- Kitajima, E. M., and Costa, A. (1968). Electron microscopy of the tristeza virus in citrus leaves. *In: 4<sup>th</sup> Conf. Int. Organ. Citrus Virol.* (J.F.Childs, Ed.), pp. 59-64., Gainesville, Florida.
- Kobayashi, S., Nakamura, Y., Kaneyoshi, J., Higo, H., and Higo, K. (1996). Transformation of kiwifruit (*Actinidia chinensis*) and trifoliolate orange (*Poncirus trifoliata*) with a synthetic gene encoding the human epidermal growth factor (hEGF). *J Japan Soc Hort Sci* **64**, 763-769.
- Kong, P., Rubio, L., Polek, M., and Falk, B. W. (2000). Population structure and genetic diversity within California citrus tristeza virus (CTV) isolates. *Virus Genes* **21**, 139-45.
- Lapidot, M., Gafny, R., Ding, B., Wolf, S., Lucas, W. J., and Beachy, R. N. (1993). A dysfunctional movement protein of tobacco mosaic-virus that partially modifies the plasmodesmata and limits virus spread in transgenic plants. *Plant J* **4**, 959-970.
- Lee, R. F., Garnsey, S. M., Brlansky, R. H., and Calvert, L. A. (1982). Purification of inclusion-bodies of citrus tristeza virus. *Phytopathology* **72**(7), 953-953.
- Lee, R. F., Calvert, L. A., Nagel, J., and Hubbard, J. D. (1988). Citrus tristeza virus - characterization of coat proteins. *Phytopathology* **78**, 1221-1226.
- Lee, R. F., Baker, P. S., and Rocha Peña, M. A. (1994). The citrus tristeza virus (CTV): an introduction to current priorities, with special reference to the worsening situation in Central America and the Caribbean. International Institute of Biological Control, Ascot, Berks. UK.
- Lesemann, D. E. (1988). Cytopathology. *In: The plant viruses: The filamentous plant viruses* (R. G. Milne, Ed.), pp. 179-235. Plenum Press, New York.
- Lindquist, S., and Craig, E. A. (1988). The heat-shock proteins. *Annu Rev Genet* **22**, 631-677.
- Lindbo, J. A., and Dougherty, W. G. (1992a). Pathogen-derived resistance to a potyvirus immune and resistant phenotypes in transgenic tobacco expressing altered forms of a potyvirus coat protein nucleotide-sequence *Mol Plant Microbe Interact* **5**, 144-153.

- Lindbo, J. A., and Dougherty, W. G. (1992b). Untranslatable transcripts of the tobacco etch virus coat protein gene sequence can interfere with tobacco etch virus-replication in transgenic plants and protoplasts. *Virology* **189**, 725-733.
- Lindbo, J. A., Silva-Rosales, L., Proebsting, W. M., and Dougherty, W. G. (1993). Induction of a highly specific antiviral state in transgenic plants - implications for regulation of gene-expression and virus-resistance. *Plant Cell* **5**, 1749-1759.
- Lomonosoff, G. P. (1995). Pathogen-derived resistance to plant-viruses. *Ann Rev Phytopathol* **33**, 323-343.
- Lopez, C., Ayllon, M. A., Navas-Castillo, J., Guerri, J., Moreno, P., and Flores, R. (1998). Molecular variability of the 5' and 3'-terminal regions of citrus tristeza virus RNA. *Phytopathology* **88**, 685-691.
- Lopez, C., Navas-Castillo, J., Gowda, S., Moreno, P., and Flores, R. (2000). The 23-kDa protein coded by the 3'-terminal gene of citrus tristeza virus is an RNA-binding protein. *Virology* **269**, 462-70.
- Luth, D., and Moore, G. (1999). Transgenic grapefruit plants obtained by *Agrobacterium tumefaciens*-mediated transformation. *Plant Cell Tissue Organ Culture* **57**, 219-222.
- Macejak, D. G., and Luftig, R. B. (1991). Association of HSP70 with the adenovirus type 5 fiber protein in infected HEp-2 cells. *Virology* **180**, 120-125.
- Macejak, D. G., and Sarnow, P. (1992). Association of heat shock protein 70 with enterovirus capsid precursor P1 in infected human cells. *J Virol* **66**, 1520-1527.
- Manjunath, K. L., Pappu, H. R., Lee, R. F., Niblett, C. L., and Civerolo, E. (1993). Studies on coat protein genes of four Indian isolates of citrus tristeza closterovirus: Cloning, sequencing and expression. In: *12<sup>th</sup> Proc. Conf. Intl. Org. Citrus Virol* (IOCV, Ed.), pp. 20-27, Riverside, California.
- Manjunath, K. L., Chandrika, R., Febres, V., Lee, R. F., and Niblett, C. L. (2000). Molecular characterization of the genome of a grapefruit stem pitting isolate of citrus trsiteza virus from Florida (Abst.). In: *14<sup>th</sup> Proc. Conf. Intl. Org. Citrus Virol* (J. Da Graca, R.F.Lee, and R. Yokomi, Eds.), Campinas, Sao Paulo, Brazil.
- Manjuntah, K. L., Lee, R. F., and Nblett, C. L. (2000b). Recent advances in the molecular biology of citrus tristeza closterovirus. In: *14<sup>th</sup> Proc. Conf. Intl. Org. Citrus Virol* (J. Da Graca, R.F.Lee, and R. Yokomi, Eds.), Campinas, Sao Paulo, Brazil
- Marano, M. R., and Baulcombe, D. (1998). Pathogen-derived resistance targeted against the negative-strand RNA of tobacco mosaic virus: RNA strand-specific gene silencing? *Plant J* **13**, 537-546.

- Mawassi, M., Gafny, R., Gagliardi, D., and Bar-Joseph, M. (1995a). Populations of citrus tristeza virus contain smaller-than-full-length particles which encapsidate sub-genomic RNA molecules. *J Gen Virol* **76**, 651-659.
- Mawassi, M., Karasev, A. V., Mietkiewska, E., Gafny, R., Lee, R. F., Dawson, W. O., and Bar-Joseph, M. (1995b). Defective RNA molecules associated with citrus tristeza virus. *Virology* **208**, 383-387.
- Mawassi, M., Mietkiewska, E., Hilf, M. E., Ashoulin, L., Karasev, A. V., Gafny, R., Lee, R. F., Garnsey, S. M., Dawson, W. O., and Bar-Joseph, M. (1995c). Multiple species of defective RNAs in plants infected with citrus tristeza virus. *Virology* **214**, 264-8.
- Mawassi, M., Mietkiewska, E., Gofman, R., Yang, G., and Bar-Joseph, M. (1996). Unusual sequence relationships between two isolates of citrus tristeza virus. *J Gen Virol* **77**, 2359-64.
- Mawassi, M., Satyanarayana, T., Albiach-Marti, M. R., Gowda, S., Ayllon, M. A., Robertson, C., and Dawson, W. O. (2000a). The fitness of citrus tristeza virus defective RNAs is affected by the lengths of their 5'- and 3'-termini and by the coding capacity. *Virology* **275**, 42-56.
- Mawassi, M., Satyanarayana, T., Gowda, S., Albiach-Marti, M. R., Robertson, C., and Dawson, W. O. (2000b). Replication of heterologous combinations of helper and defective RNA of citrus tristeza virus. *Virology* **267**, 360-9.
- Medina, V., Tian, T., Wierzchos, J., and Falk, B. W. (1998). Specific inclusion bodies are associated with replication of lettuce infectious yellows virus RNAs in *Nicotiana benthamiana* protoplasts. *J Gen Virol* **79**, 2325-9.
- Medina, V., Peremyslov, V. V., Hagiwara, Y., and Dolja, V. V. (1999). Subcellular localization of the HSP70-homolog encoded by beet yellows closterovirus. *Virology* **260**, 173-81.
- Mestre, P. F., Asins, M. J., Carbonell, E. A., and Navarro, L. (1997a). New gene(s) involved in the resistance of *Poncirus trifoliata* (L.) Raf. to citrus tristeza virus. *Theor Appl Genet* **95**, 691-695
- Mestre, P. F., Asins, M. J., Pina, J. A., Carbonell, E. A., and Navarro, L. (1997b). Molecular markers flanking citrus tristeza virus resistance gene from *Poncirus trifoliata* (L) Raf. *Theor Appl Genet* **94**, 458-464.
- Mestre, P. F., Asins, M. J., Pina, J. A., and Navarro, L. (1997c). Efficient search for new resistant genotypes to the citrus tristeza closterovirus in the orange subfamily *Aurantioideae*. *Theor Appl Genets* **95**, 1282-1288.
- Michaud, J. P. (1998). A review of the literature on *Toxoptera citricida* (Kirkaldy) (Homoptera:Aphididae). *Florida Entomologist* **81**, 1-166.

- Moore, G. A., Jacono, C. C., Neidigh, J. L., Lawrence, S. D., and Cline, K. (1992). *Agrobacterium*-mediated transformation of *Citrus* stem segments and regeneration of transgenic plants. *Plant Cell Rep* **11**, 238-242.
- Moreno, P., Guerri, J., and Munoz, N. (1990). Identification of spanish strains of citrus tristeza virus (CTV) by analysis of double stranded RNAs (dsRNA). *Phytopathology* **80**, 477-482.
- Moreno, P., Guerri, J., Ballesterolmos, J. F., Albiach, R., and Martinez, M. E. (1993). Separation and interference of strains from a citrus tristeza virus isolate evidenced by biological-activity and double-stranded-RNA (dsRNA) analysis. *Plant Pathol* **42**, 35-41.
- Moreno, P., and Guerri, J. (1997). Variability of citrus tristeza closterovirus (CTV): methods to differentiate isolates. In: *Filamentous Viruses of Woody Plants* (P.Monette, Ed.), pp. 97-107. Research Signpost, Trivandrum, India.
- Napuli, A. J., Falk, B. W., and Dolja, V. V. (2000). Interaction between HSP70 homolog and filamentous virions of the Beet yellows virus. *Virology* **274**, 232-239.
- Navas-Castillo, J., Albiach-Marti, M. R., Gowda, S., Hilf, M. E., Garnsey, S. M., and Dawson, W. O. (1997). Kinetics of accumulation of citrus tristeza virus RNAs. *Virology* **228**, 92-7.
- Nejidat, A., and Beachy, R. N. (1989). Decreased Levels of TMV coat protein in transgenic tobacco plants at elevated-temperatures reduce resistance to TMV infection. *Virology* **173**, 531-538.
- Niblett, C. L., Genc, H., Cevik, B., Halbert, S., Brown, L., Nolasco, G., Bonacalza, B., Manjunath, K. L., Febres, V. J., Pappu, H. R., and Lee, R. F. (2000). Progress on strain differentiation of citrus tristeza virus and its application to the epidemiology of citrus tristeza disease. *Virus Res* **71**, 97-106.
- Nikolaeva, O., Karasev, A. V., Gumpf, D. G., Lee, R. F., and Garnsey, S. M. (1995). Production of polyclonal antisera to the coat protein of citrus tristeza virus expressed in *Escherichia coli*: application for immunodiagnosis. *Phytopathology* **85**, 691-694.
- Ochoa-Corona, F. M. (2001). Citrus tristeza virus : molecular characterization of isolates for use in mild strain cross protection, localization of the 5'-terminus and heterologous encapsidation. PhD. Dissertation. University of Florida, Gainesville.
- Oglesbee, M., Ringler, S., and Krakowka, S. (1990). Interaction of canine distemper virus nucleocapsid variants with 70K heat-shock proteins. *J Gen Virol* **71**, 1585-90.
- Okuno, T., Nakayama, M., and Furusawa, I. (1993). Cucumber mosaic-virus coat protein-mediated protection. *Semin Virol* **4**, 357-361.

- Pappu, H., Pappu, S., Niblett, C., Lee, R., and Civerolo, E. (1993a). Comparative sequence analysis of the coat proteins of biologically distinct citrus tristeza closterovirus isolates. *Virus Genes* **7**, 255-64.
- Pappu, H. R., Pappu, S. S., Manjunath, K. L., Lee, R. F., and Niblett, C. L. (1993b). Molecular characterization of a structural epitope that is largely conserved among severe isolates of a plant virus. *Proc Natl Acad Sci U S A* **90**, 3641-4.
- Pappu, H. R., Karasev, A. V., Anderson, E. J., Pappu, S. S., Hilf, M. E., Febres, V. J., Eckloff, R. M., McCaffery, M., Boyko, V., Gowda, S., and et al. (1994). Nucleotide sequence and organization of eight 3' open reading frames of the citrus tristeza closterovirus genome. *Virology* **199**, 35-46.
- Pappu, S. S., Febres, V. J., Pappu, H. R., Lee, R. F., and Niblett, C. L. (1997). Characterization of the 3' proximal gene of the citrus tristeza closterovirus genome. *Virus Res* **47**, 51-57.
- Peña, L., Cervera, M., Juarez, J., Navarro, A., Pina, J. A., Duranvila, N., and Navarro, L. (1995a). *Agrobacterium*-mediated transformation of sweet orange and regeneration of transgenic plants. *Plant Cell Rep* **14**, 616-619.
- Peña, L., Cervera, M., Juarez, J., Ortega, C., Pina, J. A., Duranvila, N., and Navarro, L. (1995b). High-efficiency *Agrobacterium*-mediated transformation and regeneration of *Citrus*. *Plant Science* **104**, 183-191.
- Peña, L., Cervera, M., Juarez, J., Navarro, A., Pina, J. A., and Navarro, L. (1997). Genetic transformation of lime (*Citrus aurantifolia* Swing): factors affecting transformation and regeneration. *Plant Cell Rep* **16**, 731-737.
- Peña, L., Martin-Trillo, M., Juarez, J., Pina, J. A., Navarro, L., and Martinez-Zapater, J. M. (2001). Constitutive expression of Arabidopsis LEAFY or APETALA1 genes in citrus reduces their generation time. *Nature Biotechnol* **19**, 263-267.
- Peremyslov, V. V., Hagiwara, Y., and Dolja, V. V. (1999). HSP70 homolog functions in cell-to-cell movement of a plant virus. *Proc Natl Acad Sci U S A* **96**, 14771-14776.
- Pirone, T. P. (1991). Viral genes and gene products that determine insect transmissibility. *Semin Virol* **2**, 81-87.
- Powell, P. A., Nelson, R. S., De, B., Hoffmann, N., and Rogers, S. G. (1986). Delay of disease development in transgenic plants that express the tobacco mosaic virus coat protein gene. *Science* **232**, 738-743.

- Price, M., Schell, J., Grosser, J., Pappu, S.S., Pappu, H.R., Febres, V., Manjunath, K.L., Niblett, C.L., Derrick, K.S., and Lee, R.F. (1996). Replication of citrus tristeza closterovirus in citrus protoplasts. *Phytopathology* **86**, 830-833.
- Pruss, G., Ge, X., Shi, X. M., Carrington, J. C., and Vance, V. B. (1997). Plant viral synergism: The potyviral genome encodes a broad-range pathogenicity enhancer that transactivates replication of heterologous viruses. *Plant Cell* **9**, 859-868.
- Raccach, B., Roichtacher, C. N., and Barbagallo, S. (1989). Semipersistent transmission of viruses by vectors with special emphasis in citrus tristeza virus. *Adv. Dis.Vector Res.* **6**, 301-340.
- Ratcliff, F., Harrison, B. D., and Baulcombe, D. C. (1997). A similarity between viral defense and gene silencing in plants. *Science* **276**, 1558-1560.
- Rocha-Pena, M. A., Lee, R. F., Lastra, R., Niblett, C. L., Ochoa-Corona, F. M., Garnsey, S. M., and Yokomi, R. K. (1995). Citrus tristeza virus and its aphid vector *Toxoptera citricida*: Threats to citrus production in the Caribbean and Central and North America. *Plant Dis.* **79**, 437-443.
- Roistacher, C. N. (1991). *Graft-Transmissible Diseases of Citrus : Handbook for Detection and Diagnosis*. International Organization of Citrus Virologists : Food and Agriculture Organization of the United Nations, Rome.
- Rubio, L., Ayllon, M. A., Kong, P., Fernandez, A., Polek, M., Guerri, J., Moreno, P., and Falk, B. W. (2001). Genetic variation of citrus tristeza virus isolates from California and Spain: evidence for mixed infections and recombination. *J Virol* **75**, 8054-8062.
- Sambrook, J., Fritsch, E.F., Maniatis, T. (1989). *Molecular Cloning. A laboratory Manual*. (C. S. H. Laboratory, Ed.) Cold Spring Harbor, N.Y.
- Sanford, J. C., and Johnston, S. A. (1985). The concept of parasite-derived resistance - deriving resistance genes from the parasites own genome. *J Theor Biol* **113**, 395-405.
- Sagara, J., and Kawai, A. (1992). Identification of heat shock protein 70 in the rabies virion. *Virology* **190**, 845-848.
- Satyanarayana, T., Gowda, S., Boyko, V. P., Albiach-Marti, M. R., Mawassi, M., Navas-Castillo, J., Karasev, A. V., Dolja, V., Hilf, M. E., Lewandowski, D. J., Moreno, P., Bar-Joseph, M., Garnsey, S. M., and Dawson, W. O. (1999). An engineered closterovirus RNA replicon and analysis of heterologous terminal sequences for replication. *Proc Natl Acad Sci U S A* **96**, 7433-7438.

- Satyanarayana, T., Gowda, S., Mawassi, M., Albiach-Marti, M. R., Ayllon, M. A., Robertson, C., Garnsey, S. M., and Dawson, W. O. (2000). Closterovirus encoded HSP70 homolog and p61 in addition to both coat proteins function in efficient virion assembly. *Virology* **278**, 253-265.
- Schneider, H. (1959). The anatomy of tristeza virus-infected citrus. *In: Citrus virus diseases* (J. M. Wallace, Ed.), pp. 73-84. University of California Press, Berkeley.
- Schneider, H., and Sasaki, P. J. (1972). Ultrastructural studies of chromatic cells in tristeza diseased lime. *In: 5<sup>th</sup> Proc. Conf. Int. Organ. Citrus Virol* (W. C. Price, Ed.), pp. 222-228, Gainesville
- Sekiya, M. E., Lawrence, S. D., McCaffery, M., and Cline, K. (1991). Molecular cloning and nucleotide sequencing of the coat protein gene of citrus tristeza virus. *J Gen Virol* **72**, 1013-1020.
- Simon, A. E., and Bujarski, J. J. (1994). RNA-RNA recombination and evolution in virus-infected plants. *Ann Rev Phytopathol* **32**, 337-362.
- Suastika, G., Natsuaki, T., Terui, H., Kano, T., Ieki, H., and Okuda, S. (2001). Nucleotide sequence of citrus tristeza virus seedling yellows isolate. *J Gen Plant Pathol* **67**, 73-77.
- Tatusov, R. L., Koonin, E. V., and Lipman, D. J. (1997). A genomic perspective on protein families. *Science* **278**, 631-637.
- Tsai, J. H., Liu, Y. H., Wang, J. J., and Lee, R. F. (2000). Recovery of orange stem pitting strains of citrus tristeza virus (CTV) following single aphid transmission with *Toxoptera citricida* from a Florida decline isolate of CTV. *Proc. Fla. State Hort. Soc.* **113**, 75-78.
- Vázquez, J. (2001). Catalytic analysis of the two putative cysteine proteases of citrus tristeza virus. PhD. Dissertation. University of Florida, Gainesville.
- Vives, M. C., Rubio, L., Lopez, C., Navas-Castillo, J., Albiach-Marti, M. R., Dawson, W. O., Guerri, J., Flores, R., and Moreno, P. (1999). The complete genome sequence of the major component of a mild citrus tristeza virus isolate. *J Gen Virol* **80**, 811-816.
- Wisler, G., Duffus, J., Liu, H., and Li, R. (1998). Ecology and epidemiology of whitefly-transmitted closteroviruses. *Plant Dis.* **82**, 270-280.
- Yang, G., Mawassi, M., Gofman, R., Gafny, R., and Bar-Joseph, M. (1997). Involvement of a subgenomic mRNA in the generation of a variable population of defective citrus tristeza virus molecules. *J Virol* **71**, 9800-9802.

- Yang, G., Che, X., Gofman, R., Ben-Shalom, Y., Piestun, D., Gafny, R., Mawassi, M., and Bar-Joseph, M. (1999). D-RNA molecules associated with subisolates of the VT strain of citrus tristeza virus which induce different seedling-yellowings reactions. *Virus Genes* **19**, 5-13.
- Yang, Z. N., Mathews, D. M., Dodds, J. A., and Mirkov, T. E. (1999). Molecular characterization of an isolate of citrus tristeza virus that causes severe symptoms in sweet orange. *Virus Genes* **19**, 131-142.
- Yang, Z. N., Ingelbrecht, I. L., Louzada, E., Skaria, M., and Mirkov, T. E. (2000). *Agrobacterium*-mediated transformation of the commercially important grapefruit cultivar Rio Red (*Citrus paradisi* Macf.). *Plant Cell Rep* **19**, 1203-1211.
- Yang, Z. N., Ye, X. R., Choi, S., Molina, J., Moonan, F., Wing, R. A., Roose, M. L., and Mirkov, T. E. (2001). Construction of a 1.2-Mb contig including the citrus tristeza virus resistance gene locus using a bacterial artificial chromosome library of *Poncirus trifoliata* (L.) Raf. *Genome* **44**, 382-393.
- Yokomi, R. K., Lastra, R., Stoetzel, M. B., Damgsteet, V. D., Lee, R. F., Garnsey, S. M., Rocha-Pena, M. A., and Niblett, C. L. (1994). Establishment of the brown citrus aphid *Toxoptera citricida* (Kirkaldy) (Homoptera: *Aphididae*) in Central America and the Caribbean basin, and its transmission of citrus tristeza virus. *J. Econ. Entomol.* **87**, 1078-1085.
- Yoshida, T., Schichijo, T., Ueno, I., Kihara, T., Yamada, Y., Hirai, M., Yamada, S., Ieki, H., and Kuramoto, T. (1983). Survey for resistance of citrus cultivars and hybrids seedlings to citrus tristeza virus (CTV). *Bull Fruit Tree Res Stn (Okitsu)* **B10**, 51-58.
- Zhang, Z. C., Li, D. W., Zhang, L., Yu, J. L., and Liu, Y. (1999). Virus movement protein gene mediated resistance against cucumber mosaic virus infection. *Acta Botan Sinica* **41**, 585-590.

## BIOGRAPHICAL SKETCH

Inés-Marlene Rosales was born in 1968 in Santiago, Chile. She earned a Bachelor of Science degree in biochemistry at the University of Chile, in December 1994. Her undergraduate research thesis, “Molecular Characterization of the Chilean Plum Pox Isolate,” was conducted at the INIA (Instituto de Investigaciones Agropecuarias), Santiago, Chile. After her graduation she continued working at the same Institute in the plant biotechnology laboratory, and in 1997 she was awarded by INIA with a scholarship to pursue the Doctor of Philosophy degree in the field of plant pathology at the University of Florida.